AFAL-TR-73-399
PART I

004970-1-T

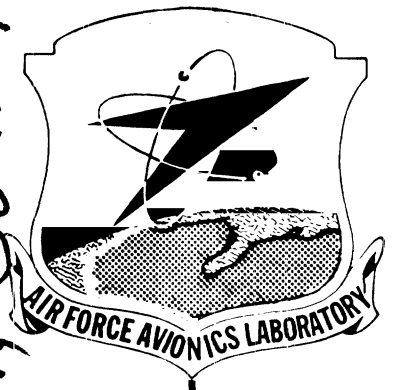

VHF-UHF Phased Array Techniques

PART I. CALCOMP Studies of Linear Arrays with Non-Uniformly Spaced Isotropic Elements

JOHN A. M. LYON, PHILIP H. FISKE,
MOHAMED A. HIDAYET, and JESS B. SCOTT

November 1973

Technical Report AFAL-TR-73-399, PART I

Air Force Avionics Laboratory
Air Force Systems Command
Wright-Patterson Air Force Base, Ohio

NOTICE

When Government drawings, specifications, or other data are used for any purpose other than in connection with a definitely related Government procurement operation, the United States Government thereby incurs no responsibility nor any obligation whatsoever; and the fact that the government may have formulated, furnished, or in any way supplied the said drawings, specifications, or other data, is not to be regarded by implication or otherwise as in any manner licensing the holder or any other person or corporation, or conveying any rights or permission to manufacture, use, or sell any patented invention that may in any way be related thereto.

Copies of this report should not be returned unless return is required by security considerations, contractual obligations, or notice on a specific document.

VHF-UHF PHASED ARRAY TECHNIQUES

PART I: CALCOMP STUDIES OF LINEAR ARRAYS WITH NON-UNIFORMLY SPACED ISOTROPIC ELEMENTS

John A. M. Lyon
Philip H. Fiske
Mohamed A. Hidayet
Jess B. Scott

FOREWORD

This report describes research performed by The University of Michigan Radiation Laboratory, 2455 Hayward Street, Ann Arbor, Michigan 48105 and constitutes the first of two interim reports required under USAF Contract F33615-71-C-1495, Task 05, Project 6099, "VHF-UHF Phased Array Techniques". The work was sponsored by the Electronic Technology Division, Air Force Avionics Laboratory and the Technical Monitor was Mr. Harold E. Weber, AFAL/TEM-3.

The original work statement for this contract was quite different from the modified work statement which was made available on 13 October 1972. The present report covers items which were in the original work statement. A second interim report will give coverage primarily to the amended work statement of 13 October 1972.

This report covers the time period 5 March 1971 through 30 June 1973 and was prepared by John A. M. Lyon, Philip H. Fiske, Mohamed A. Hidayet and Jess B. Scott; Professor Lyon also served as the Principal Investigator. The report has been designated Radiation Laboratory Report Number 004970-1-T for internal control purposes. It was submitted for sponsor approval on 3 October 1973.

ABSTRACT

This report contains information obtained by numerous computer studies of linear arrays of isotropic elements. A large range of numbers of elements were used. Various formulations were used to provide control on the degree of non-uniformity of spacing. Provision was made so as to provide a gradation in the illumination of the various elements used. It was found that a simple exponential relation provided illumination corresponding simultaneously to a Tchebyscheff type radiation pattern.

It was decided that for practical purposes some restraint should be provided on the grading of the slot illumination from the center slot to either extreme end slot. Therefore, in some of the studies utilizing an exponential variation of illumination, an arbitrary limit was imposed which required the illumination on the end slot to be either 9 or 12 dB below that of the center slot.

Considerable work was done on an optimization process, which has been classified as the method of steepest descent. In the steepest descent method a change in spacing is made in the direction that causes the most rapid rate of change (reduction) in the difference between a prescribed radiation pattern and the obtained radiation pattern. In other words, the change to be made was always in the direction so as to decrease the error or difference between the two patterns most rapidly. In applying this optimization procedure it was decided that it was appropriate to start with an array already reasonably well designed. For instance, if a broadside Tchebyscheff array was selected, the optimization process would be applied and changes would be made in the spacings of the elements so that the sidelobe levels would be reduced.

TABLE OF CONTENTS

LIST OF ILLUSTRATIONS

LIST OF ILLUSTRATIONS
(continued)

LIST OF ILLUSTRATIONS
(continued)

LIST OF ILLUSTRATIONS
(continued)

LIST OF ILLUSTRATIONS
(continued)

LIST OF ILLUSTRATIONS
(continued)

I. INTRODUCTION

Originally the contract F33615-71-C-1495 was to cover the period 15 April 1971 through 1 March 1974. The original statement of work was dated 4 March 1971. In this work statement four tasks were indicated with titles as follows: Task 1 was Dual Frequency Microwave Array, Task 2 VHF Ferrite Array, Task 3 UHF Constant K Lens with Multiple Feeds, and Task 4 Broadband and Special Array Elements. Although the contract period officially started 15 April 1971 there was an early indication by conversations with sponsors that some changes would be made in the work statement. In response to an inquiry on 28 June 1971 the chief investigator of this project was told by sponsor representatives that a new work statement had been formulated two weeks earlier and that this statement would be received in another two to three weeks. Later, on 14 August 1971, the sponsor representative indicated by telephone that the new work statement had been prepared and was now in final form. Finally a formal work statement, dated 27 January 1972, was received which called for a redirection of effort. This work statement was classified, however, there is no need in this report to refer to the classified objectives. Essentially the new work statement discontinued Tasks 2, 3 and 4 of the previous work statement. Task 1 of the previous work statement was expanded in its coverage. The main unclassified titles which persisted in this new work statement were: Dual Frequency Microwave Array, Array Design Configuration, Element Evaluation, Array Section Evaluation. On 31 March 1972 the project director and principal investigator outlined in a letter the work proposed by the sponsor at an earlier meeting on 16 March 1972. The outline in the letter showed six tasks. Task 1 was Fifteen-Element Linear Array. Task 2 was Fifteen-by-Fifteen Element Planar Array. Task 3 was Fifteen-Element Linear S-Band Array with Interleaved Five-Element L-Band Array. Task 4 was Use of Multi-Terminal/Multi-Mode Elements for Scanning. Task 5 was Fifteen-by-Fifteen Element S-Band Array with Interleaved Five-by-Five Element L-Band Array. Task 6 was Large

Interleaved S- and L-Band Planar Arrays.

On 17 August 1972 a discussion was held with the sponsors at Wright-Patterson Air Force Base. Shortly thereafter on 24 August 1972 a sponsor representative called and indicated that the laboratory had decided to restrict future work on the project to Tasks 1, 2 and 4 as defined in the University of Michigan letter dated 31 March 1972.

The new work statement providing for three tasks was formalized by a written statement dated 13 October 1972. Task 1 was Fifteen-Element Linear Array. Task 2 was Fifteen-by-Fifteen Element Planar Array. Task 3 was Use of Multi-Terminal/Multi-Mode Elements for Scanning. As can be seen, the new work statement incorporated Tasks 1, 2 and 4 as shown in the University of Michigan letter of 31 March 1972.

The work described in this report falls under the category of Task 1 -- Dual Frequency Microwave Array, as on the original work statement of 4 March 1971. The work also can be considered to fall under Task 1 -- Dual Frequency Microwave Array as shown in the contract modification of 27 January 1972. Under the original statement a minimal amount of work was done under Task 2 -- VHF Ferrite Array and Task 4 -- Broadband and Special Array Elements. Actually no work was done on Task 3 -- UHF Constant-K Lens with Multiple Feeds, as described in the original work statement. The work described in this report is also supportive of the work described in the final work statement of 13 October 1972, particularly Tasks 1 and 2.

In a contract modification effective 17 October 1972 the due date for the final interim report was changed to 30 July 1973. This represented an early termination of the contract. In a later contract modification (3 May 1973) the due date for the final interim report was changed to 30 September 1973.

The conventional array with elements uniformly spaced at half wavelength intervals is a "filled" array. The mutual coupling in such an array is often

sufficient to cause undesirable changes in the aperture illumination. It is obvious that an aperture that contains M-elements, equally spaced at half wavelength intervals, will contain more elements than if the spacings between elements are made unequal, and if the minimum spacing is a half wavelength. Since the unequally spaced array will contain fewer elements than the conventional array occupying the same aperture it is said to be "thinned". The radiation pattern of the thinned array cannot be controlled as well as that of a filled array, and the sidelobe level relative to the main lobe will not be as low. If the thinning is not too severe (no more than half the elements removed) the peak sidelobes can be kept to a reasonable value and can be made competitive with that of a uniformly spaced array.

Unequally spaced arrays may be used to obtain radiation patterns with low peak sidelobes without the need for an amplitude taper. This may be of importance in applications where it is not convenient to individually adjust the amplitude of the illumination at each element. Since the beamwidth of an array is determined primarily by the extent of the aperture and is relatively insensitive to the arrangement of elements within the aperture (compare, for example, the pattern of the circular planar aperture with that of a ring), the array with unequally spaced elements can approximate the beamwidth of a conventional filled array. Although the beamwidth of the unequally spaced array may be as narrow as that of the filled array, the theoretical resolution capabilities are not as good, since resolution depends upon both the beamwidth and the received signal-to-noise ratio. The latter depends upon the number of elements.

In the operation of a conventional equally spaced array over a wide frequency range it is quite likely that undesirable grating lobes will be formed. Grating lobes occur when the array beam is scanned if the element spacing exceeds one-half wavelength by a slight margin. For example, the spacing must be less than 0.59λ for a scan angle of $\pm 45^{o}$. If "s" is the spacing, λ is the wavelength in the same units, θ_o is the angle from broadside position of the main lobe, then θ_1

gives the position(s) of the grating lobe(s) according to the formula (Skolnik, 1970):

$$\sin\theta_1 = \sin\theta_o \pm \frac{n}{s/\lambda} \quad . \tag{1.1}$$

The unequally spaced array permits the antenna to operate over a wide frequency range without the appearance of grating lobes. In addition the unequally spaced array can be scanned over a wide range without the formation of grating lobes such as could appear with an equally spaced array.

The availability of the spacing as an additional parameter provides, in principle, more flexibility in array pattern synthesis. However, this property is restricted in practice by requirements on permitted spacing.

In individual studies of various linear arrays the technical objectives obtained from the overall work statement of this project originally were these:

0.8 degrees beamwidth,
maximum scan position 60^o from broadside,
maximum sidelobe level 40 dB below main lobe.

Subsequently, the work statement was drastically modified and the numerical values above were eliminated. In the studies related to these objectives the variables which were utilized were the number of array elements, the amplitude of excitation of each element, and the spacings from one element to another. Discussion of the studies involving a wide selection of linear arrays with various numbers of elements, various spacings, and various illumination arrangements are given in Section II.

Numerical iterative methods have been used in many optimization procedures. In particular, an iterative method based upon the principle of steepest descent has been shown to be useful in radiation pattern synthesis. Such a method can make use of the available parameters of element amplitudes and phases, element spacing, and frequency. In the optimization by this method which is recorded here, the method was restricted to optimization by changing the element spacing. In the studies made by this method, even though there is no complete assurance

that a true optimum was obtained, nevertheless, it is possible to see that a progressive improvement has been obtained in the performance of a standard array. Furthermore, it has been possible to see that this improvement has been carried out very nearly to the limit of such improvements.

Section II presents the results of the linear array studies and includes the development of the formulations for the computer, the use of CALCOMP as a design tool, the use of the method of steepest descent and related studies. Section III contains a discussion of the results and presents our conclusions.

II. USE OF COMPUTER IN ARRAY PATTERN STUDY

2.0 Linear Array Formulation*

A linear array of isotropic radiators is shown in Fig. 1. The number of radiators is N where N is odd. The symbols to be used are defined as:

a = amplitude of excitation, for example, current;

ϕ = phase relative to center element;

z = distance from center element;

Δz = incremental distance between elements.

For the odd number of elements as shown in Fig. 1, certain conditions including symmetry are specified in the following manner:

$$
\begin{aligned}
&\text{(a)} \quad a_o = 1 && \text{for } n \geq 1 \\
&\text{(b)} \quad a_n = a_{-n} && \\
&\text{(c)} \quad \phi_o = 0 && \text{for } n \geq 1 \\
&\text{(d)} \quad \phi_n = -\phi_{-n} && \\
&\text{(e)} \quad z_o = 0 && \text{for } n \geq 1 \\
&\text{(f)} \quad z_n = z_{-n} && \\
&\text{(g)} \quad \Delta z_n = \Delta z_{-n} &&
\end{aligned}
\tag{2.1}
$$

Now restrict the problem to far field conditions where the range to the observation point is such that the radiated fields decrease as one over the distance.

For this situation Fig. 2 may be used, where the desired direction of the main lobe of the radiation pattern is specified by angle θ_m relative to the linear array. To accomplish this the phase of the radiation from each individual element

---

*This formulation for linear arrays has been taken from the notes of Professor Charles W. McMullen of The University of Michigan. Mr. John Barnes was responsible for much of the programming for the CALCOMP method.

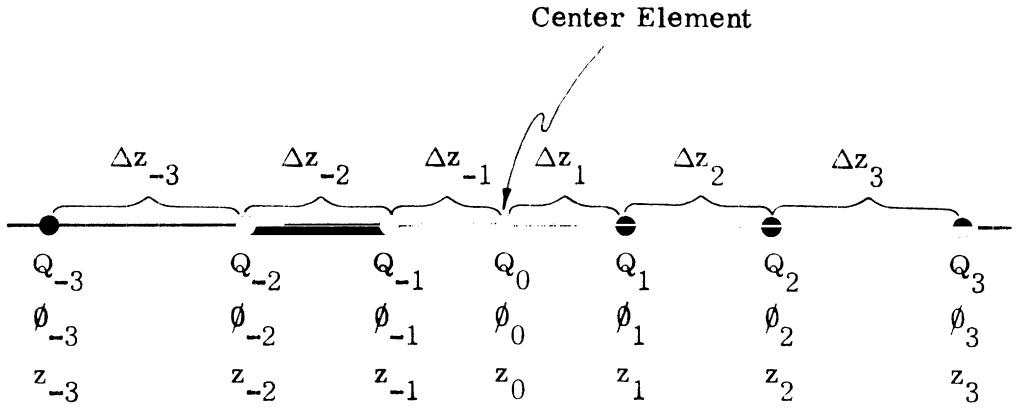

Fig. 1: Linear Array of Elements, Consisting of N Isotropic Elements, where N is Odd.

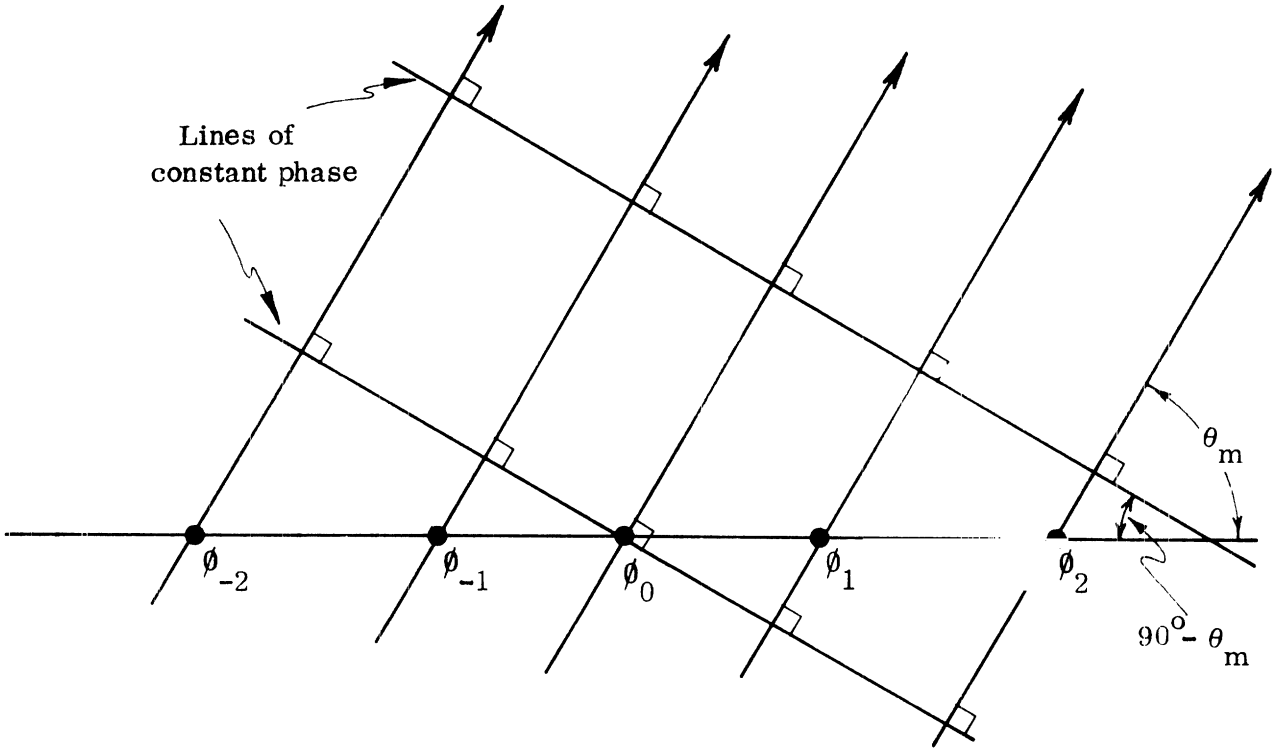

Fig. 2: Determination of ϕ's for Linear Array of Elements.

must be the same along lines of constant phase. As shown in Fig. 2, these are at an angle of $90^{o} - \theta_{m}$ with respect to the array.

It is required then that

$$\begin{aligned} &(a) \quad \phi_{n} = -\beta z_{n} \cos\theta_{m} = -\phi_{-n} \ , \\ &(b) \quad \beta = \frac{2\pi}{\lambda} \ , \end{aligned} \tag{2.2}$$

where λ is the wavelength. It is evident from Eq. (2.2) that the phase of elements to the right of center in Fig. 2 are retarded in phase, while those to the left are advanced in phase, each relative to the center element for which $\phi_{o} = 0$.

The incremental distances between elements in the array are specified by the functional relationships:

$$\begin{aligned} &(a) \quad \Delta z_{1} = C_{z1}\lambda \ , \\ &(b) \quad \Delta z_{n} = C_{z2}(\Delta z_{n-1})^{C_{z3}} \ , \end{aligned} \tag{2.3}$$

where C_{z1}, and C_{z3} are constants to be specified. These constants allow the spacing and spreading of the elements in the array to be controlled. It follows than from Fig. 1 and Eq. (2.3) that the distance of elements from the center is expressed as:

$$\begin{aligned} &(a) \quad z_{1} = \Delta z_{1} \ , \\ &(b) \quad z_{n} = z_{n-1} + \Delta z_{n} \quad \text{for } n \geq 2 \ . \end{aligned} \tag{2.4}$$

Finally the amplitude of excitation for elements in the array is given by the functional relationship

$$a_{n} = e^{-\frac{z_{n}^{2}}{C_{a}}} \tag{2.5}$$

where C_{a} is a constant to be specified. It allows the taper of excitation to be controlled as one moves away from the center element. Later in subsection 2.1

computer terminology is used and C_a becomes CA1 and a_n is called A(N).

Thus Eqs. (2.1) through (2.5) completely specify the linear array antenna by giving the separation, phase, and amplitude of the elements. With this information one may use Fig. 3 to calculate the field strength F in any direction θ relative to the array.

Since the distance of the field point P is large, the directions of r_1, r_2, r_{-1}, and r_{-2} in Fig. 3 may be approximated as the same kind of r_o, that is, at angle θ with respect to the array. This same idea was used in Fig. 2 where parallel lines are drawn from each element in the direction of power concentration. It follows then from Fig. 3 that:

$$\begin{aligned} r_1 &= r_o - z_1 \cos\theta \quad , \\ r_{-1} &= r_o + z_1 \cos\theta \quad , \\ r_2 &= r_o - z_2 \cos\theta \quad , \\ r_{-2} &= r_o + z_2 \cos\theta \quad . \end{aligned} \tag{2.6}$$

Now at some distant point as shown in Fig. 3, the contributions of each element of the array may be summed to get the field strength F. Thus

$$\begin{aligned} F = {} & a_o e^{-j\beta r_o} + \\ & a_1 e^{j\phi_1} e^{-j\beta r_1 \cos\theta} + a_{-1} e^{j\phi_{-1}} e^{-j\beta r_{-1}\cos\theta} + \\ & a_2 e^{j\phi_2} e^{-j\beta r_2 \cos\theta} + a_{-2} e^{j\phi_{-2}} e^{-j\beta r_{-2}\cos\theta} \quad . \end{aligned} \tag{2.7}$$

Combining Eqs. (2.1b), (2.1d), (2.2a), (2.6) and (2.7), as well as noting that antenna field patterns usually involve only the magnitude of F, one may write:

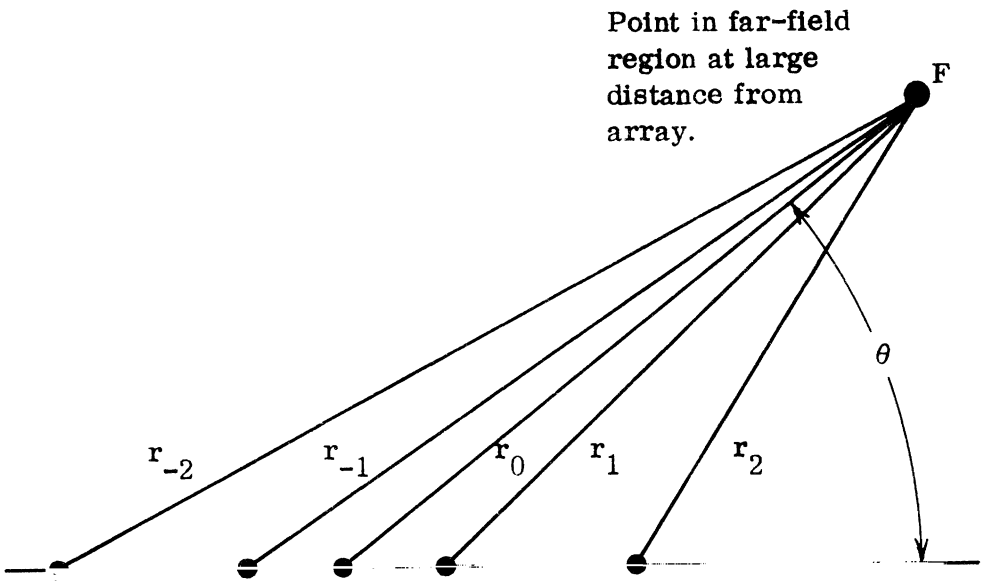

Fig. 3: Determination of Field Strength F for Linear Array of Elements.

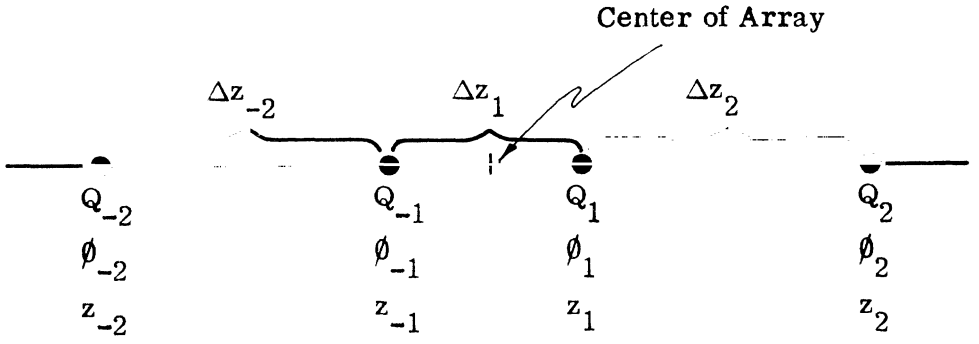

Fig. 4: Linear Array of Elements, Consisting of N Isotropic Radiators, where N is Even.

$$\left| F_e^{\,j\beta r_o} \right| = \left| a_o + 2a_1 \frac{e^{j\beta z_1(\cos\theta_m - \cos\theta)} + e^{-j\beta z_1(\cos\theta_m - \cos\theta)}}{2} + 2a_2 \frac{e^{j\beta z_2(\cos\theta_m - \cos\theta)} + e^{-j\beta z_2(\cos\theta_m - \cos\theta)}}{2} \right|$$

or

$$\left| F \right| = \left| a_o + 2a_1 \cos\left[\beta z_1(\cos\theta_m - \cos\theta)\right] + 2a_2 \cos\left[\beta z_2(\cos\theta_m - \cos\theta)\right] \right| \quad . \quad (2.8)$$

Furthermore, antenna field patterns are normally a plot of $|F|/|F|_{max}$ versus angle θ, where

$$\left| F \right|_{max} = \left| F \right|_{\theta = \theta_m} \quad . \quad (2.9)$$

Finally with Eqs. (2.8) and (2.9) combined and expressed in general form, there results

$$\frac{|F|}{|F|_{max}} = \frac{\left| a_o + 2 \sum_{n=1}^{(N-1)/2} a_n \cos\left[\beta z_n(\cos\theta_m - \cos\theta)\right] \right|}{a_o + 2 \sum_{n=1}^{(N-1)/2} a_n} \quad (2.10)$$

where N is an odd integer giving the total number of elements in the linear array. Antenna field patterns may now be calculated using Eq. (2.10).

Consider the linear array antenna in Fig. 4, consisting of N isotropic radiators, where N is even. It may be readily shown that the antenna field pattern is given by the expression:

$$\frac{|F|}{|F|_{max}} = \frac{\left| \sum_{n=1}^{N/2} a_n \cos\left[\beta z_n (\cos\theta_m - \cos\theta)\right] \right|}{\sum_{n=1}^{N/2} a_n} \qquad (2.11)$$

where all terms are the same as for an odd number of elements except

$$\begin{aligned} &(a)\quad a_o = 0 \quad , \\ &(b)\quad a_n = e^{-\frac{z_n^2 - z_1^2}{C_a}} \quad \text{for } n \geq 1 \quad , \\ &(c)\quad z_1 = \Delta z_1/2 \quad . \end{aligned} \qquad (2.12)$$

2.1 Linear Array Program

A computer program was devised based upon the elementary array considerations described in the previous subsection. The radiation patterns which were recorded in this report have been achieved using a CALCOMP display tube arrangement. Using this equipment it was possible to call for the desired program and then to insert the appropriate data for the array to be studied. For instance, the number of elements to be used would be inserted as data by specifying NANT = followed by the number of elements desired. In a similar way appropriate data would be inserted for the quantities CZ 1, CZ 2, CZ 3, and CA 1. Note that as required by computer language instead of Cz1 as written in subsection 2.0, the symbol is now written CZ 1. Similar adaptations are made for other symbols. The first three parameters mentioned serve to specify the spacing to be used. The last one mentioned serves to specify the amplitude of the individual elements. The insertion of a single value for CA 1 would be used in the program together with the exponential expression which produces A(N). In this way the amplitude

of the illumination for each element was then known. Other quantities which were specified were THETAM for the angle of the main lobe, (this angle is measured upward from the line of the array elements), THTMAX for the maximum angle in the rectangular plot, and THTMIN for the minimum angle in the rectangular plot. These last two quantities are the extreme points for the range of scan in the plot. Another important data input was designated as NSTP which was chosen according to the number of steps (maximum possible 361) desired in the computation of the rectangular plot. These points were spaced evenly between the extreme values of scan position. Another useful input point was designated as NTB, which was given equal to one if a polar plot in the top half only was required. NTB was made equal to two if a polar plot in the bottom half only was required and equal to three if a polar plot covering both halves was required.

In addition, keys were available on the CALCOMP display unit to specify polar plot, if required, rectangular plot, and also overlay. The use of the overlay button permitted the plotting of a second array situation on top of a previous one. In order to do this the previous plot should not be erased but one should immediately proceed to use the overlay button and then to insert the appropriate new data. This allowed quick comparison between two arrays of interest.

In utilizing the provision for polar plot it is found that the plotting program provides printed information on beamwidth, number of elements, the choice of CZ1, CZ2, CZ3, CA1, THETAM, Z(N), A(N), and PHI(N). The last quantity, PHI(N), is the measured phase of any element compared with the center element which is referenced as zero phase. In the actual construction of an array the values of A(N), Z(N), and PHI(N) would be used. The advantages of a polar plot are these: (1) good for easy detection of grating lobes; (2) good for small numbers of elements where general trends only are desired.

For a rectangular plot there is a computer printout on the face of the CALCOMP tube indicating the number of elements, CZ1, CZ2, CZ3, CA1, and THETAM. Since the rectangular plots are, in general, used for large arrays

provision was made to store Z(N), the distance to each element and A(N), the illumination of each element, and PHI(N). For large numbers of elements these three items of data would involve many points and there might not be room enough adjacent to the rectangular plot. For this reason this type of data was stored and, of course, there is provision at any time to call for a printout of this data. The rectangular plots were used especially for large numbers of array elements. The obvious advantages of rectangular plots are: (1) observation of exact side-lobe structure; (2) observation of specific portions of a pattern in great detail. The use of the overlay provision was available for either polar plots or rectangular plots.

2.2 Major Steps in Using CALCOMP

The CALCOMP unit provides for a visual display on a cathode ray tube. Otherwise it functions much like any terminal on the IBM 360/67 computer. A separate printout unit is associated with CALCOMP, making it unnecessary to photograph the display on the cathode ray tube. The major steps in the use of CALCOMP are tabulated below.

1. Sign On
2. $GLAB: SETUP
   ECHO OFF (Computer Response)
3. $ RUN SOURCE PROGRAM + GLAB; GILBCI
4. Press desired function button such as POLAR RECT OVERLAY NEATEN STOP.
5. &IN ☐Array Specs ☐& OUT
   Array Specs such as
   CA 1 = 1.00, CA 1 = 0.333, NTB = 1, etc.
   NTB = 1 calls for a polar plot in the top half only. This plot will be printed.
6. Press OVERLAY
7. &IN ☐Array Specs ☐& OUT
   Plot in lower half will be made.

8. Press NEATEN
   Grid and array spacings, amplitudes and phases will be displayed.

2.3 Physical Constraints on Array

It is necessary that for each prescribed amplitude distribution chosen for the elements there must be an appropriate feed network to provide for this. In the cases considered, isotropic elements are involved and the problem of providing the necessary feeds is neglected for the time being. In an actual physical array the mutual coupling effects can be of paramount importance. Such coupling effects may very well mean that the actual illuminations obtained on each element aperture will not be simply related to the powers fed to the element by the feed network. This means that a complete analysis of an array must go beyond a simple array in which element illuminations are assumed. Although in these pattern studies coupling effects are not considered, nevertheless, the chosen illumination distributions have been made with possible alterations due to coupling in mind. For this reason, in some of the studies, the minimum level of illumination obtained at an end element was limited to a prescribed dB level below the illumination level of the central element. This restriction on illuminations recognized that to go to still lower levels of illumination would be quite meaningless since such levels would be completely upset by mutual coupling effects.

The element spacings used in these arrays were restricted to values of the order of 0.4λ to 0.5λ. This range of spacings is the one most frequently used for simple, broadside antenna arrays. Furthermore, this range of spacing provides adequate clearance between the individual elements and inhibits the formation of grating lobes. It should be noted that some grating lobes can be tolerated, provided that they are positioned in such a fashion as to be cancelled out by nulls in the patterns of the individual elements. In a few cases studied where the spacing was greater than 0.5λ, grating lobes were formed.

Although the design studies here described show certain performance would be obtained with the assumed values of illumination, amplitude, and phase, together with the assumed values of spacing, yet the exact same radiation patterns would very likely not be obtained on a physical antenna array using the same prescribed illumination and spacing values. Some departures could result because the physical model did not adequately reproduce the conditions assumed in the analysis model. For instance, the isotropic elements assumed here would not be obtainable in practice.

A very considerable range was used in the number of elements chosen for the various linear array studies. Naturally it is desired to keep the number of elements to a minimum, thereby keeping the complexity of the array to a minimum. As will be easily noticed in this study a very large number of elements was used in order to approach the directivity and beamwidth requirements which were originally set as objectives. Careful consideration was given in extending the studies to longer and longer linear arrays. It was important to assess the advantage of adding additional elements.

2.4 Random Errors in Arrays

Although the benefits of increasing the number of elements in the assumed case of isotropic radiators may seem worthwhile, the practicality of adding elements should be questioned. One can, in principle, specify the distribution of illumination across the array aperture and expect the resulting radiation pattern to be as predicted. In practice, however, there will be unavoidable errors in the illuminations excited at the aperture, and the actual radiation pattern will differ from that predicted by theory. The agreement between the two depends upon how well the desired distribution of illumination across the array aperture can be achieved.

Errors in the aperture illumination can be divided into two types depending upon whether they are predictable or random. An example of a predictable error is the finite quantization of the phase produced by a digital phase-shifter. Random

errors are caused by the accidental deviations of the antenna parameters from design values. Although these errors may be small, they are always present and can limit the minimum sidelobe level that can be achieved just as random noise limits the sensitivity of a radio receiver. Random errors will increase the sidelobe level, cause a reduction in the gain, and cause errors in the direction of the main beam.

An array antenna radiation pattern may differ from the desired radiation pattern because of: (1) errors in the illuminations at each element, (2) errors in the phase of the illuminations, (3) missing or inactive elements (due to catastrophic failure), (4) rotation of the radiating element (faulty alignment of element polarization), (5) translational errors in the element location, and (6) errors in the radiation patterns of individual elements.

2.5 25-Element Arrays with Uniform Illumination but Varied Spacings

This set of studies designated with the prefix A and shown in Figs. 5 to 13 inclusively, consists of a number of computer studies on 25-element arrays. Each of the arrays is characterized by uniform illumination over the array aperture. The fact that the uniform illumination persists is implied by the choice of CA 1 which is a very large value. The unequal spacing is described by the values of CZ 1, CZ 2, CZ 3. Refer to the legend given on pages 8 and 9 for a description on the use of the various parameters mentioned. The studies in this section are preliminary in the sense that they were the first studies to be made using the computer display tube. These early studies were made with polar plots which were convenient for the small number of elements used. However, it was soon learned, as shown in subsequent studies, that a rectangular plot was much preferred, especially for large arrays with many side lobes. Each array pattern shown in this group actually has two major lobes. The narrower main lobe at 90° in each case corresponds to an illumination so that the array radiates in a broadside direction. An additional plot has been made which shows the array

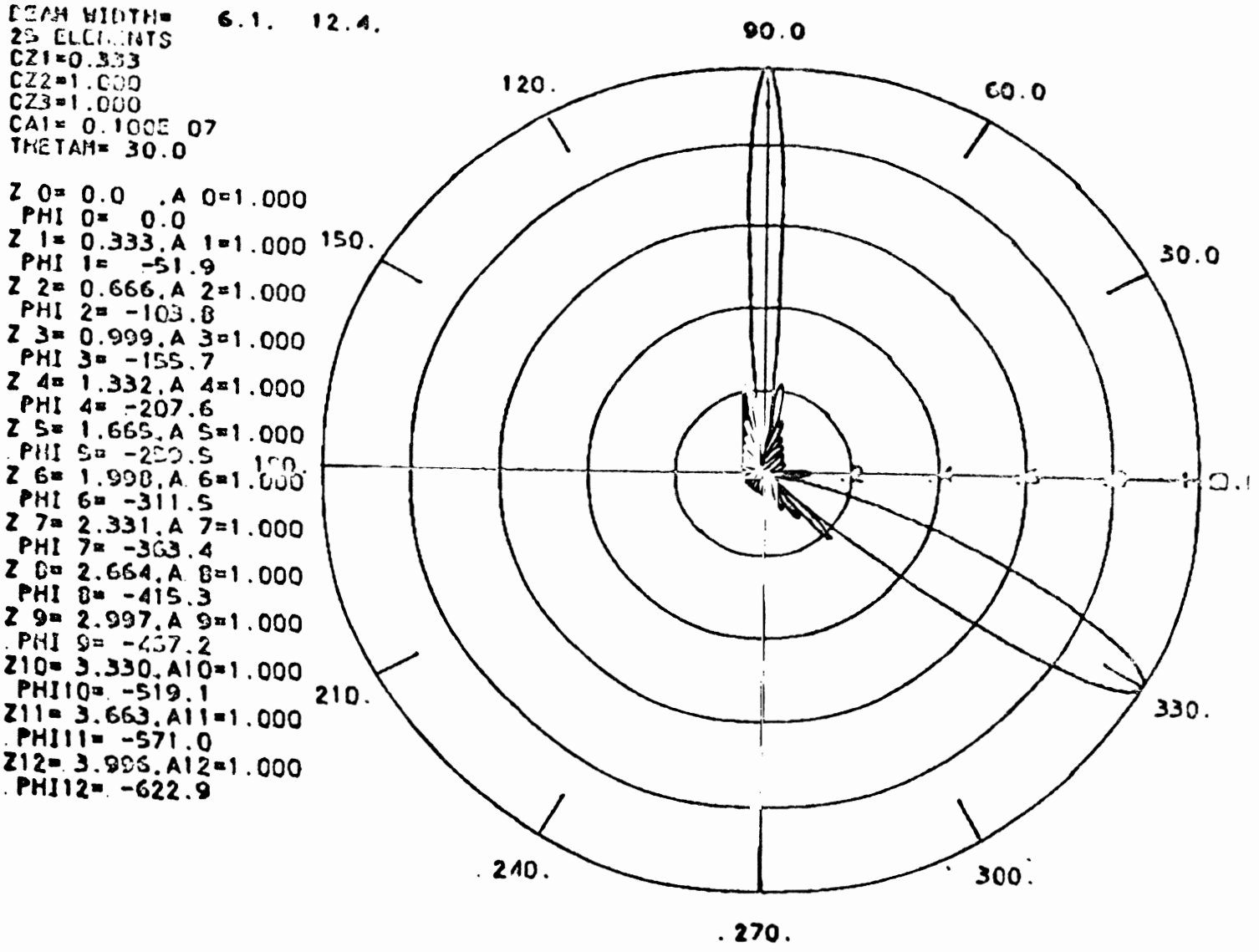

Fig. 5: Study A-1. 25-Elements — Uniform Illumination and Uniform Spacing of 0.333λ.

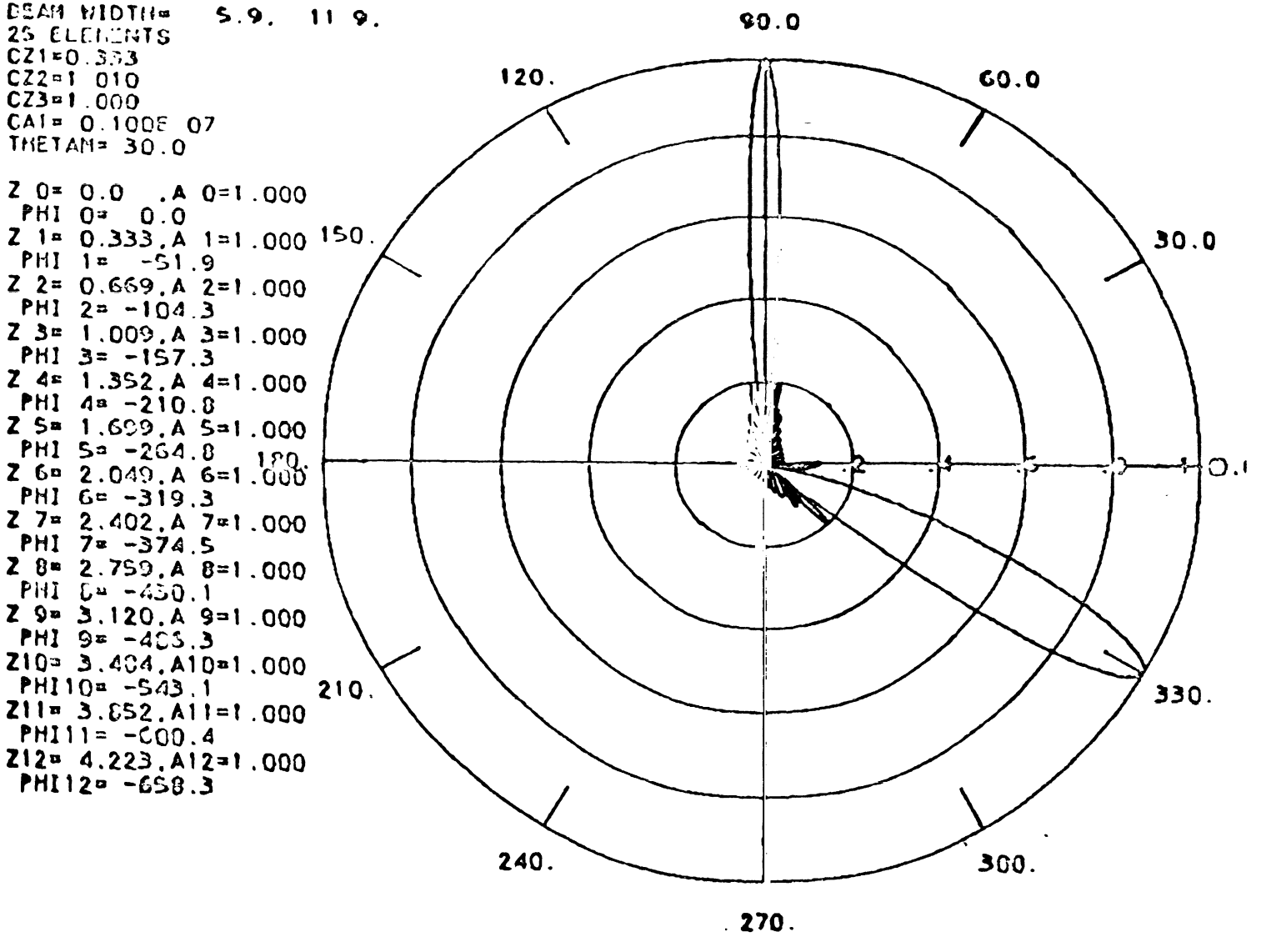

Fig. 6: Study A-2. 25-Elements — Uniform Illumination; Range of Spacing 0.333λ to 0.371λ.

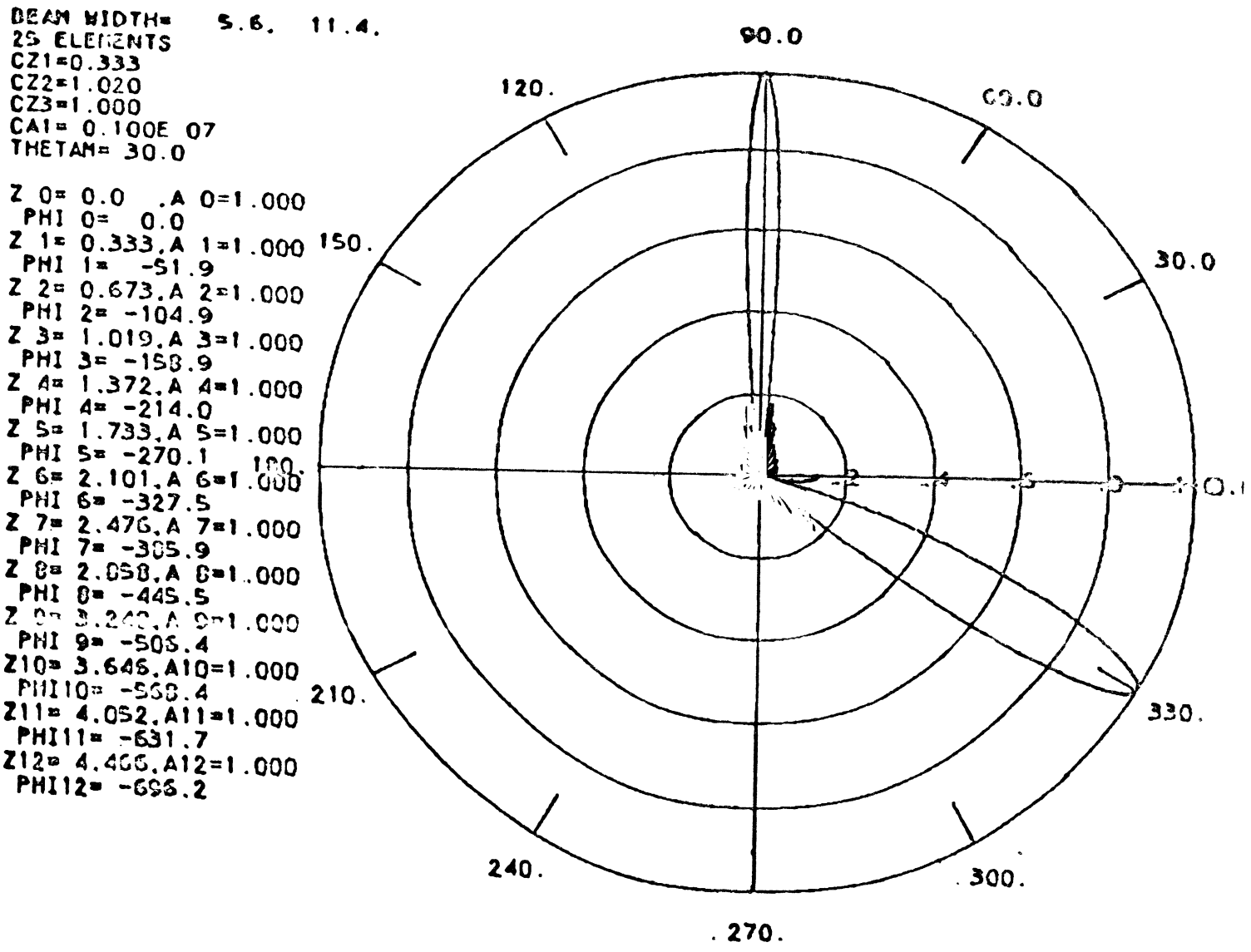

Fig. 7: Study A-3. 25-Elements — Uniform Illumination; Range of Spacing 0.333λ to 0.414λ.

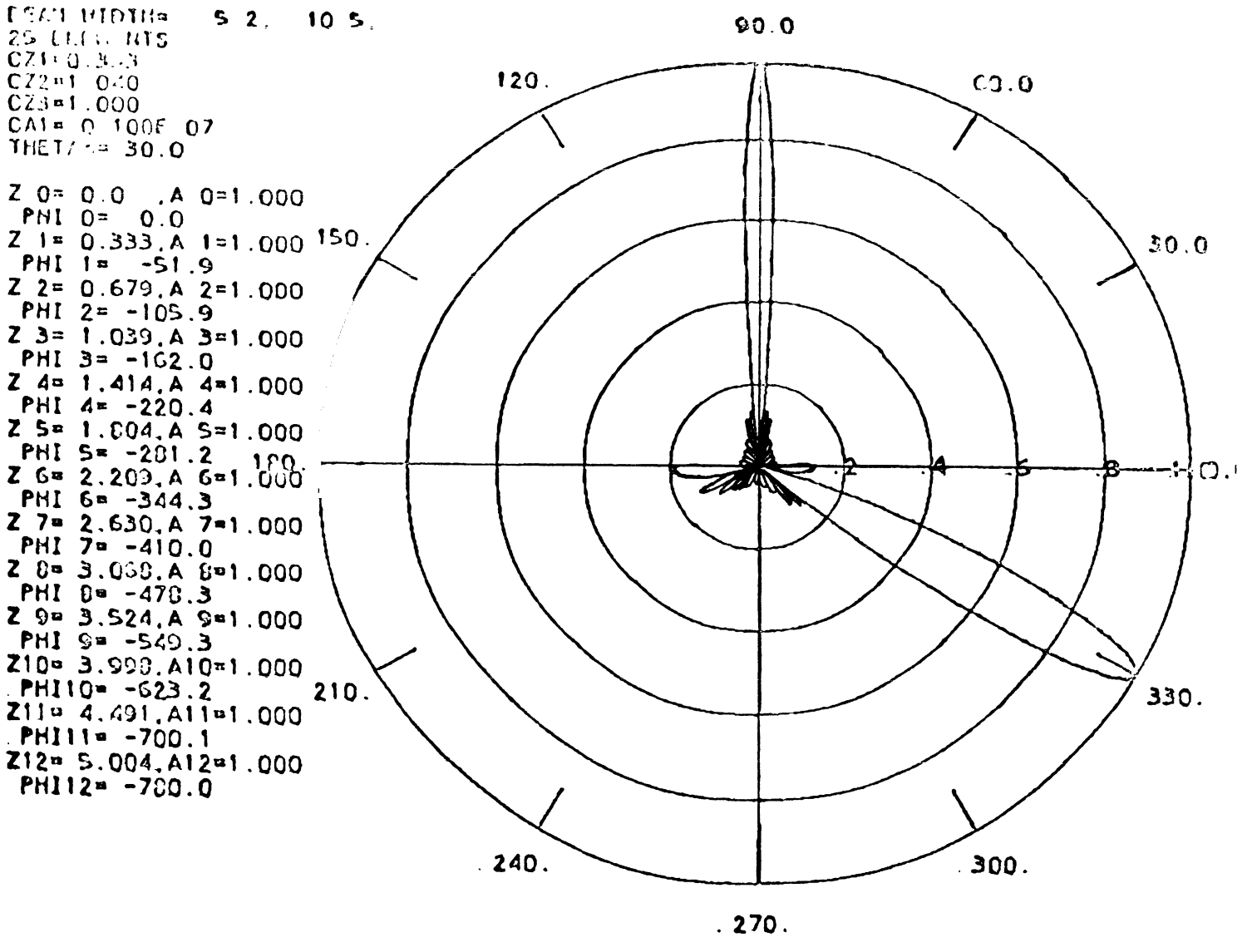

Fig. 8: Study A-4. 25-Elements— Uniform Illumination; Range of Spacing 0.333λ to 0.513λ.

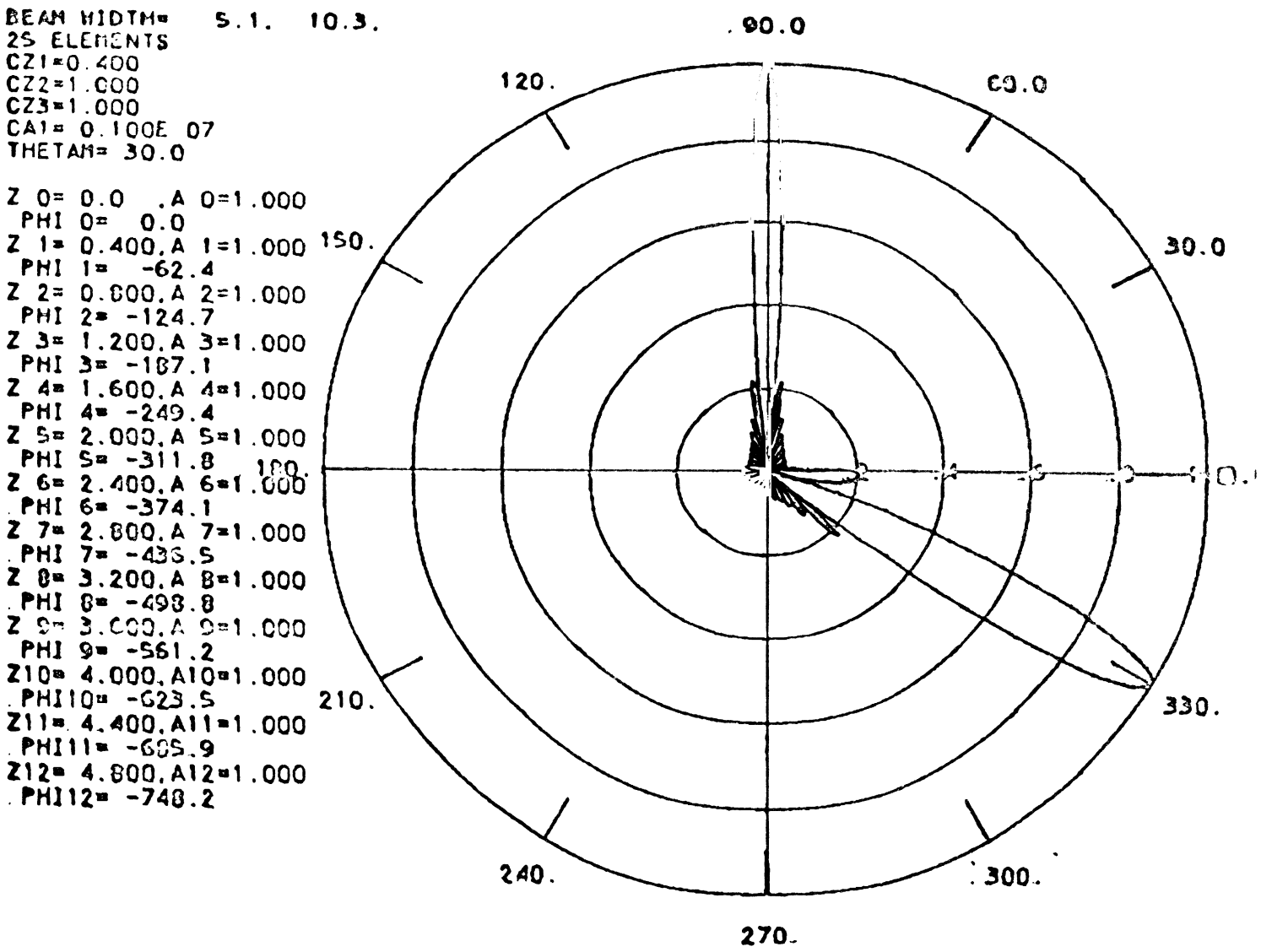

Fig. 9: Study A-5. 25-Elements — Uniform Illumination and Uniform Spacing of 0.400λ.

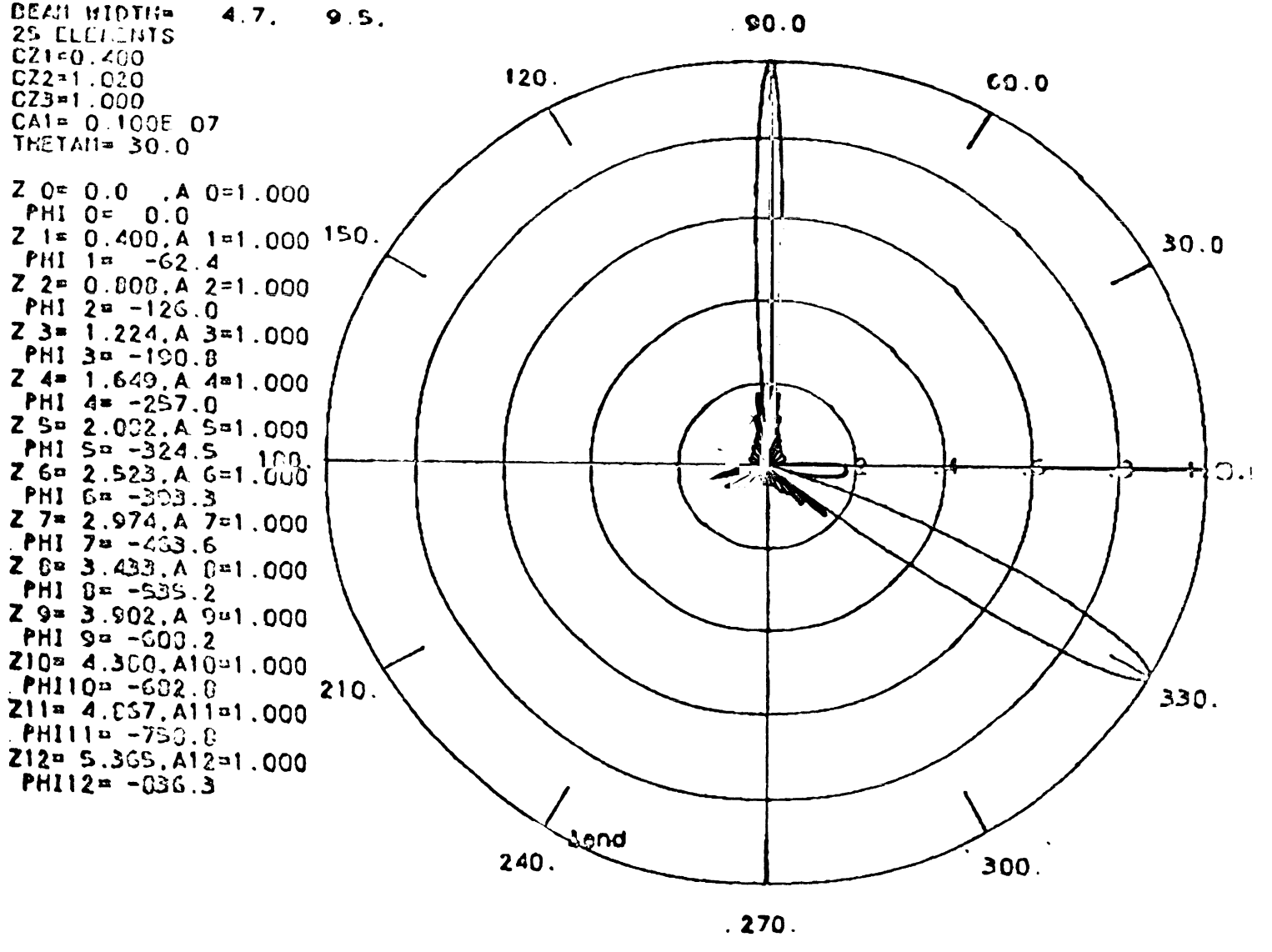

Fig. 10: Study A-6. 25-Elements — Uniform Illumination; Range of Spacing 0.400λ to 0.498λ.

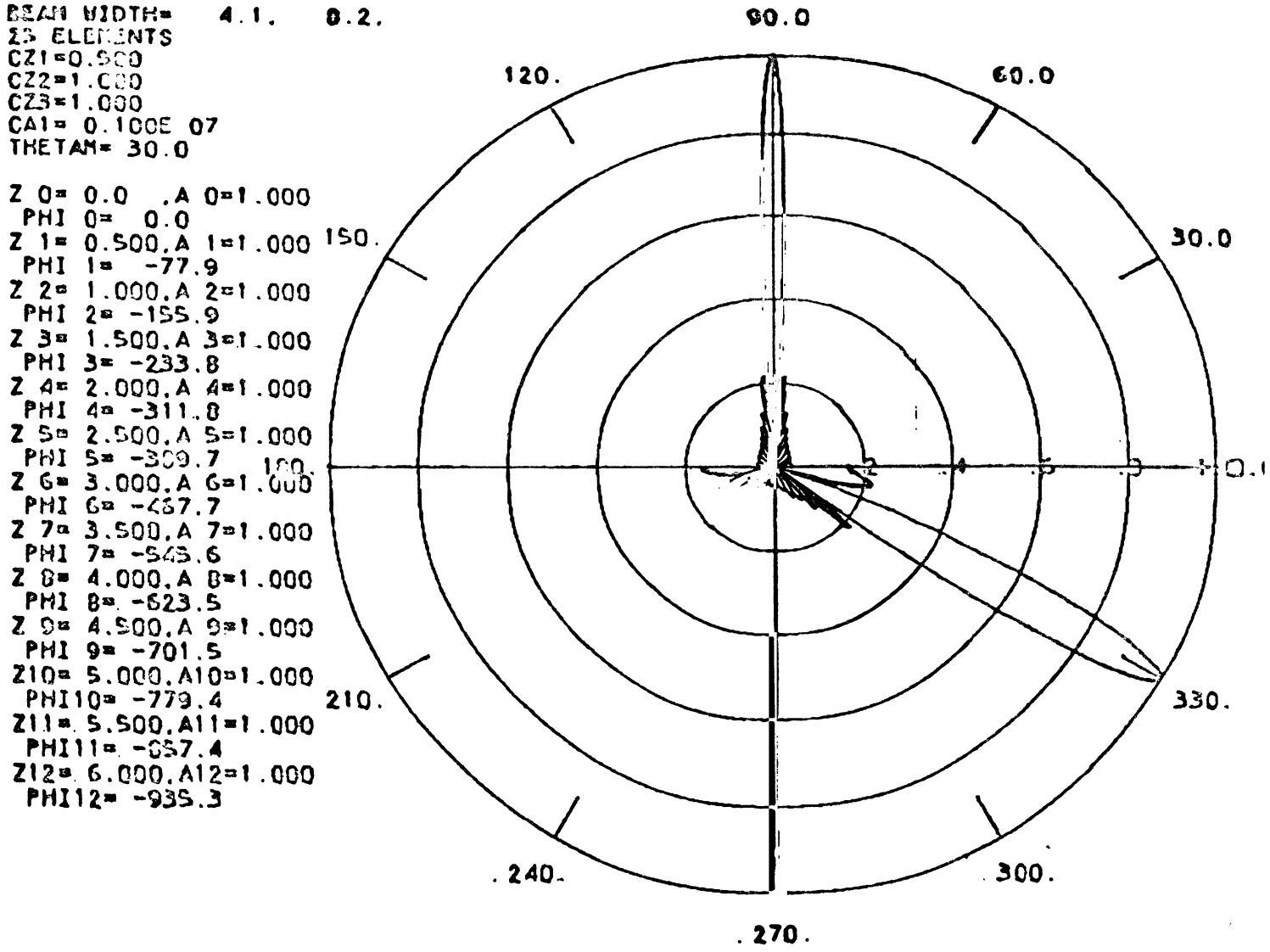

Fig. 11: Study A-7. 25-Elements — Uniform Illumination and Uniform Spacing of 0.500λ.

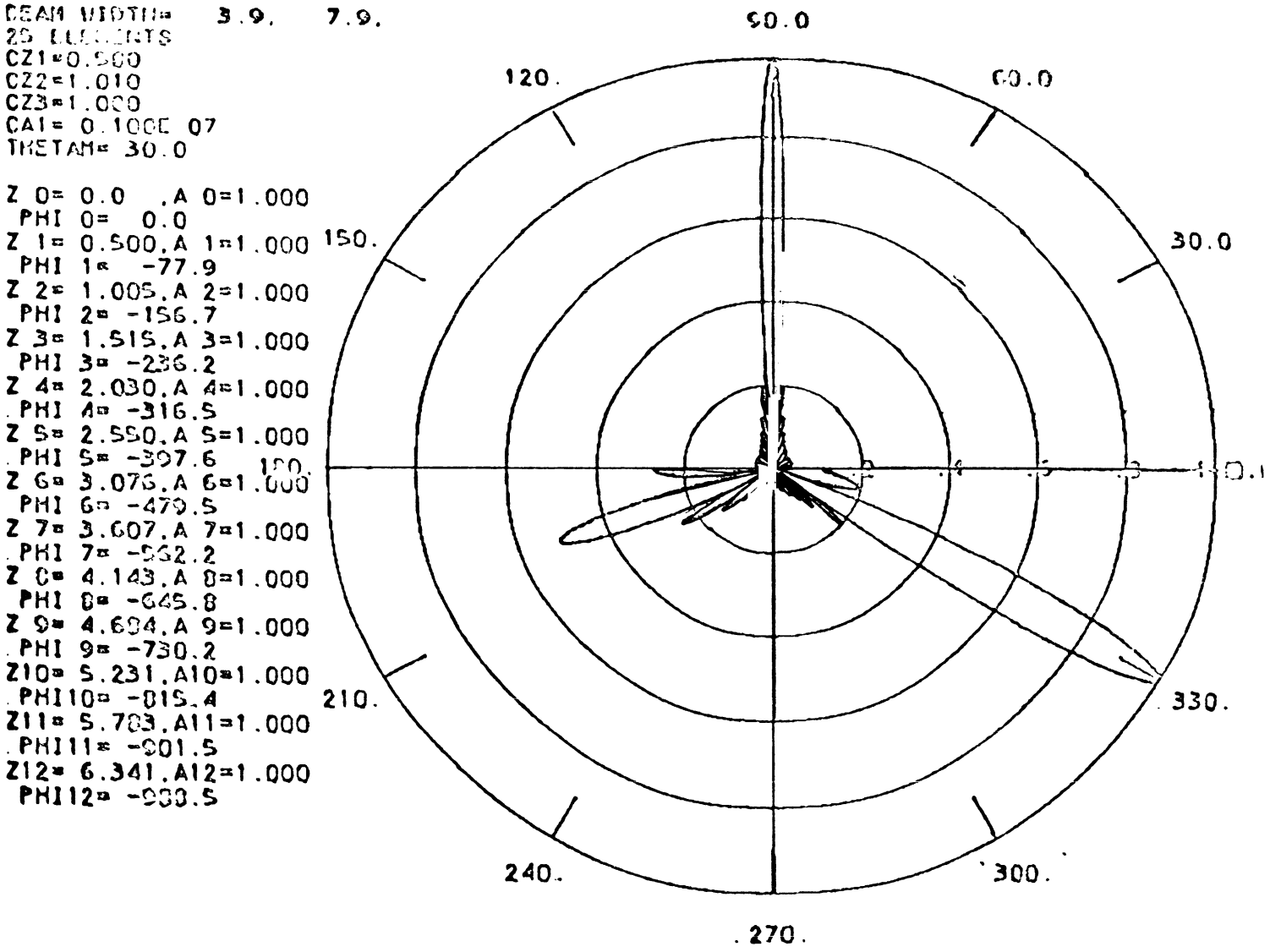

Fig. 12: Study A-8. 25-Elements — Uniform Illumination; Range of Spacing 0.500λ to 0.558λ.

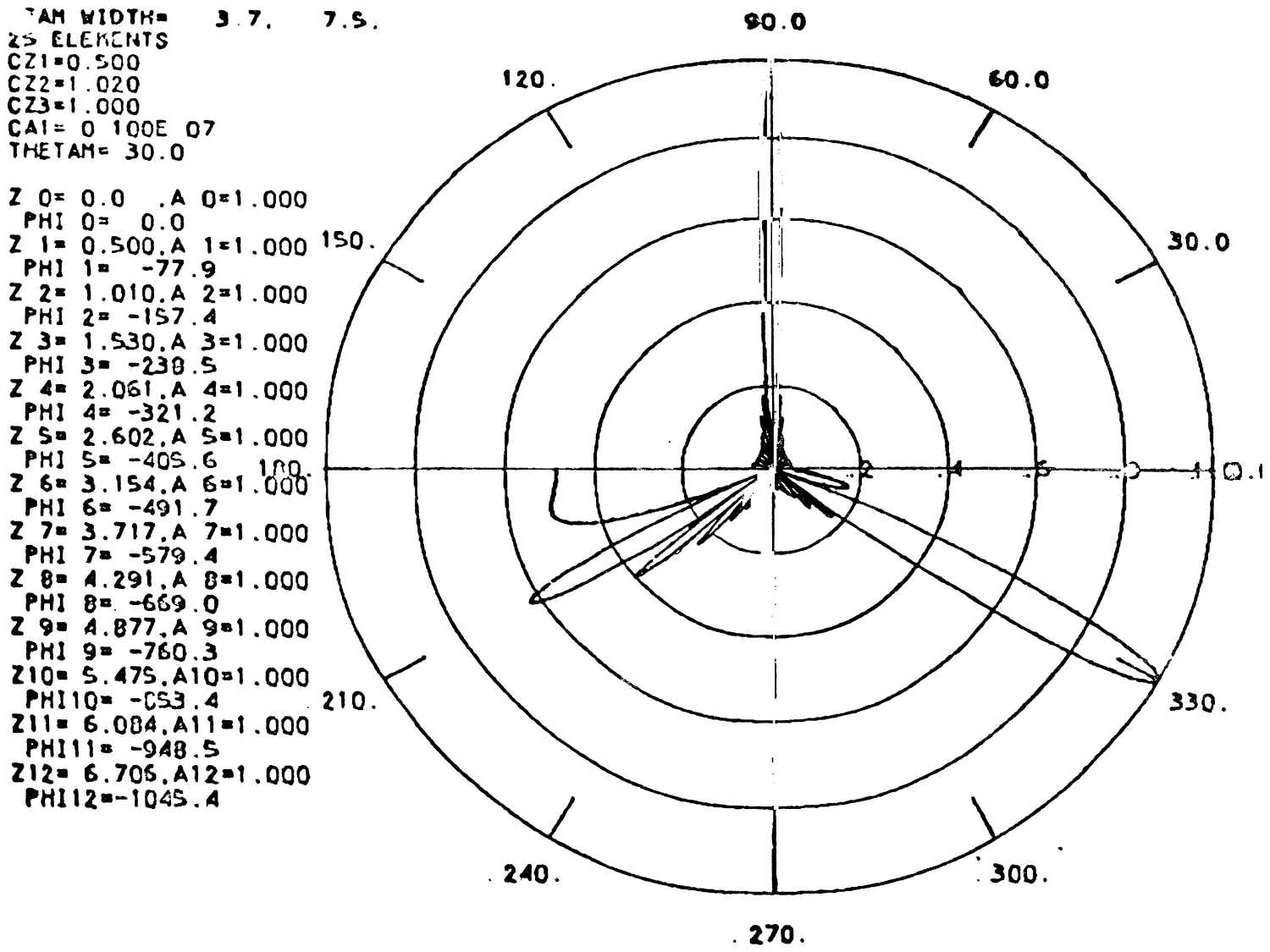

Fig. 13: Study A-9. 25-Elements — Uniform Illumination; Range of Spacing 0.500λ to 0.622λ.

radiating with the phasing adjusted for a scan angle of 60^{o} from broadside position. However, this has been plotted as a mirror image to minimize overlapping in the sidelobes. It is to be noticed that the beam is wider than a main beam as would be expected. To re-state the above, the wide lobe which appears to be at 330^{o} is really the main beam at a position of 30^{o}; that is, the beam as shown in the fourth quadrant should really be in the first quadrant. In observing these preliminary studies it will be noted that the small number of elements with uniform spacing and various illuminations provide beams that are considerably wider than required. Likewise the sidelobe levels which are observed are not sufficiently low to approach the requirements as originally stated. The plots shown are based on a linear power scale.

It will be noted that some examples in this group of preliminary studies commenced with the basic spacing of 0.33λ at the center with the successive spacings increasing slightly as one progresses outward from the center. Values of the parameter CZ 2, which influence the spacing, were from 1.0 to 1.04. The parameter CZ 3 was kept constant throughout these studies. It is to be noted at the top of each study, the beamwidths for the two positions of the main beam have been printed on the computer output.

The following trends are observed: In cases where the spacing increased most rapidly in departing from the center, it can be seen that the beamwidths tend to be less than in other studies. There is some limitation on this phenomenon because ultimately as the spacing increases the problem of grating lobes occurs, resulting in an undesirable high level of lobes. It is also noted that with the beam in the scan position 60^{o} from broadside, the beamwidth is increased by the secant of the angle of 60^{o}, or in other words, for this scan position the beamwidth is twice that for the broadside beam position. Of course the principal reason that the beamwidths are as large as they are is that in this series of studies the restriction of 25-elements has been imposed. Also it is to be observed that the relatively high sidelobe level corresponds to the fact that the illumination of elements was main-

tained uniformly throughout the array. A tapered illumination would be helpful in reducing the sidelobe level. This latter variation is implemented in subsequent studies. The studies in this group are labeled consecutively starting with A-1 and running through the number A-9.

For illustration in interpreting the studies consider Study A-1. The top half of the display shows the beam in broadside position; the beamwidth is printed out as 6.1^{o}. Since an array of isotropic radiators is considered the radiation pattern around the axis of the array is circular. The directivity for study A-1 with the beamwidth mentioned is 12.7 dB; this value neglects the sidelobes. The bottom half of the display shows the beam in a scanned position of 60^{o} from broadside; its beamwidth as printed out is 12.4^{o}. Note there are 25 elements. The value of CZ 1 being 0.333 and CZ 2 being 1.000 and CZ 3 being 1.000 indicate a uniform spacing between elements of 0.333λ. The value of CA 1 being 0.1×10^{7} assures that, practically speaking, the illumination is without taper (all elements have the same illumination). The values of Z printed give the positions of all elements since symmetry exists. For this particular study all of the A's are equal to 1. This indicates each element has the same illumination of normalized value 1. Other studies may be interpreted in a similar way. Occasional reference to subsection 2.1 will help.

It is interesting to contrast Studies A-1 through A-7, all having uniform spacing, with Studies A-8 and A-9, which have non-uniform spacings. The latter two studies each show a substantial second lobe for the scanned position of 60^{o} from broadside of the main beam. For Study A-8 the large secondary lobe is about 70^{o} from broadside (130^{o} from main lobe). For Study A-9 the large secondary lobe is 60^{o} from broadside (120^{o} from main lobe). These large secondary lobes are not strictly grating lobes since they are not as large as the main lobes. However, these secondary lobes have their origin in the increased spacing (above 0.5λ) of some elements, in particular, elements near the ends of the two arrays involved. Since all elements do not have the necessary excessive spacing a full size grating

lobe does not occur in Studies A-8 and A-9. Note in Study A-8 the element spacing at the extreme end of the array is 0.622λ whereas the spacing at the center of the array is 0.5λ.

2.6 Studies on Variation of Tapered Illumination

In these B-series studies shown in Figs. 14 to 29 inclusively, the spacing was uniform for all studies. For some of the studies arrays of 150 elements were used and in others 250 elements were used. The illumination in each case is controlled by the parameters CA 1. the use of this parameter is described in subsection 2.1. Smaller values of the parameter CA 1 correspond to greater amounts of tapering. The direct computer plots on these studies have been made on a rectangular coordinate basis. Please notice that here the vertical scale corresponds to dB power. The horizontal scale is a degree scale. The overall extent of the horizontal scale is 180^{o}, which corresponds to 18^{o} markings on the scale. The computer program provides for an expanded horizontal scale wherever necessary. It is possible to call for this expanded scale and this has been done in some studies. This expanded scale is extremely useful for determining the beamwidth and also to show further detail on the sidelobe structure. It is to be noticed that in the data on the 150-element arrays the beamwidth of the main beam is very small, being of the order of 1^{o}. The beamwidth of the main beam is even smaller on the 250-element studies, as can easily be observed. It is to be noted that with 250 elements improved performance can be observed. For instance, in Study B-12, using 250 elements and with considerable illumination taper, it is found that a significant directivity has been achieved. Unfortunately, a printout of the beamwidth for the rectangular plots was not requested; this request could have been made as in the polar plots of the A series. Reading the beamwidth from the rectangular plot would enable the directivity to be computed approximately although such a reading is not at all precise. The main beam can be measured more accurately on an expanded scale as is shown in a later figure which indicates that it is about 1^{o}. Note that the sidelobe structure is such

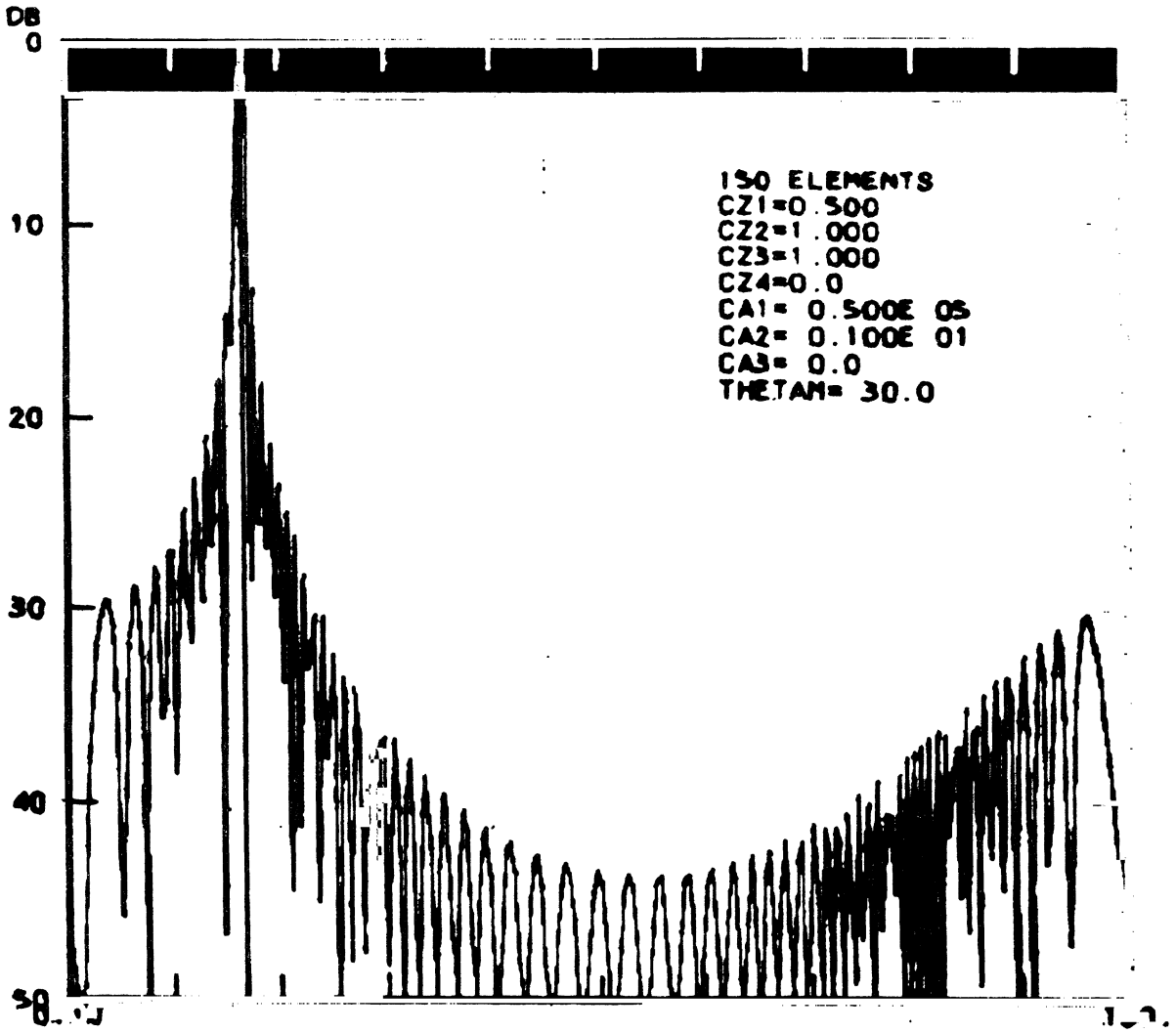

Fig. 14: Study B-1. 150 Elements with Uniform Spacing of 0.500λ. Taper Factor CA 1 = 0.500×10^5. Each Abscissa Scale Unit is 18^0.

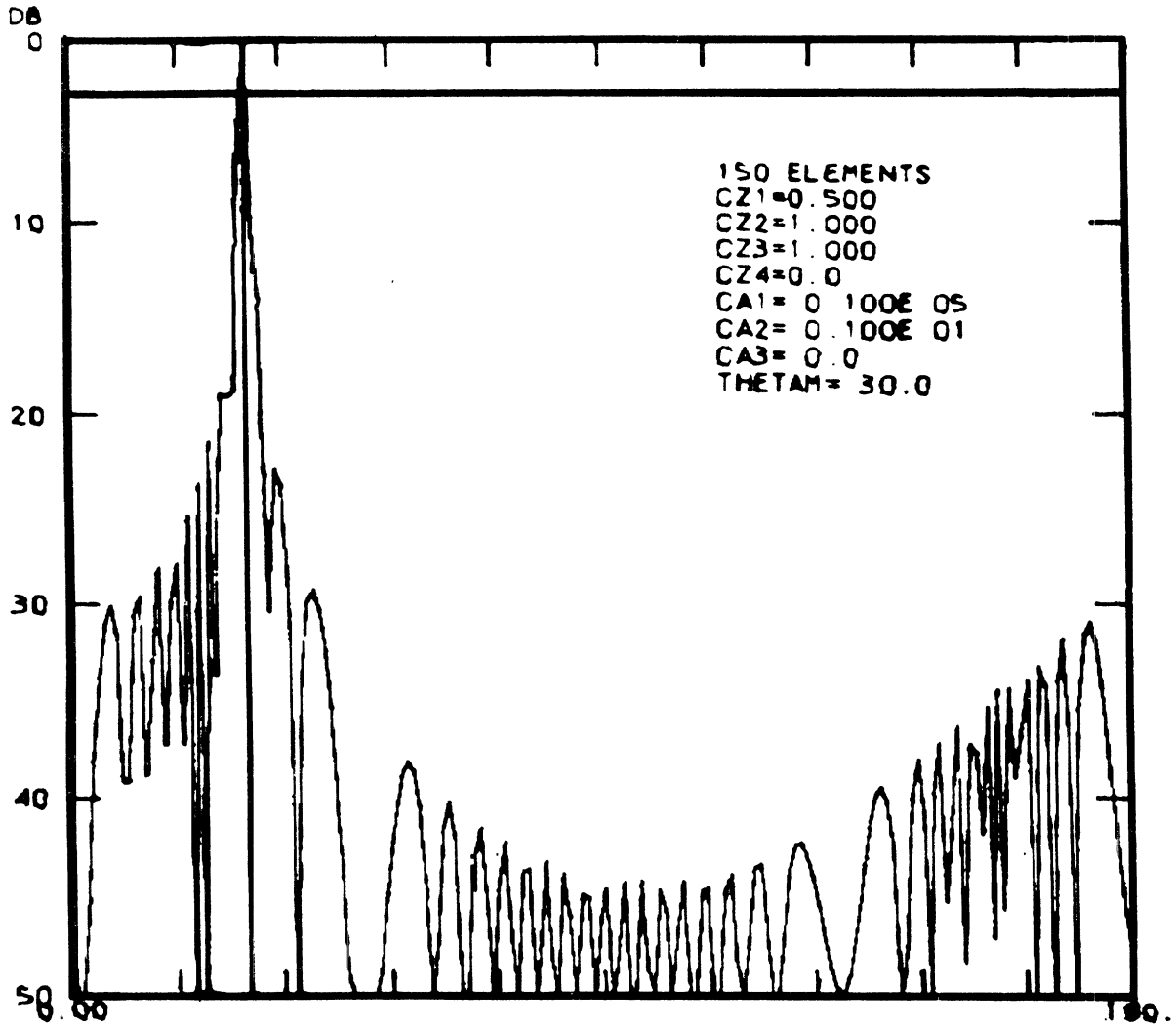

Fig. 15 Study B-2. 150 Elements with Uniform Spacing of 0.500λ. Taper Factor CA 1 = 0.100×10^5. Each Abscissa Scale Unit is 18°.

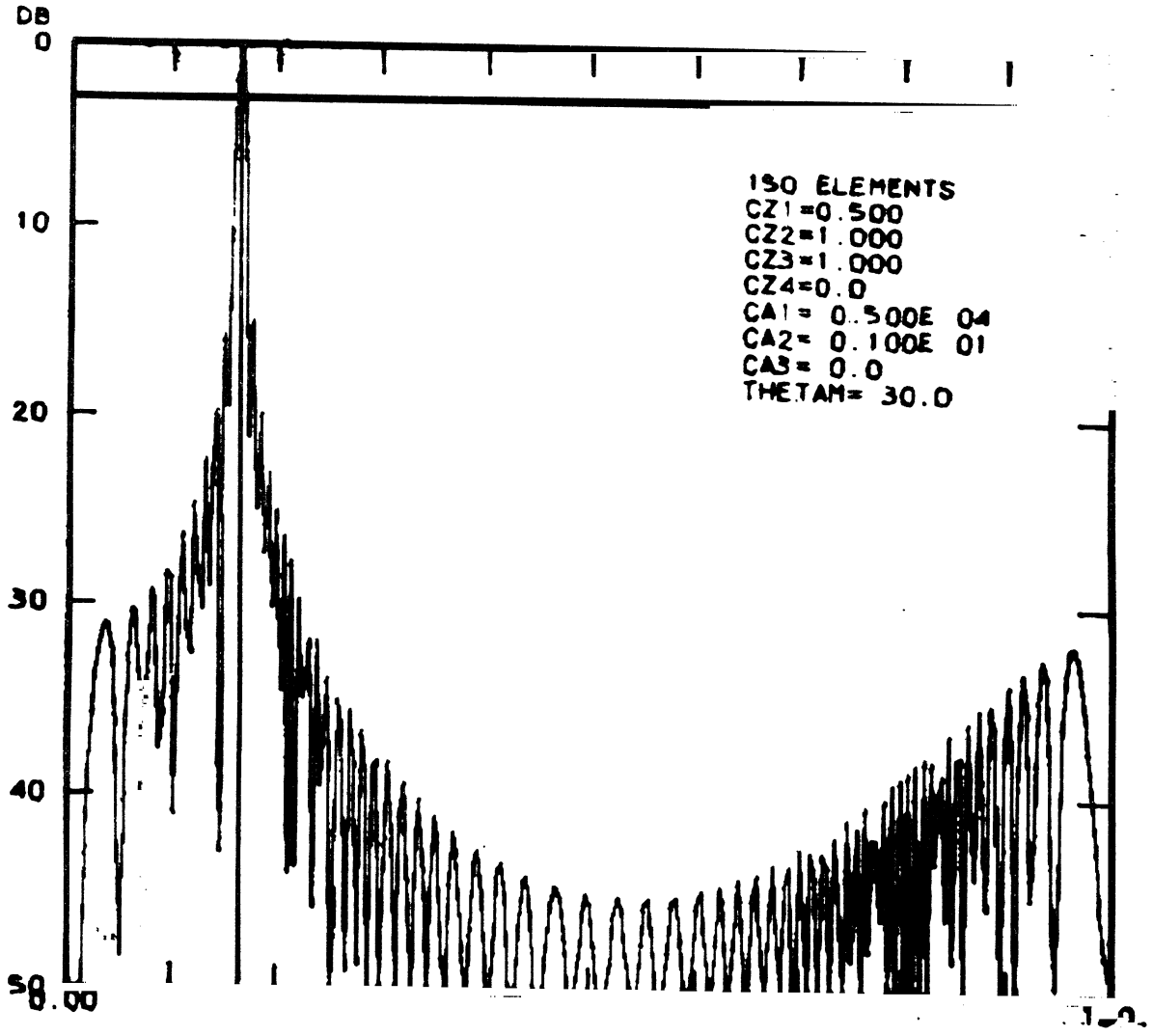

Fig. 16: Study B-3. 150 Elements with Uniform Spacing of 0.500λ. Taper Factor CA 1 = 0.500×10^4. Each Abscissa Scale Unit is 18^o.

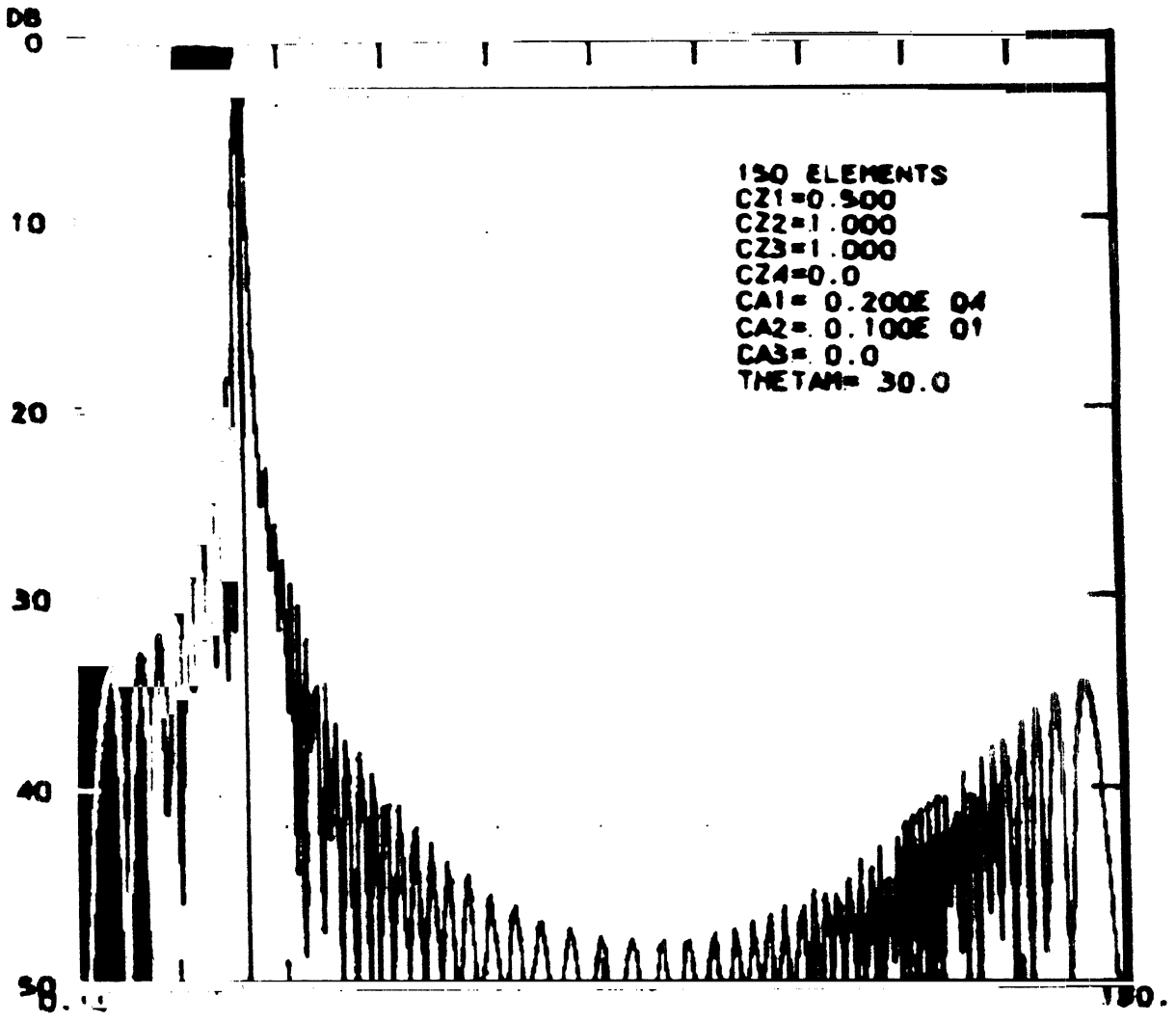

Fig. 17: Study B-4. 150 Elements with Uniform Spacing of 0.5 λ. Taper Factor CA 1 = 0.200×10^4. Each Abscissa Scale Unit is 18^o.

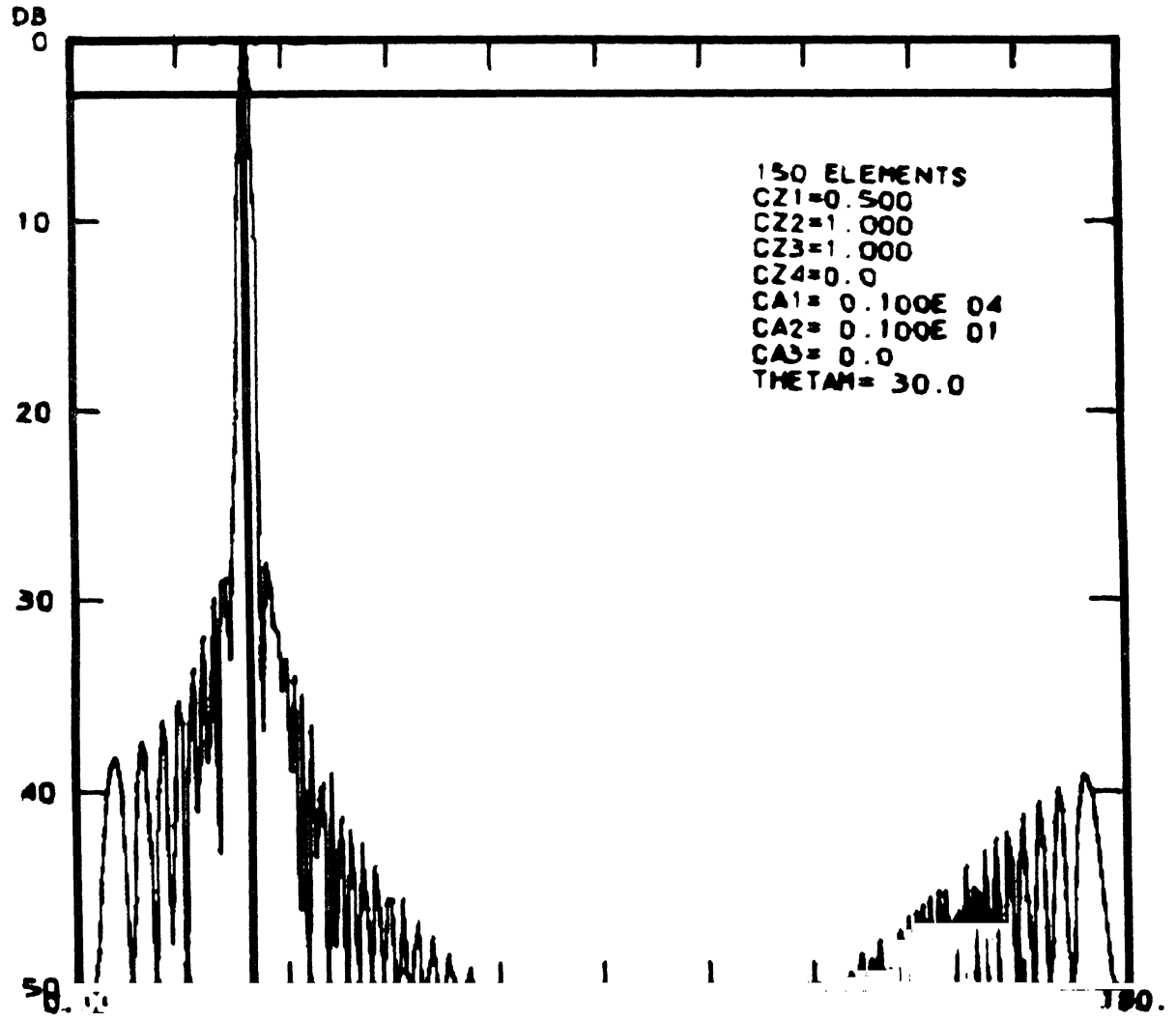

Fig. 18: Study B-5. 150 Elements with Uniform Spacing of 0.500λ. Taper Factor CA 1 = 0.100×10^4. Each Abscissa Scale Unit is 18^o.

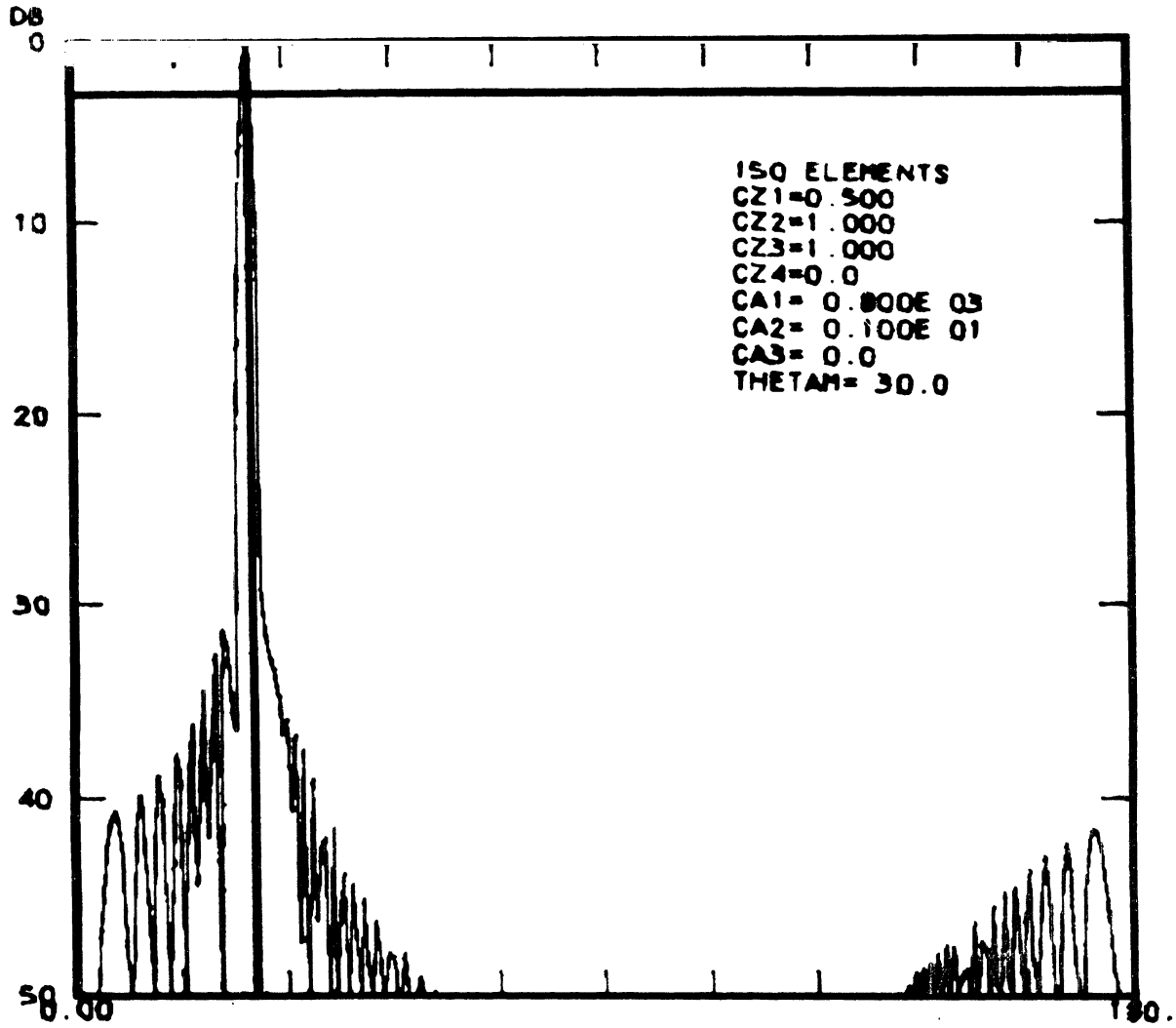

Fig. 19: Study B-6. 150 Elements with Uniform Spacing of 0.500λ Taper Factor CA1 = 0.800×10^3. Each Abscissa Scale Unit is 18°.

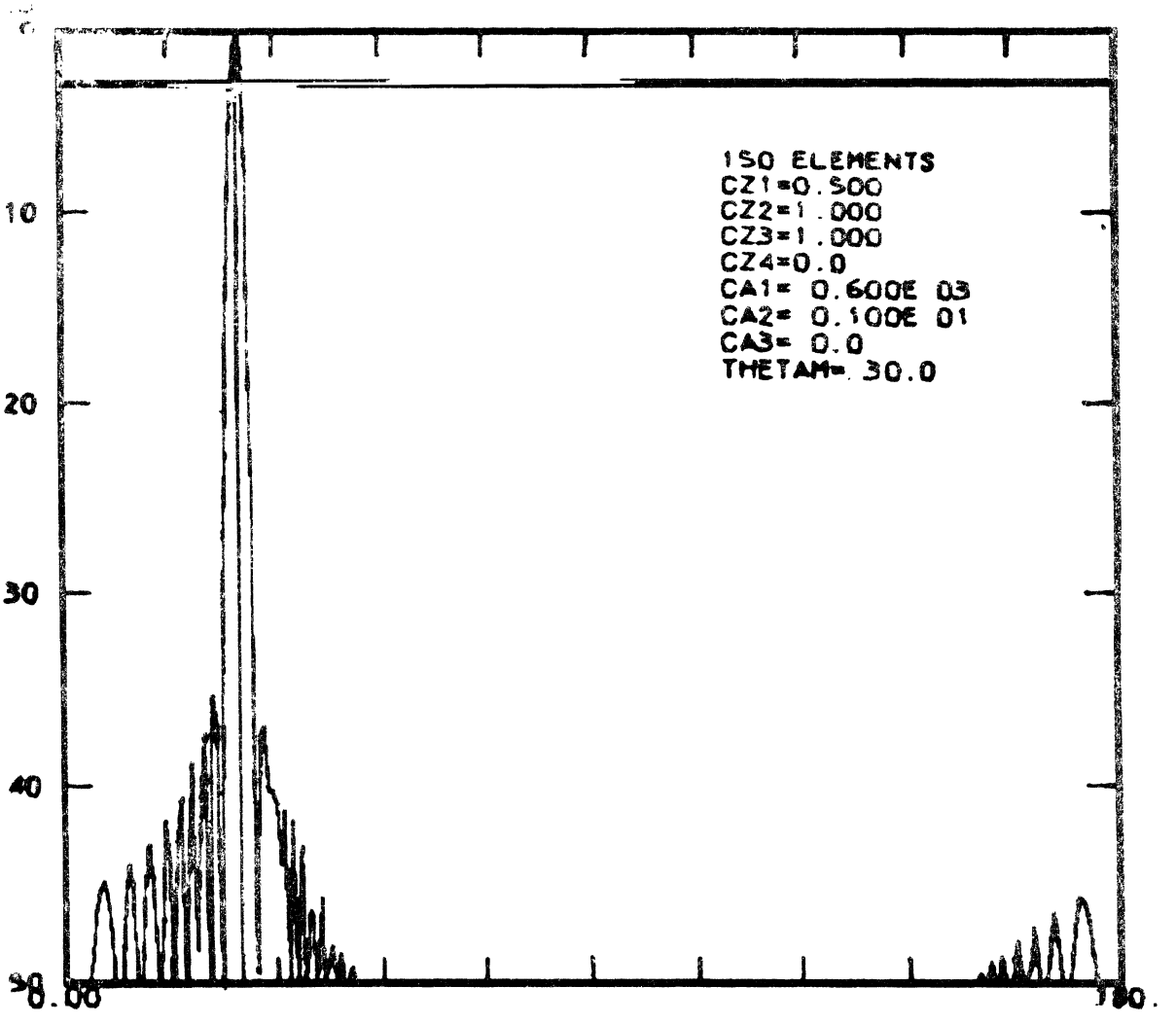

Fig. 20: Study B-7. 150 Elements with Uniform Spacing of 0.500λ Taper Factor CA1 $= 0.600 \times 10^3$. Each Abscissa Scale Unit is 18°.

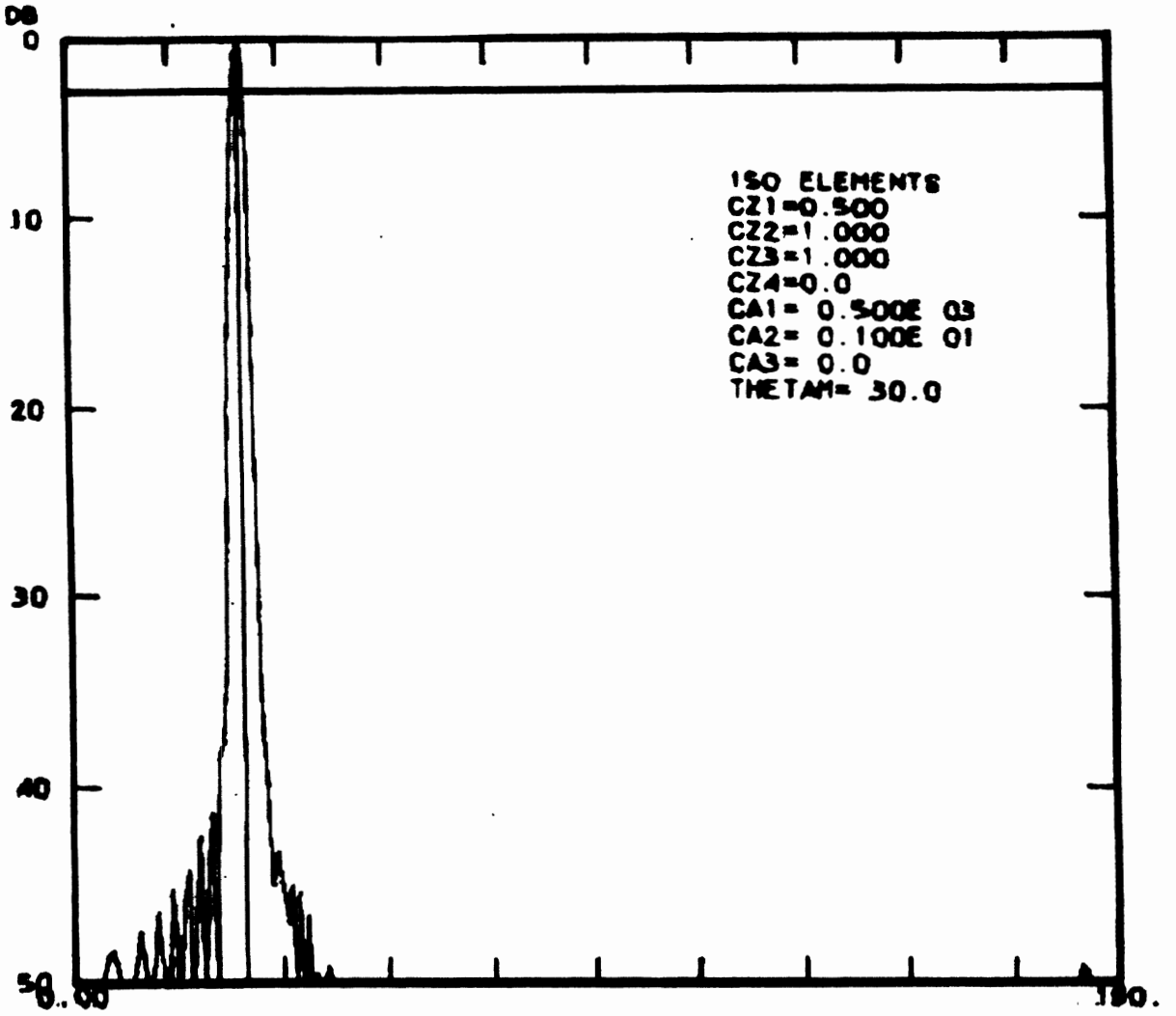

Fig. 21: Study B-8. 150 Elements with Uniform Spacing of 0.500λ. Taper Factor CA 1 = 0.500×10^3. Each Abscissa Scale Unit is 18°.

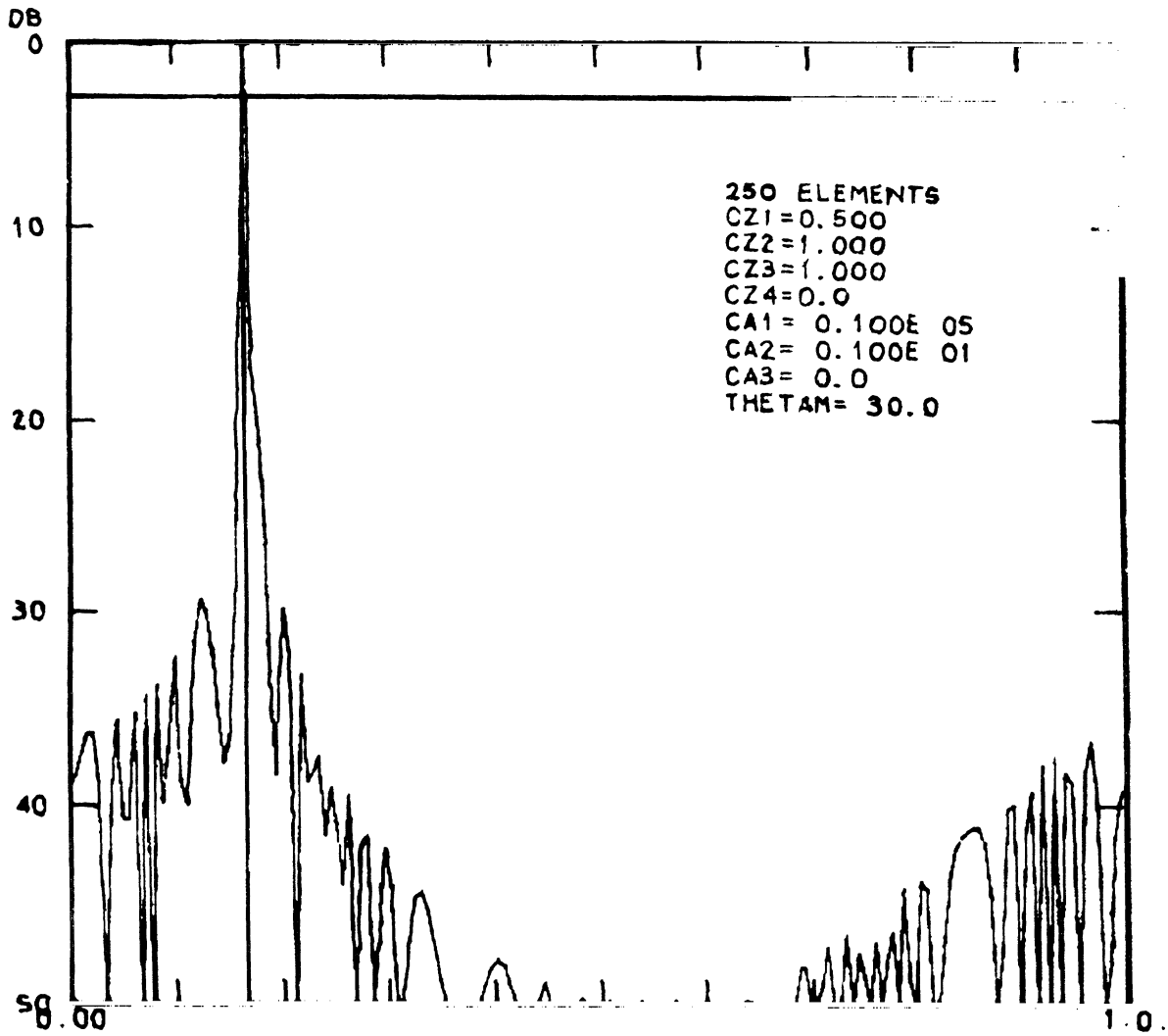

Fig. 22: Study B-9. 250 Elements with Uniform Spacing of 0.500λ. Taper Factor $CA = 0.100 \times 10^5$. Each Abscissa Scale Unit is 18^o.

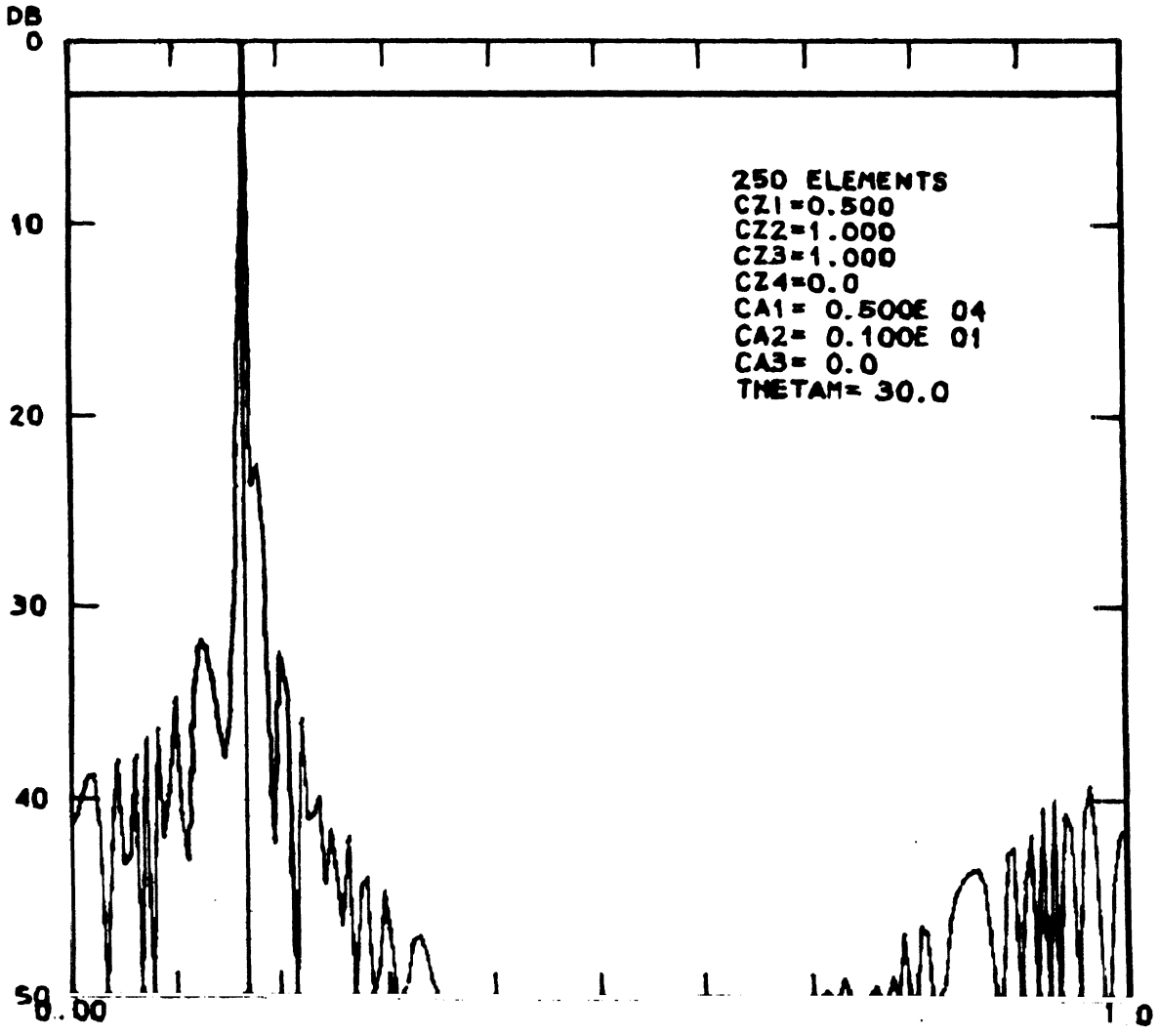

Fig. 23: Study B-10. 250 Elements with Uniform Spacing of 0.500λ. Taper Factor CA $1 = 0.500 \times 10^4$. Each Abscissa Scale Unit is 18^o.

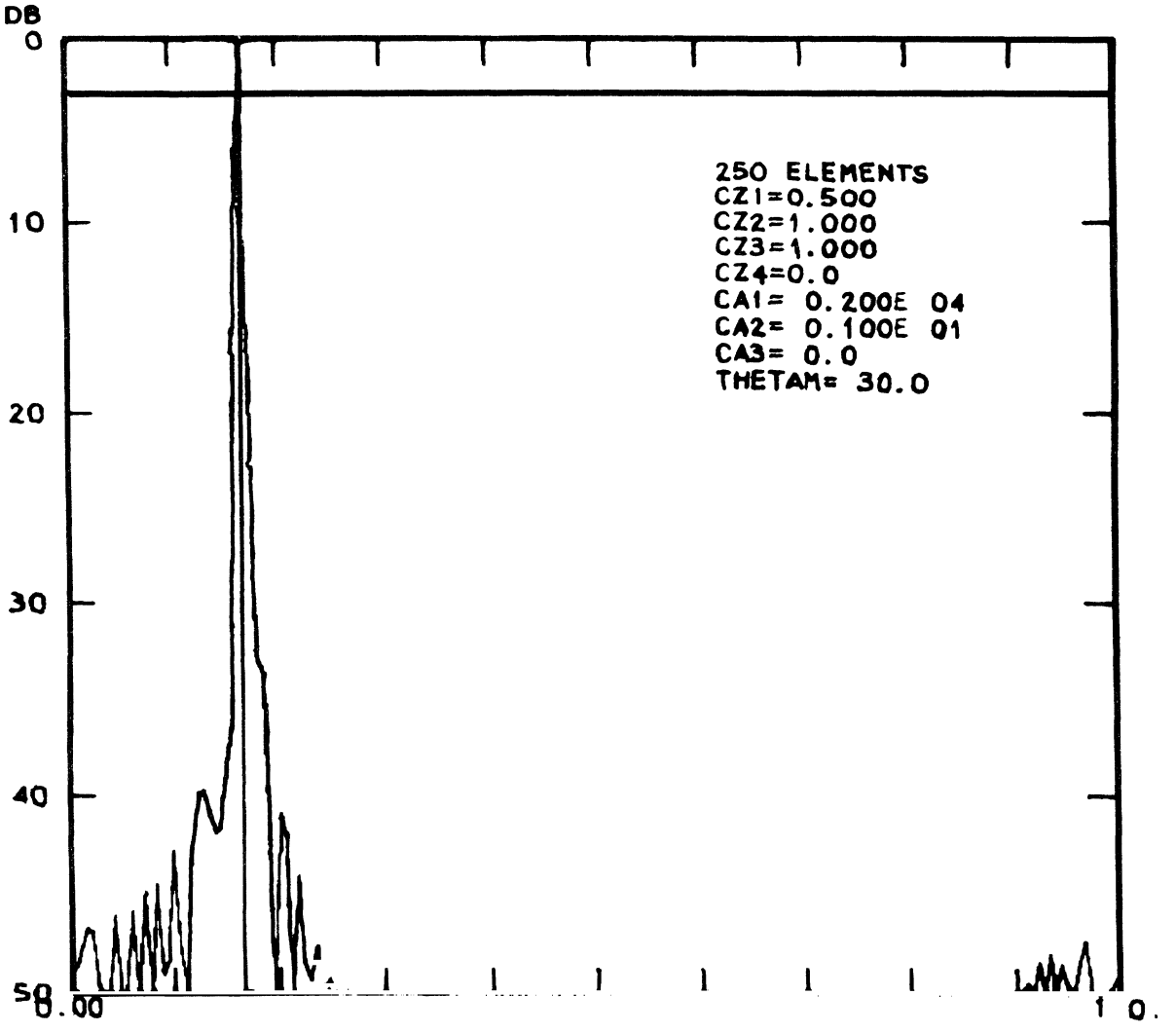

Fig. 24: Study B-11. 250 Elements with Uniform Spacing of 0.500λ. Taper Factor CA 1 = 0.200×10^4. Each Abscissa Scale Unit is 18°.

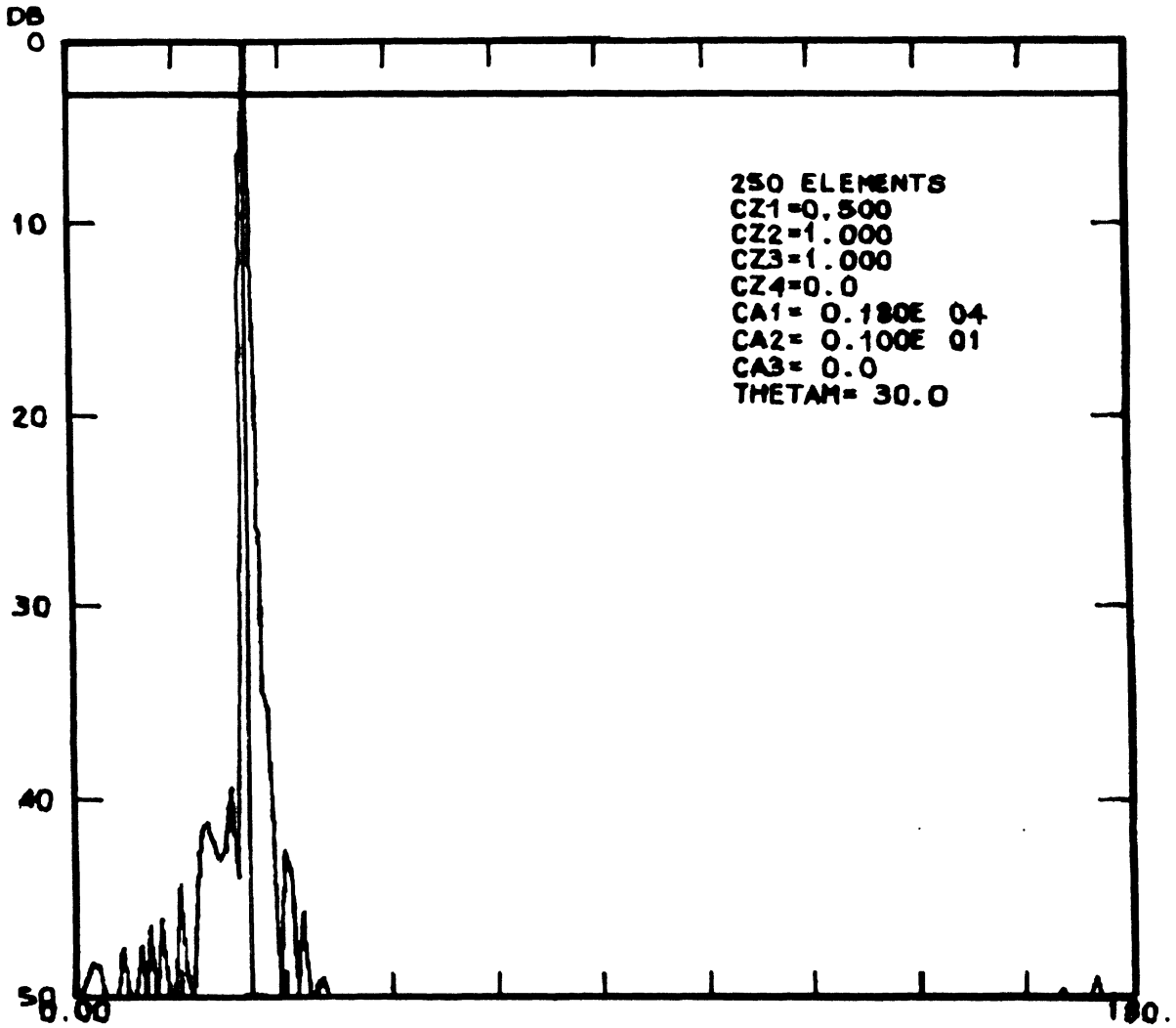

Fig. 25: Study B-12. 250 Elements with Uniform Spacing of 0.500λ. Taper Factor CA 1 = 0.180×10^4. Each Abscissa Scale Unit is 18^o.

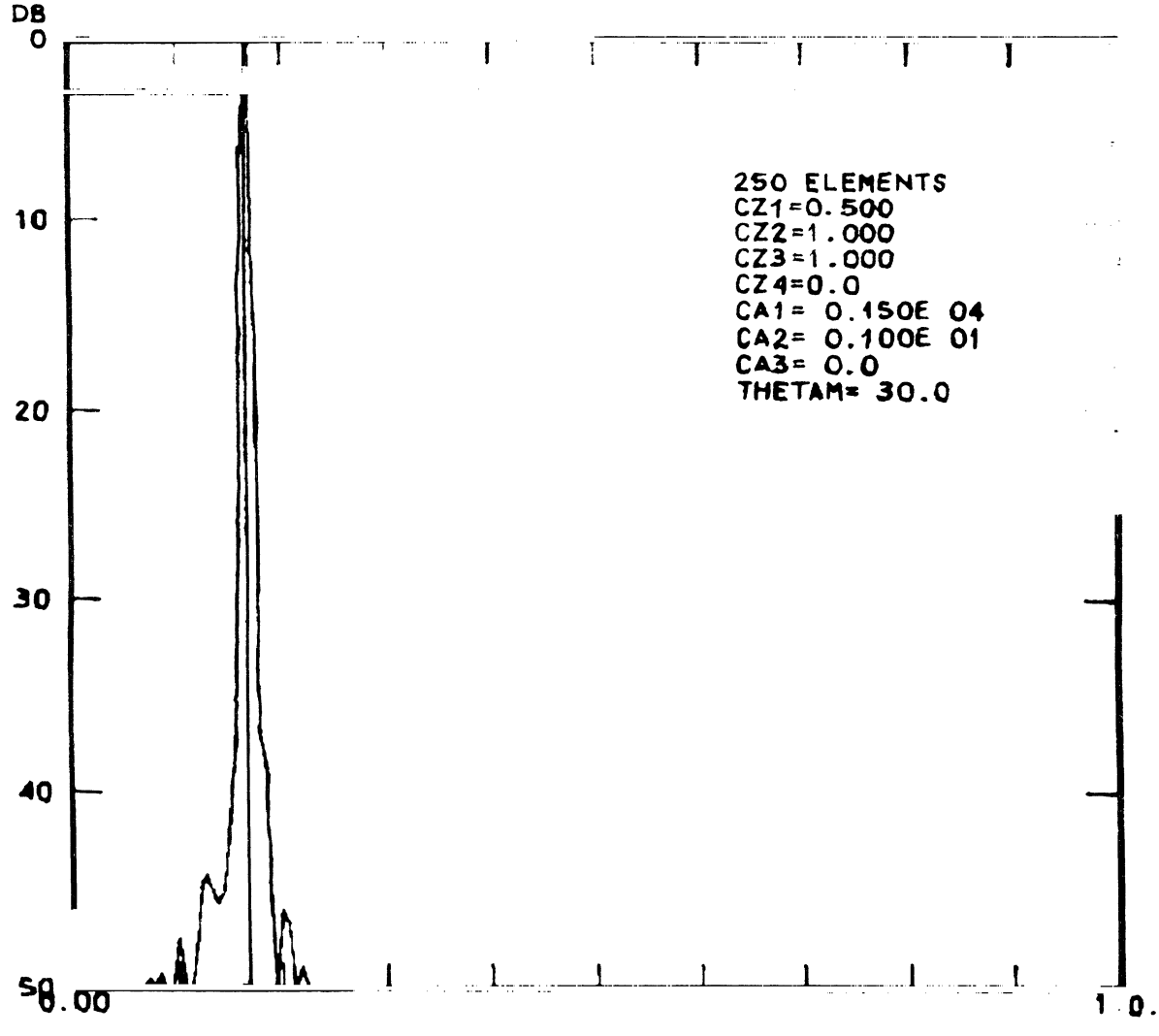

Fig. 26: Study B-13. 250 Elements with Uniform Spacing of 0.500λ. Taper Factor CA $1 = 0.150 \times 10^4$. Each Abscissa Scale Unit is 18°.

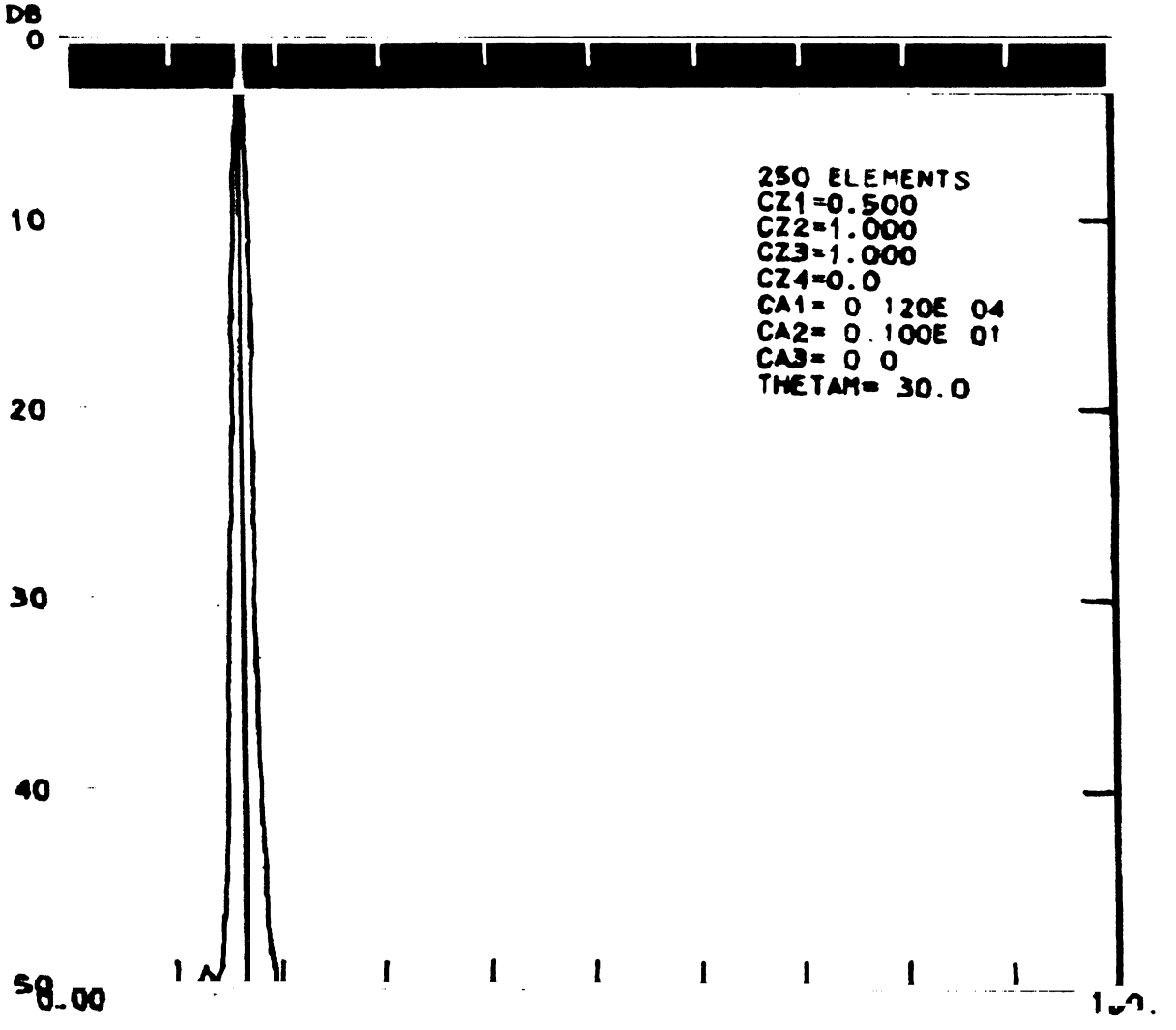

Fig. 27: Study B-14. 250 Elements with Uniform Spacing of 0.500λ. Taper Factor CA 1 = 0.120×10^4. Each Abscissa Scale Unit is 18^o.

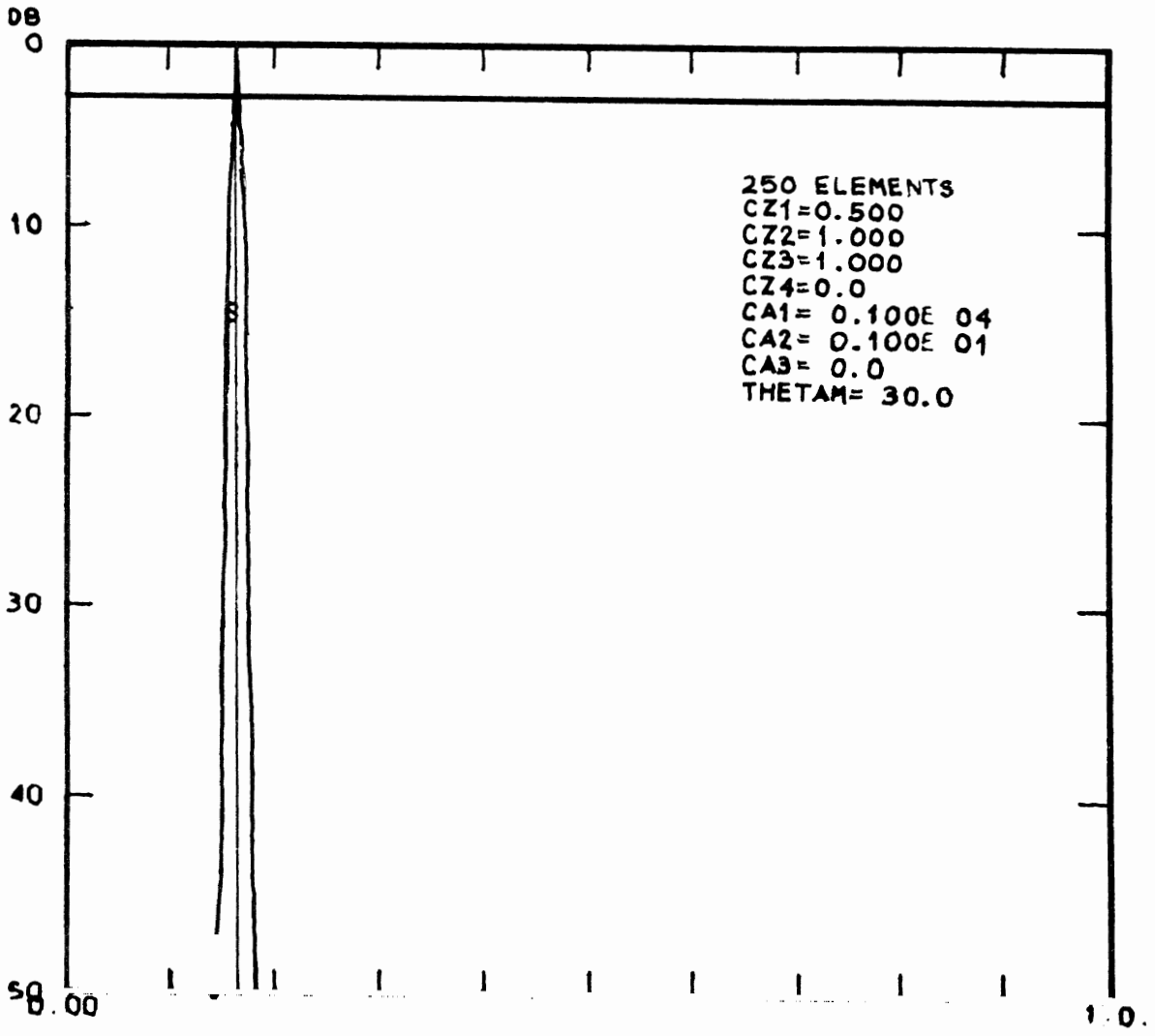

Fig. 28: Study B-15. 250 Elements with Uniform Spacing of 0.500λ. Taper Factor CA 1 = 0.100×10^4. Each Abscissa Scale Unit is 18^o.

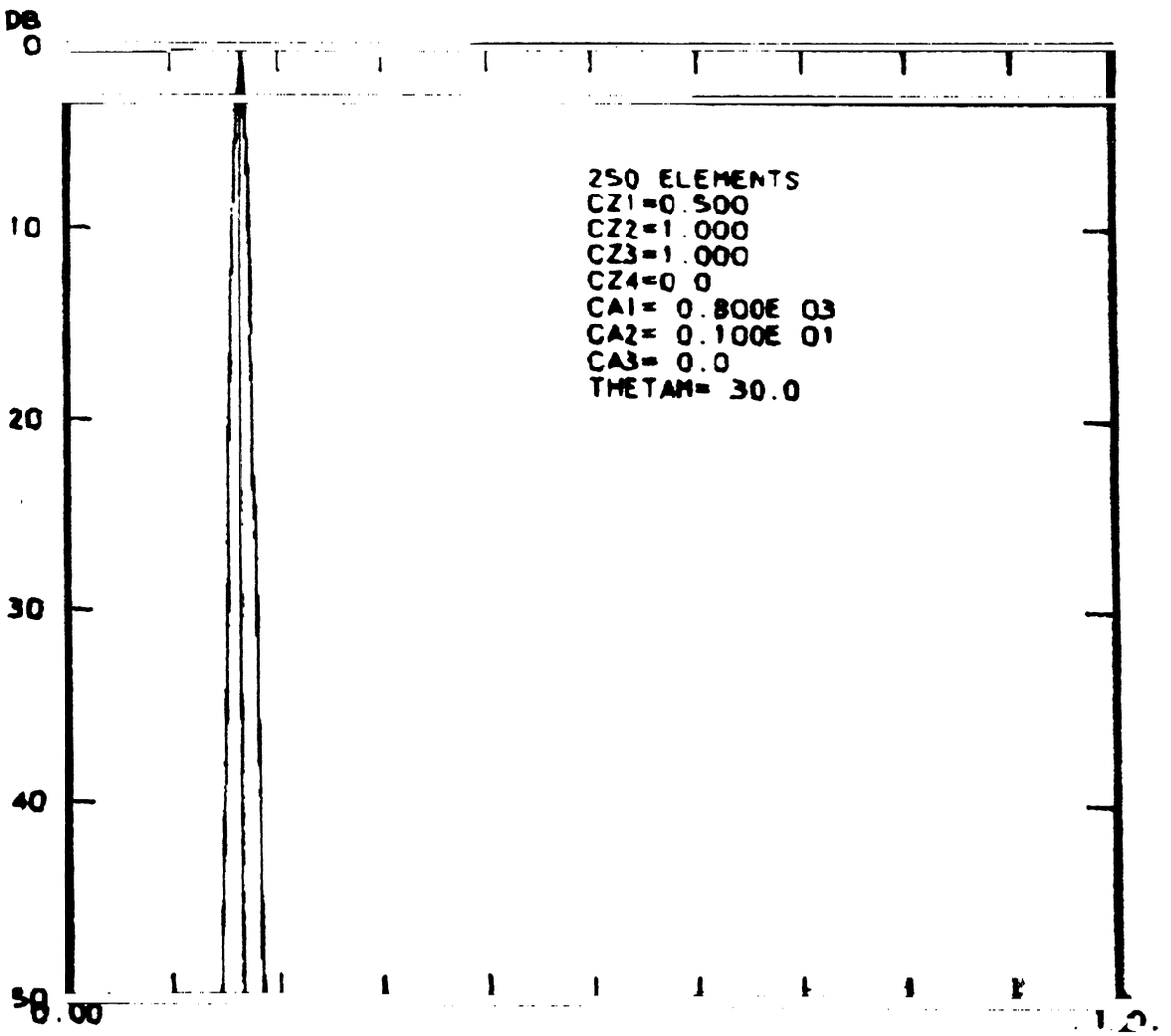

Fig. 29: Study B-16. 250 Elements with Uniform Spacing of 0.500λ. Taper Factor CA $1 = 0.800 \times 10^3$. Each Abscissa Scale Unit is 18^o.

that all lobes are below 40 dB as compared with the main beam.

Please note in the studies relating to graded illumination of elements that all of the studies were made for a scan angle corresponding to 60^{o} from the broadside position or as noted on the individual figures corresponding to an angle of 30^{o} as measured from the plane of the array. In commenting on the observed results it should be pointed out that the great reduction of sidelobe level which occurs with the cases showing a steep gradation of illumination is strictly in accordance with what would be anticipated from analysis. Analysis of this type of dependence of sidelobe structure has been made in the literature. Just as a square pulse needs high frequency components in order to be synthesized, so a square distribution of illumination (uniform distribution of illumination of elements) corresponds to the occurence of many sidelobes with substantial level of such sidelobes. Thus we see a distinct advantage for large amounts of taper. However, large amounts of taper also pose problems which must yet be considered. In an actual antenna array a large amount of taper is difficult to maintain accurately because of mutual coupling effects. Loss in efficiency also occurs with a high degree of taper in the illumination.

2.7 Studies Illustrating the Grating Lobe

All of the C-series of studies, shown in Figs. 30 to 35 inclusively, were made with arrays of 250 elements. Some of the studies were made with 0.6λ uniform spacing. In others of the studies, a uniform spacing of 0.75λ was used. Please notice that both of these spacings exceed the 0.5λ spacing which is commonly used for many arrays. Grating lobes are possible only when the uniform spacing exceeds 0.5λ. Actually the onset of grating lobes depends on the scan angle (see equation (1.1)). For a scan angle of $\pm 60^{o}$ no grating lobes occur for uniform spacing less than 0.53λ; for a scan of $\pm 45^{o}$ no grating lobes occur for spacing less than 0.59λ. The various amounts of illumination taper were used in these studies. It is to be observed that illumination taper does not provide a means for eliminating grating lobes. On the other hand, for arrays

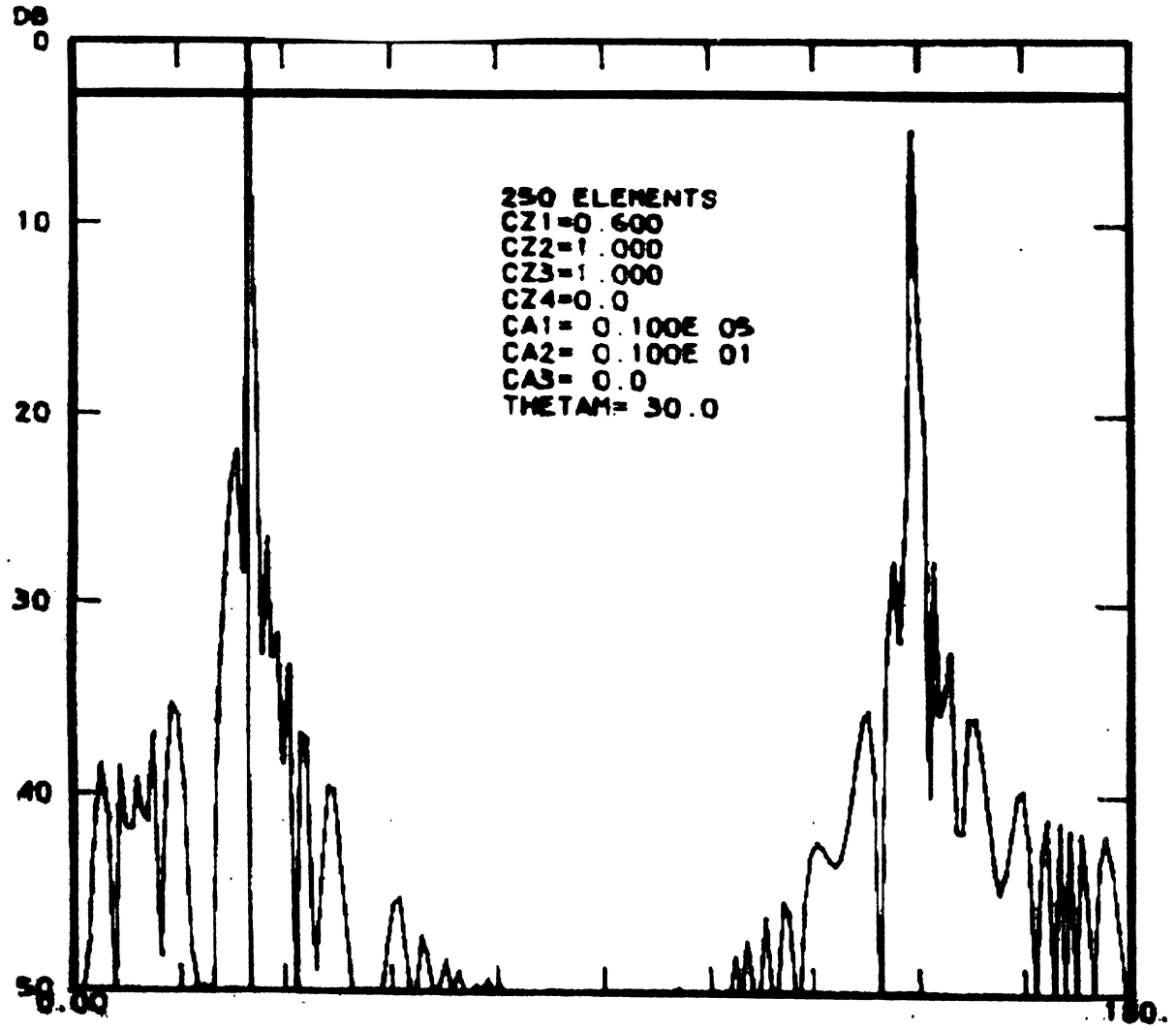

Fig. 30: Study C-1 on Grating Lobes. 250 Elements with Uniform Spacing of 0.600λ. Taper Factor CA 1 = 0.100×10^5. Each Abscissa Scale Unit is 18^o.

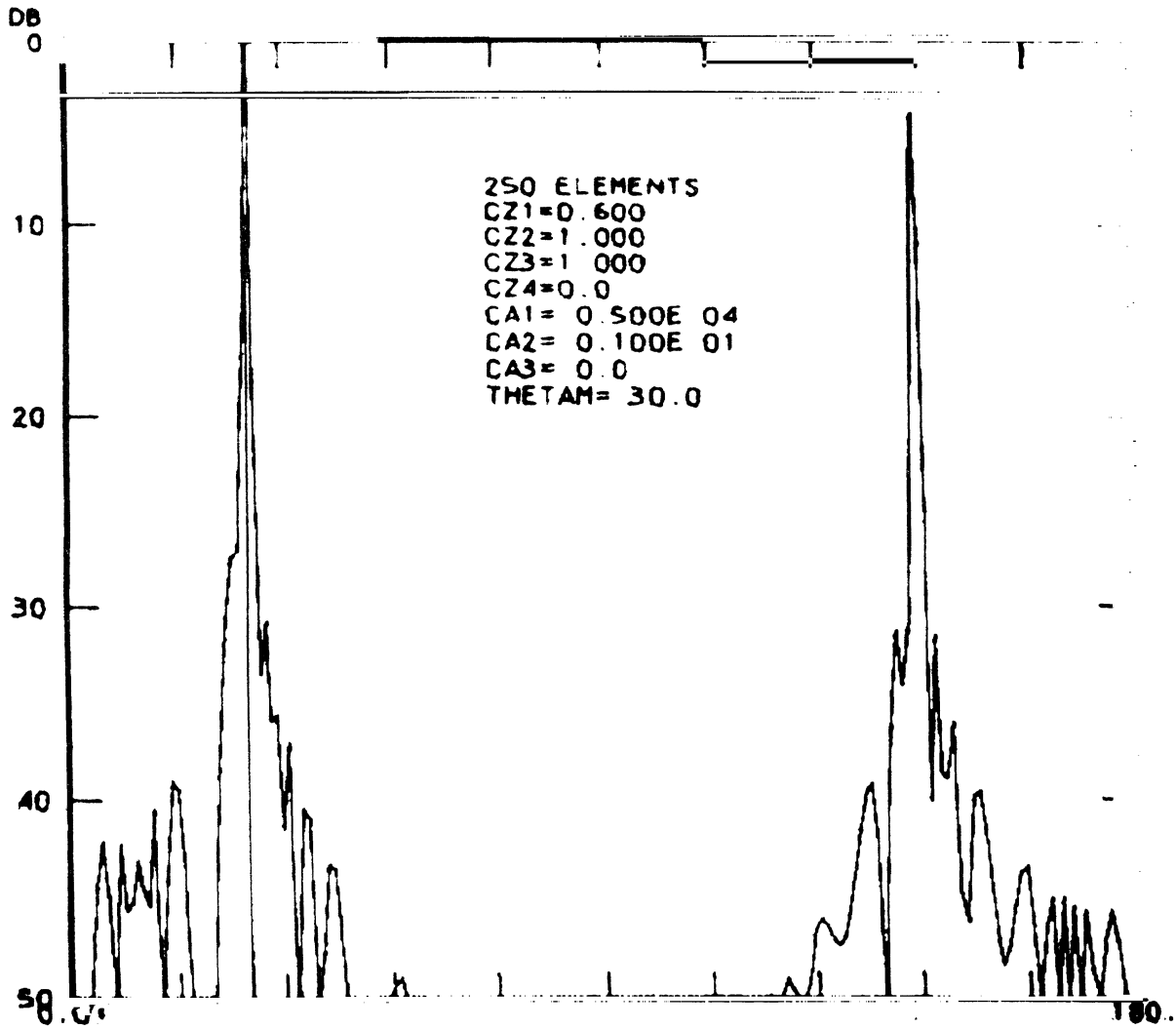

Fig. 31: Study C-2 on Grating Lobes. 250 Elements with Uniform Spacing of 0.600λ. Taper Factor CA 1 = 0.500×10^4. Each Abscissa Scale Unit is 18^{o}.

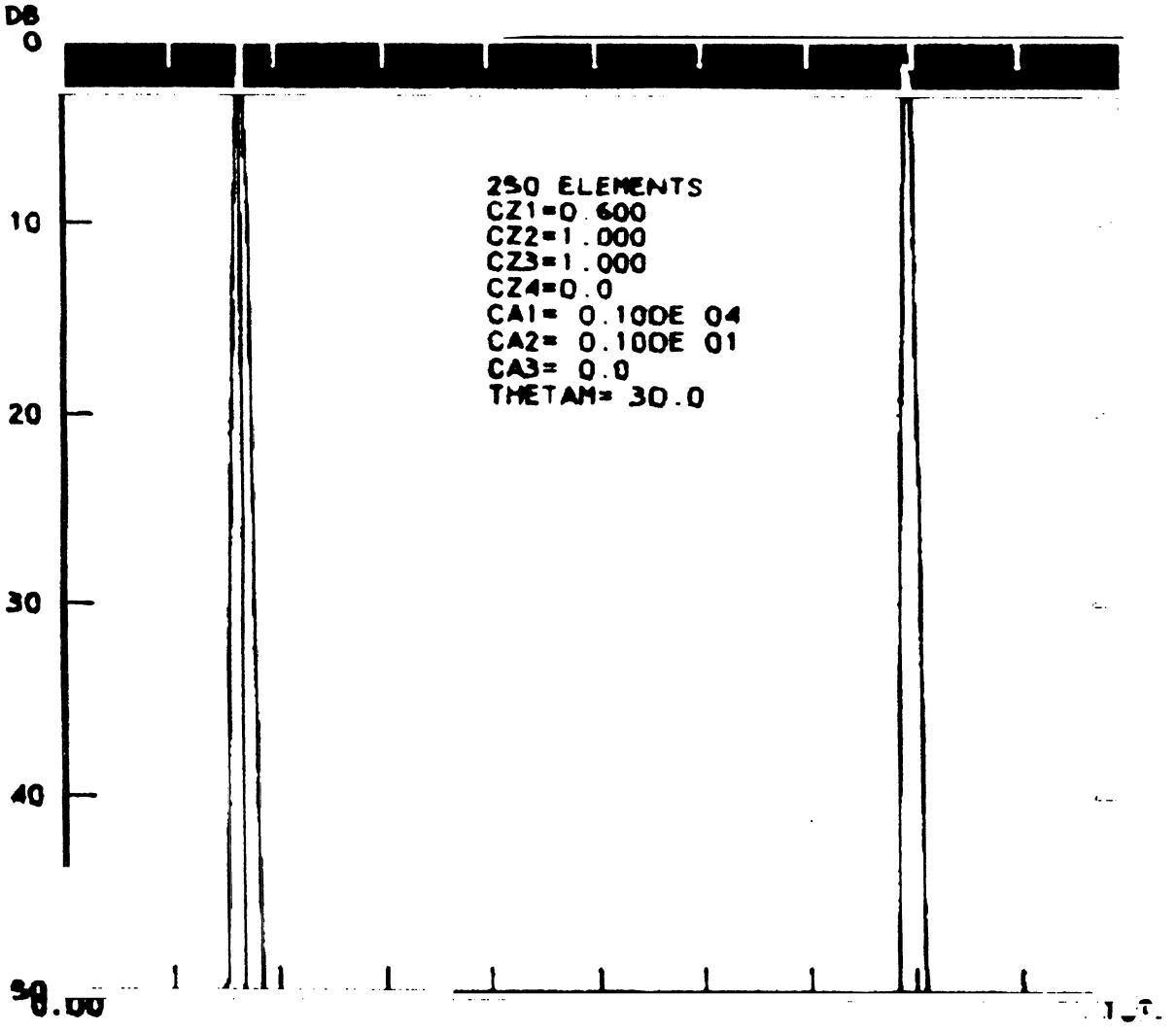

Fig. 32: Study C-3 on Grating Lobes. 250 Elements with Uniform Spacing of 0.600λ. Taper Factor CA 1 = 0.100×10^4. Each Abscissa Scale Unit is 18^o.

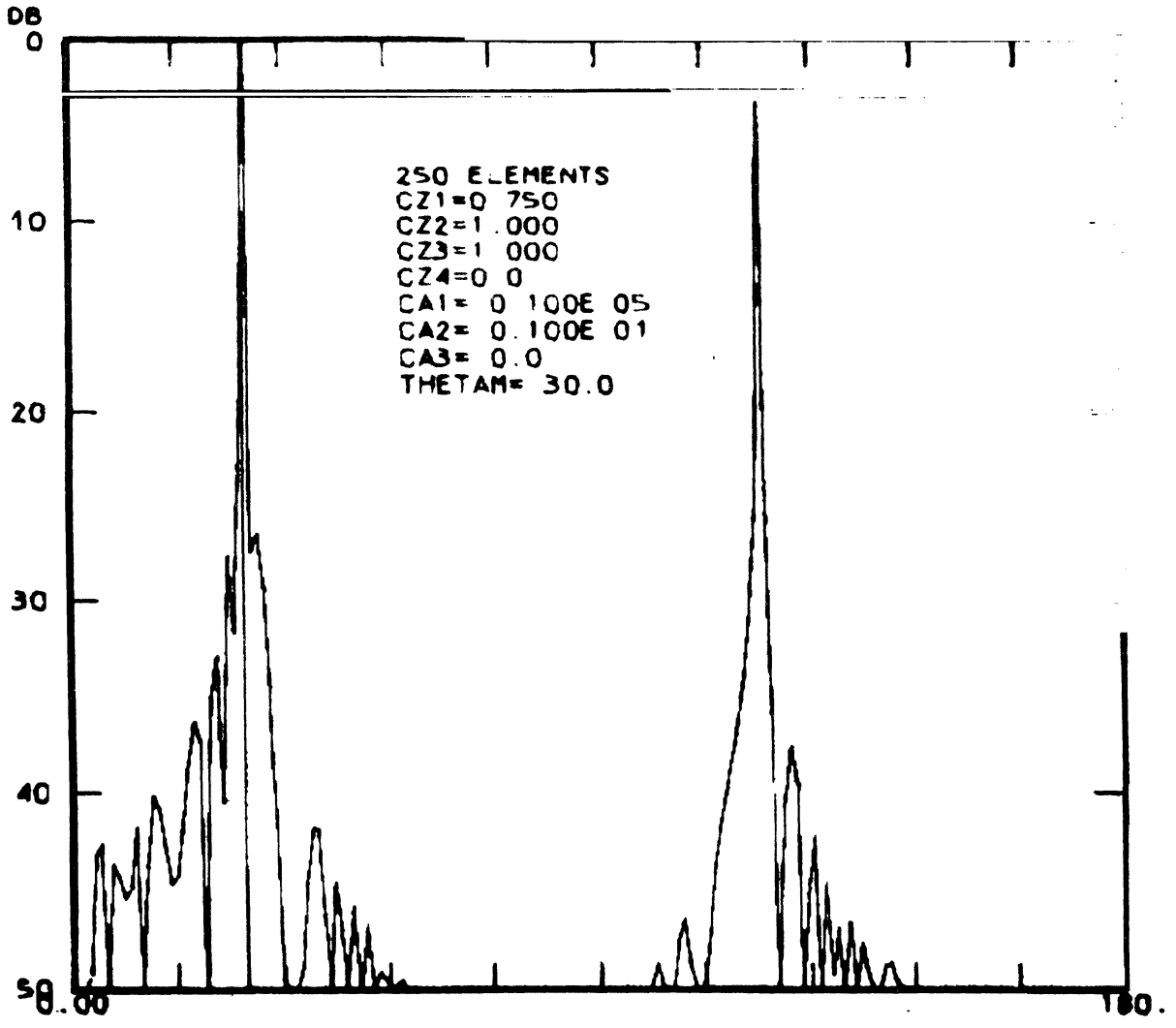

Fig. 33: Study C-4 on Grating Lobes. 250 Elements with Uniform Spacing of 0.750λ. Taper Factor CA = 0.100×10^5. Each Abscissa Scale Unit is 18°.

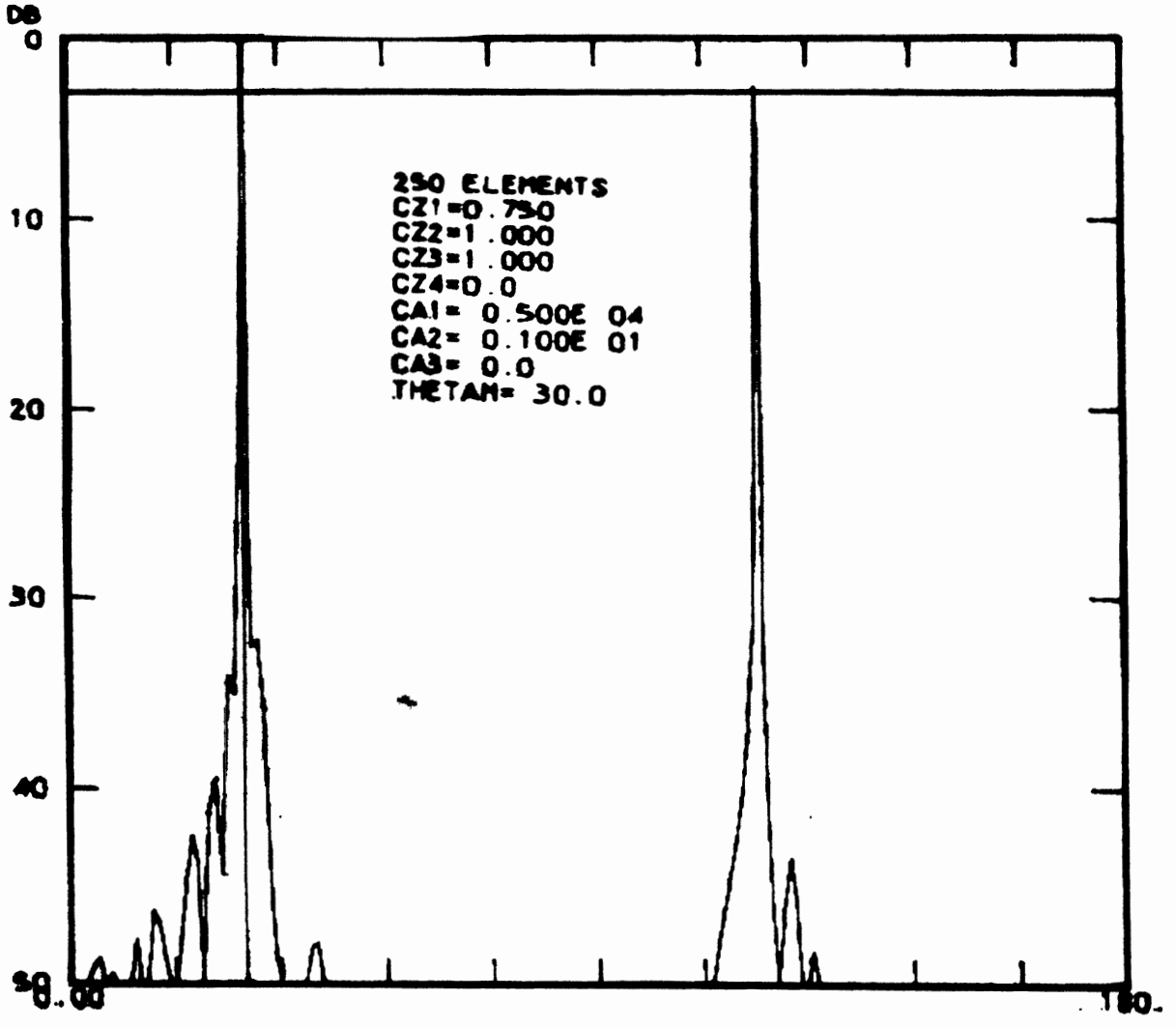

Fig. 34: Study C-5 on Grating Lobes. 250 Elements with Uniform Spacing of 0.750λ. Taper Factor CA 1 = 0.500×10^4. Each Abscissa Scale Unit is 18^o.

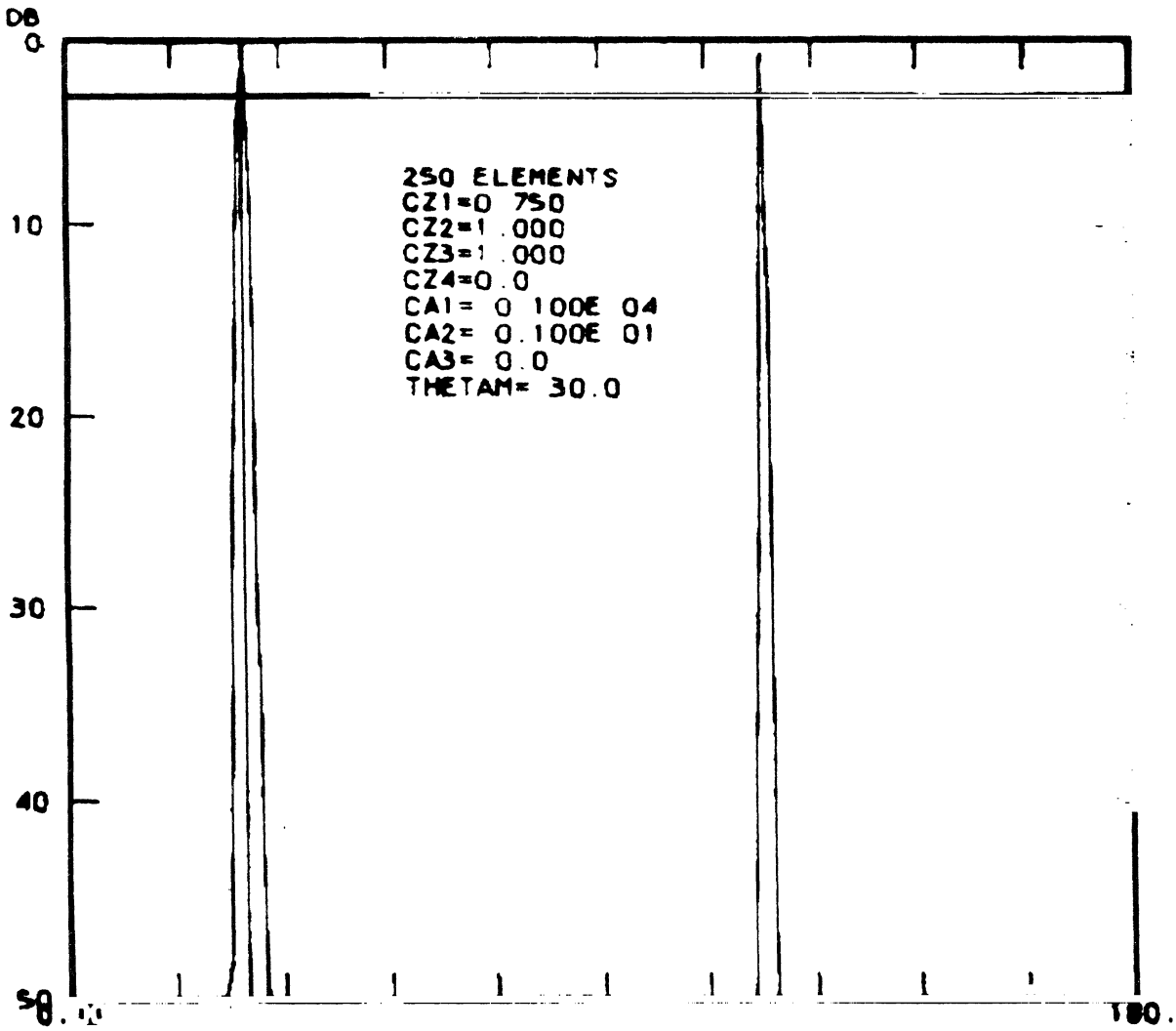

Fig. 35: Study C-6 on Grating Lobes. 250 Elements with Uniform Spacing of 0.750λ. Taper Factor CA 1 = 0.100×10^4. Each Abscissa Scale Unit is 18^o.

which have unequal spacings of elements it is possible to have some spacings exceed the critical values mentioned without running into the presence of grating lobes or large secondary lobes. It should be mentioned that a grating lobe is a second main lobe in the visible region. Strictly speaking, grating lobes do not occur for arrays with non-uniform spacing. Please note that the grating lobes shown in this series of figures are about the same size as the main lobe. There appears to be some tendency in the cases computed for the grating lobe to increase slightly in magnitude as the amount of illumination taper increases. Studies numbered C-3 and C-6 are cases which illustrate the slight increase in grating lobe level which has been observed as the illumination taper has become relatively large. So far no simple explanation for this situation has been found. Again in this group of studies the computer has provided information for the extreme scan angle position of 60^{o} from broadside. As depicted in a series of illustrations here, the range of angles shown from 0 to 180^{o} is what is considered to comprise the visible region for a linear or planar array.

2.8 Computer Simulations of Tschebyscheff Arrays

The series D patterns show the results obtained from the study of Tschebyscheff illumination on linear arrays; the patterns are shown in Figs. 36 to 42 inclusively. An antenna array having a radiation pattern corresponding to the curve of a Tschebyscheff polynomial is one for which the sidelobes are of uniform height. Also this uniform height corresponds to having the lowest sidelobe level of any possible illumination distribution among the elements of the array. Other illuminations which would result in a different sidelobe structure must have one or more sidelobes higher than the others. The order of the Tschebyscheff polynomial which corresponds to the radiation pattern is related to the number of elements in the array. In the studies on Tschebyscheff array simulation not all of the patterns correspond to true Tschebyscheff curves. The reason for this is that it was found that the illumination taper, in order to provide a true Tschebyscheff pattern, was, of necessity, very steep. This meant that there was an

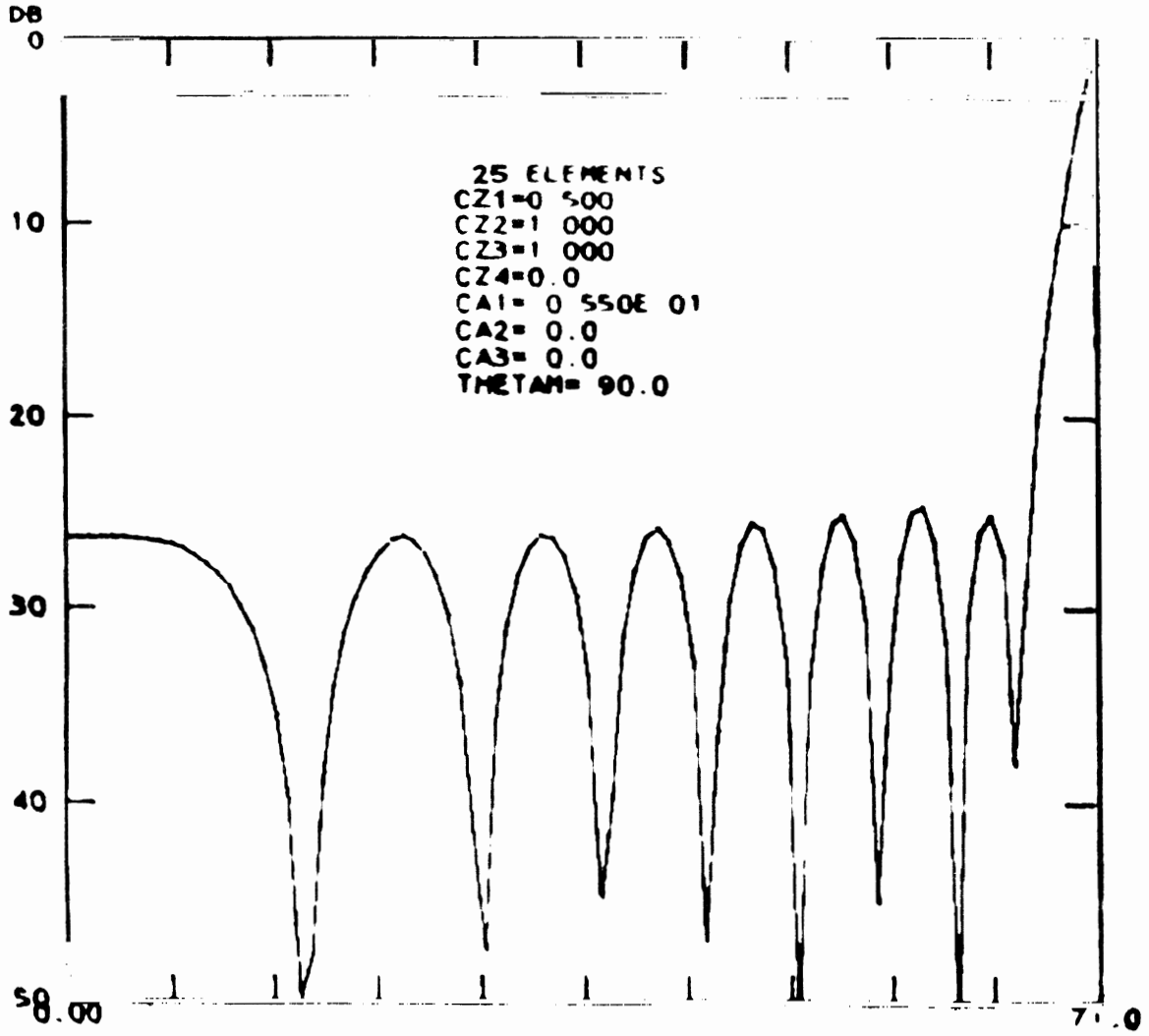

Fig. 36: Study D-1 on Tschebyscheff Simulation. 25 Elements with Uniform Spacing of 0.500λ. Taper Factor CA 1 = 0.550 x 10. Each Abscissa Scale Unit is 7^{o}.

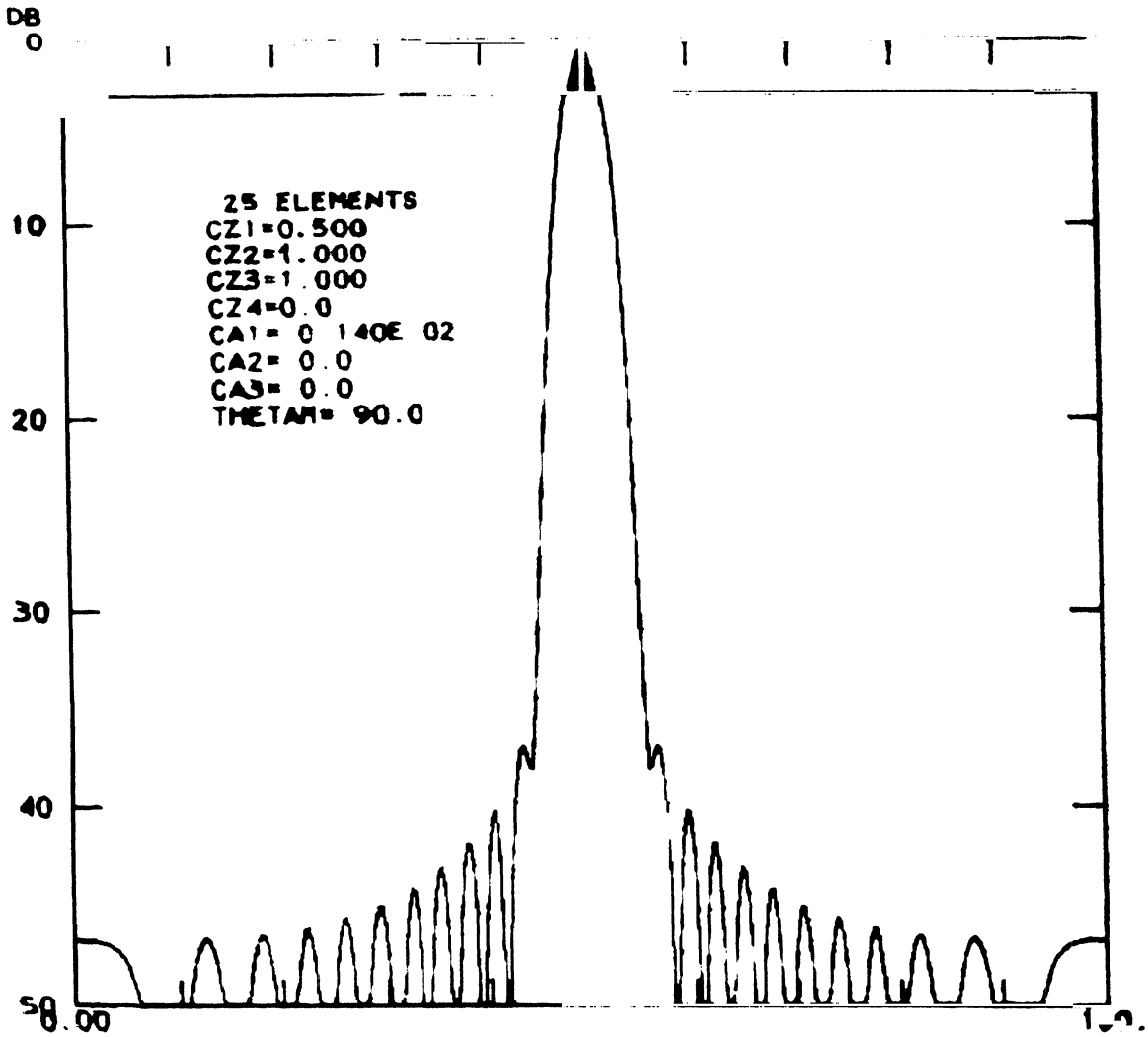

Fig. 37: Study D-2 on Tschebyscheff Simulation. 25 Elements with Uniform Spacing of 0.500λ. Taper Factor CA 1 = 0.140×10^2. Each Abscissa Scale Unit is 18^o.

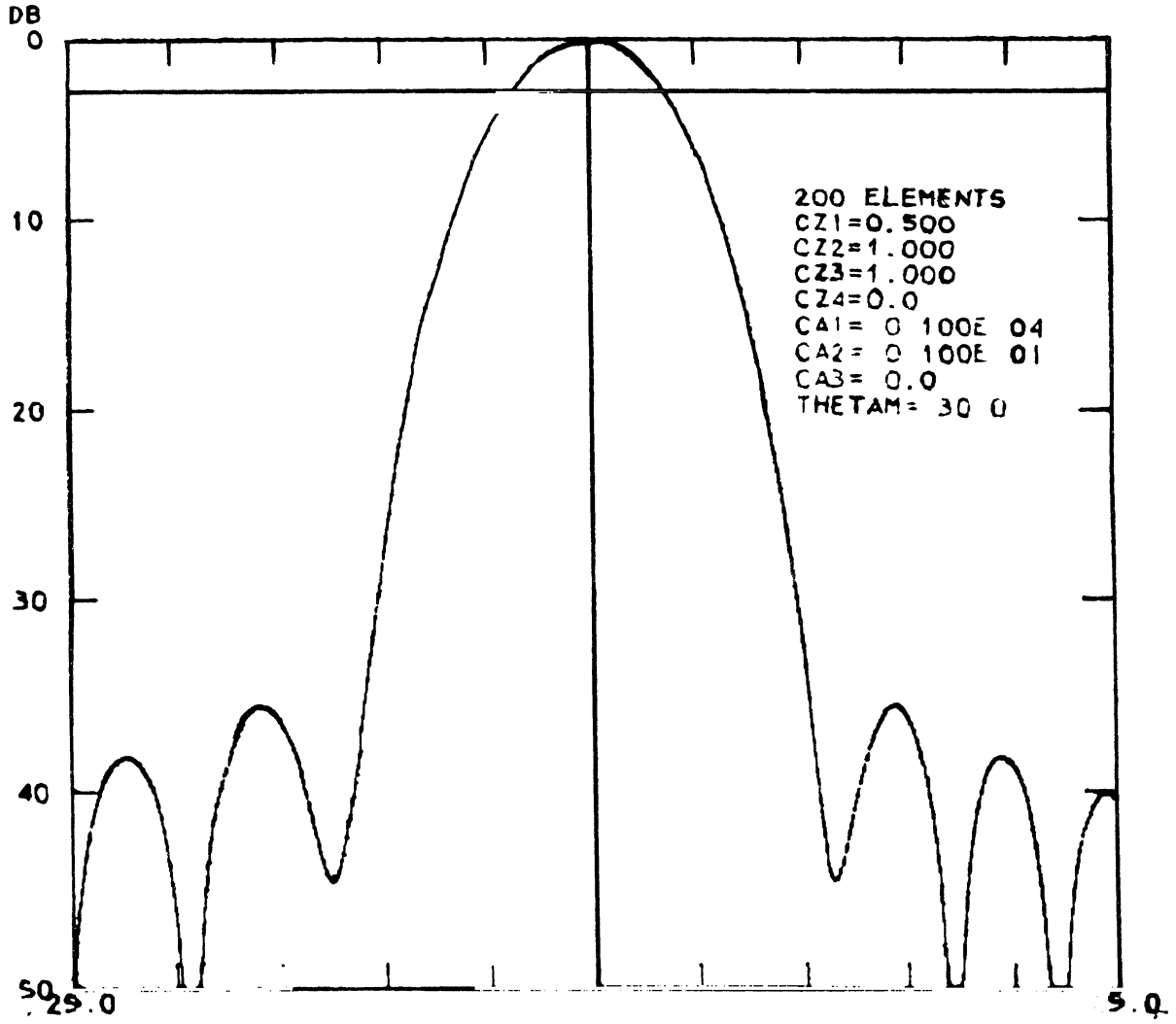

Fig. 38: Study D-3 on Tschebyscheff Simulation. 200 Elements with Uniform Spacing of 0.500λ. Taper Factor CA 1 = 0.100×10^4. Each Abscissa Scale Unit is 0.6°.

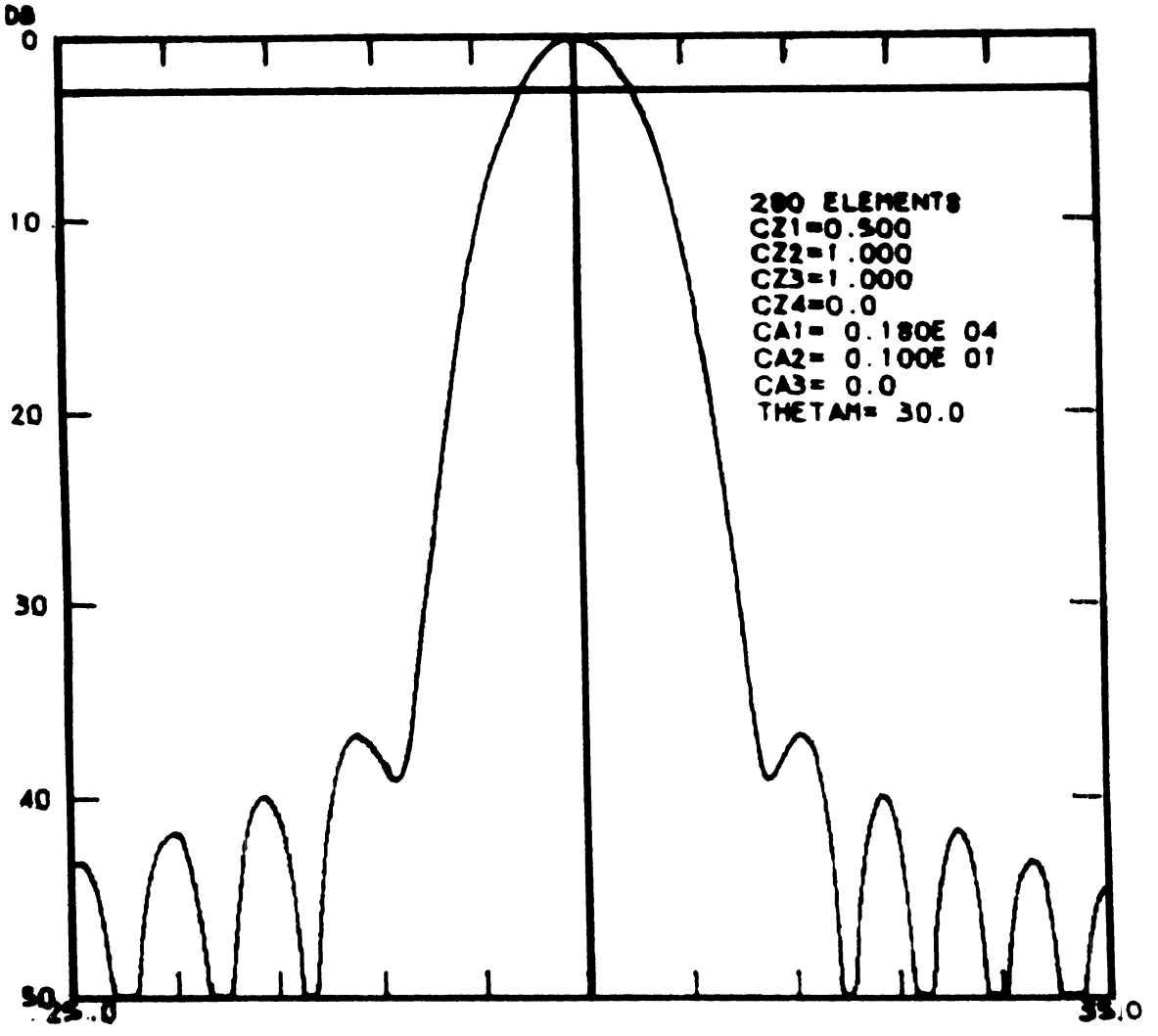

Fig. 39: Study D-4 on Tschebyscheff Simulation. 280 Elements with Uniform Spacing of 0.500λ. Taper Factor CA 1 = 0.180×10^4. Each Abscissa Scale Unit is 1^o.

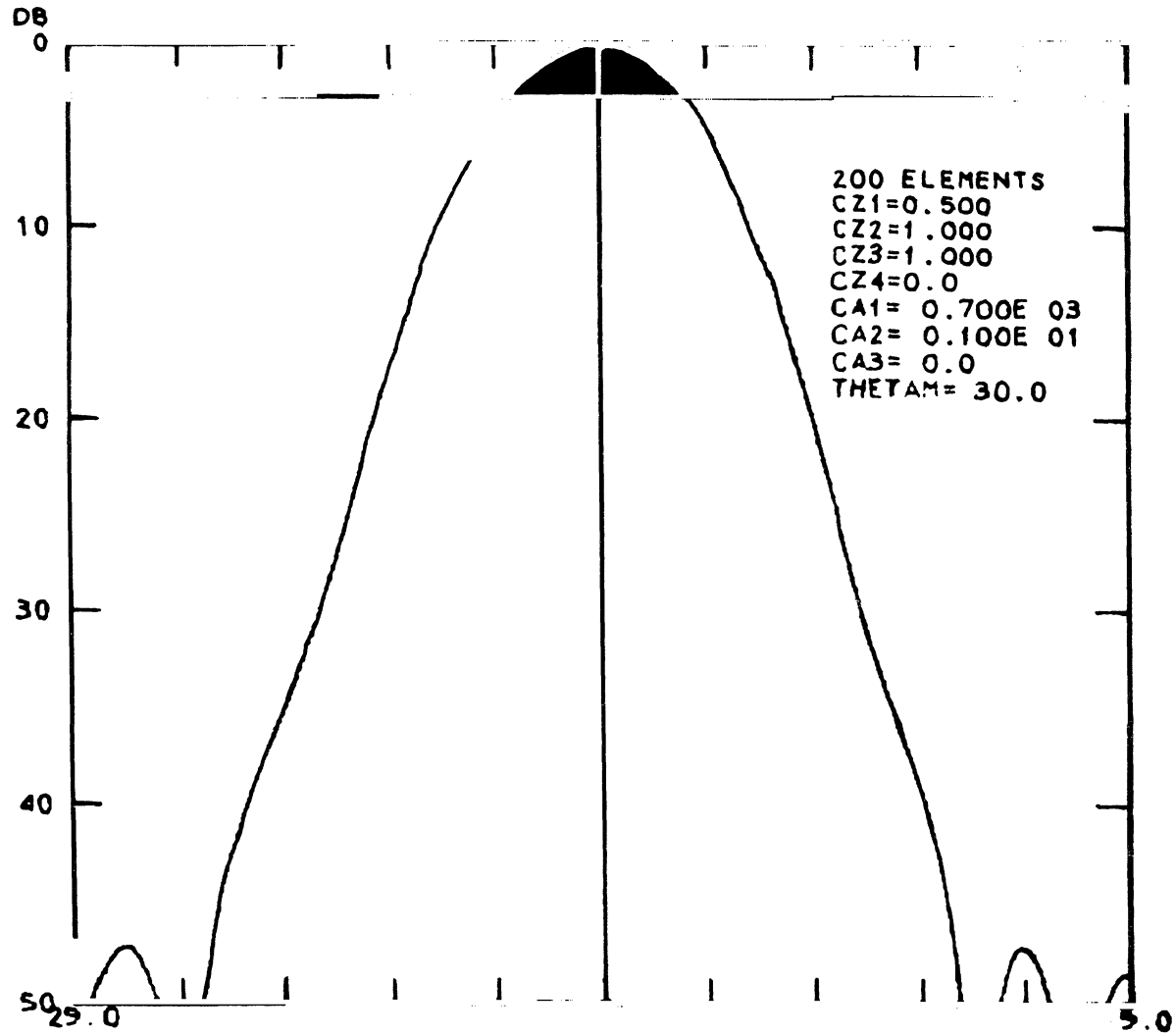

Fig. 40: Study D-5 on Tschebyscheff Simulation 200 Elements with Uniform Spacing of 0.500λ. Taper Factor CA 1 = 0.700×10^3. Each Abscissa Scale Unit is 0.6°.

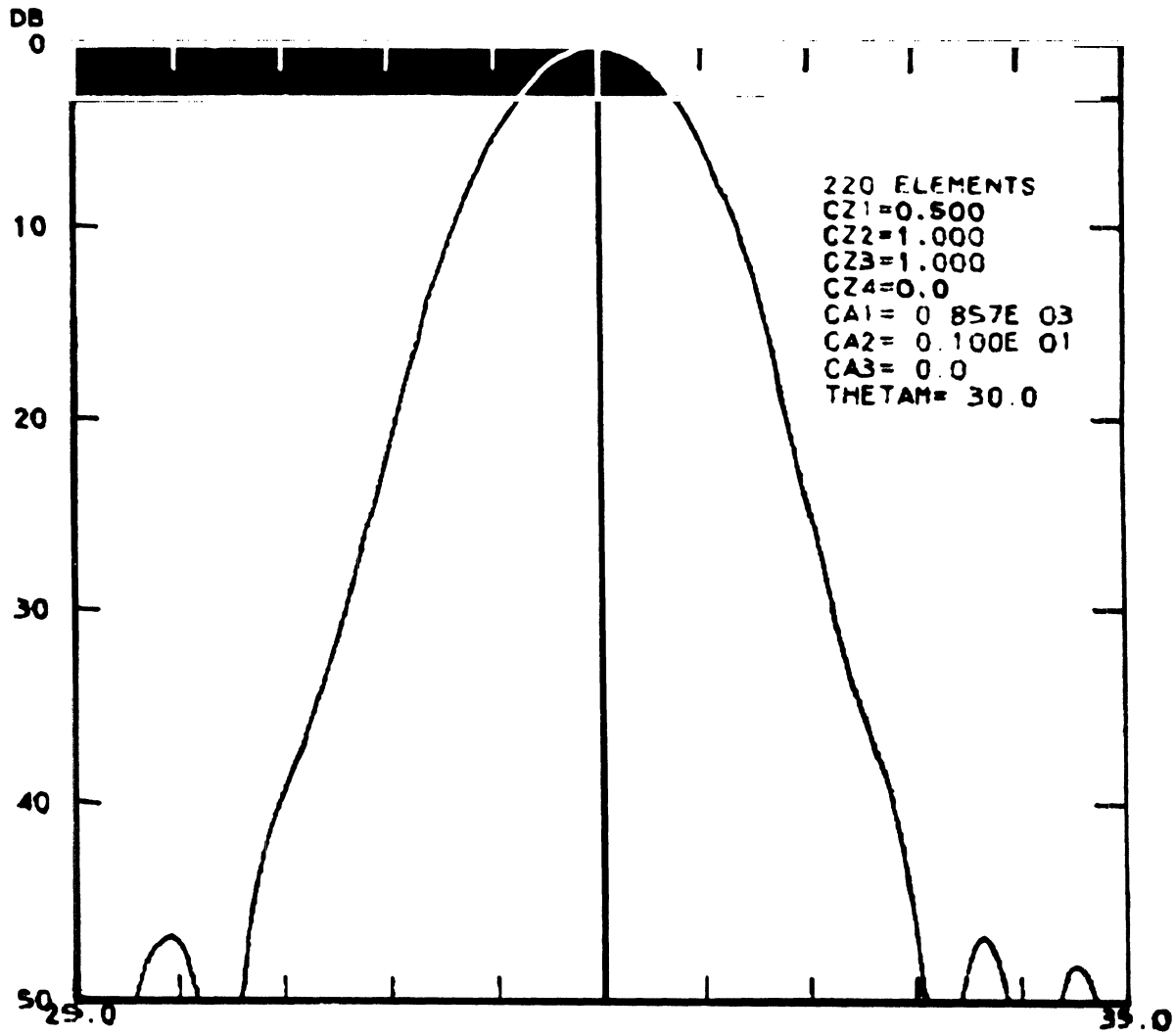

Fig. 41: Study D-6 on Tschebyscheff Simulation. 220 Elements with Uniform Spacing of 0.500λ. Taper Factor CA 1 = 0.857×10^3. Each Abscissa Scale Unit is 0.6^{o}.

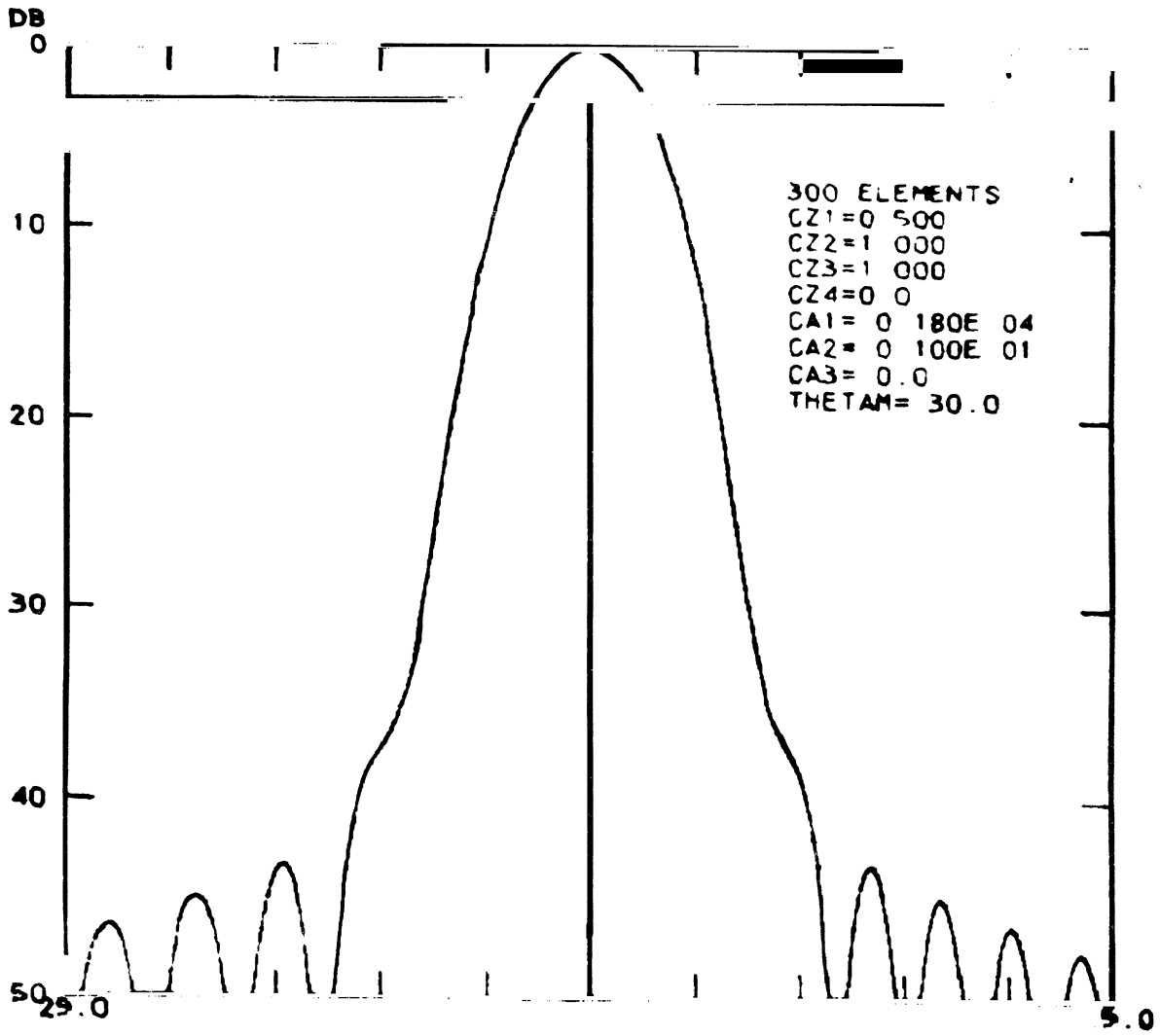

Fig. 42: Study D-7 on Tschebyscheff Simulation 300 Elements with Uniform Spacing of 0.500λ. Taper Factor CA 1 = 0.180×10^4. Each Abscissa Scale Unit is 0.6°.

extreme range of power level between the center element and the end element of an array. It is interesting to note that in order to achieve a Tschebyscheff pattern the required illumination function to provide the appropriate tapered illumination is approximately in the form of a simple exponential of the common base "e" to a negative exponent. This negative exponent has as its value distance squared divided by the parameter CA 1 where the distance is that from the element involved to the array center. For this mathematical form you are referred to subsection 2.1 which indicates the various formulas which utilize the specified parameters for the arrays. The computer simulations of Tschebyscheff patterns use various numbers of elements. However, each study involved a uniform spacing of 0.5λ. The degree to which an actual Tschebyscheff pattern was realized depends upon the steepness of taper of the illumination. The exponential distribution of illumination used varies from study to study. A large negative exponent in this exponential corresponds to a severe tapering of the illumination. It is to be noted that the case with the largest negative exponent provides the best Tschebyscheff radiation pattern. However, it is also necessary to consider that the size of the negative exponent does not depend alone on CA 1 but rather on the squared distance from the center to the element involved divided by CA 1. There is no printout on the patterns shown which indicates simply the greatest taper. In judging the patterns in this respect both the number of elements and the values of the parameter CA 1 must be considered. Note that the horizontal scales for the patterns in this group vary from pattern to pattern.

Pattern D-1 shown for a 25-element array, resembles closely a true Tschebyscheff curve. This pattern was taken for a main lobe in the normal broadside position although part of the main lobe is not shown. If the peak of the main lobe was shown it would be noted that the sidelobe level is very low compared to cases in series A using the same number of elements.

Radiation pattern D-2 is for the same number of elements as D-1 except that the illumination taper is less; correspondingly it can be observed that the pattern departs from the true Tschebyscheff type and there is a marked variation

in the levels of the various sidelobes present. In this radiation pattern it is possible to be misled because of the small angular scale. At first glance, it would appear that the highest sidelobe is lower than the highest sidelobe in the previous radiation pattern D-1. However, this is not the case since other sidelobes are obscured because of the small angular or horizontal scale. Those sidelobes which are not immediately apparent have appeared to merge with the main beam; however, they are present and a more detailed representation of the pattern using a larger angular scale would immediately show up the presence of additional sidelobes.

Pattern D-3 shows the influence of increasing the number of elements to 200. The beamwidth has now become 1.43^{o} as compared to the 6.6^{o} for the previous 25-element array.

In radiation pattern D-4 the number of elements has been increased to 280 and, as would be expected the beamwidth is reduced still further. The beamwidth now is approximately 1^{o}.

Radiation pattern D-5 taken for a 200-element array with a very steep illumination taper shows a pattern which very closely approximates a Tschebyscheff curve. With the large angular scale here most of the sidelobe structure is not available for study. Notice here that the beamwidth is 1.7^{o}. This should be compared with case D-3 which was for 200-elements which has 1.4^{o} beamwidth. By more closely approximating the Tschebyscheff radiation pattern we have reduced the sidelobe level approximately 10 dB for a given number of elements (200) but in achieving this there has been some increase in the beamwidth.

The radiation pattern shown in case D-6 for 220 elements is close to the case previously described in D-5. However, the additional elements have caused the beamwidth to be reduced to 1.48^{o}. The large illumination taper is close to optimum for a Tschebyscheff radiation pattern. In comparing D-3 and D-6 it is observed that the beamwidths in the two are almost exactly the same, but the sidelobe level in D-6 has been greatly reduced. This has been accomplished by having the more nearly optimum illumination for a Tschebyscheff radiation

pattern. Of course it has been necessary to increase the number of elements to maintain the beamwidth of the D-3 pattern.

In the radiation pattern depicted for case D-7, it is to be noted that increasing the number of elements to 300 has provided a pattern with a beamwidth of 1.07 degrees. The sidelobe level is still more than 40 dB below the main beam.

2.9 Optimization in the Presence of Power Constraints

In this phase of the study, the ratio of the power fed to the center element with that fed to the end element was kept constant. This constraint is practical since in an actual array synthesis problem, mutual coupling effects tend to limit the range of power levels fed to individual elements in an array. The two levels of power constraints utilized in these studies were -9 dB and -12 dB, or in other words, the amount of power fed to the end element in the array was 1/8 and 1/16, respectively, of that fed to the center element. All cases studied in this section utilized the familiar negative exponential taper as discussed in section 2.8.

Three separate cases using the idea of power constraints were examined. The first two involved the application of -9dB and -12dB constraints to uniform arrays with half-wavelength spacing. The third case concerned the application of a -9 dB constraint to space-tapered arrays. Each case involved 8 arrays ranging in size from 50 to 400 elements in increments of 50 elements. A scan position of 60° from broadside was used for each array. Array patterns were plotted on a rectangular scale and the detailed sidelobe structure about the main lobe was studied carefully to determine the correct level of the maximum sidelobe.

The first case to be considered is the application of a -9 dB power constraint to uniformly spaced arrays. The array patterns for this case are designated by the letter E and are shown in Figs. 43 through 46, inclusively. These patterns indicate that the sidelobe level remains relatively constant at a level of -20 dB independent of the number of elements in the array. As expected, the beamwidth tends to decrease as the number of elements increases. The

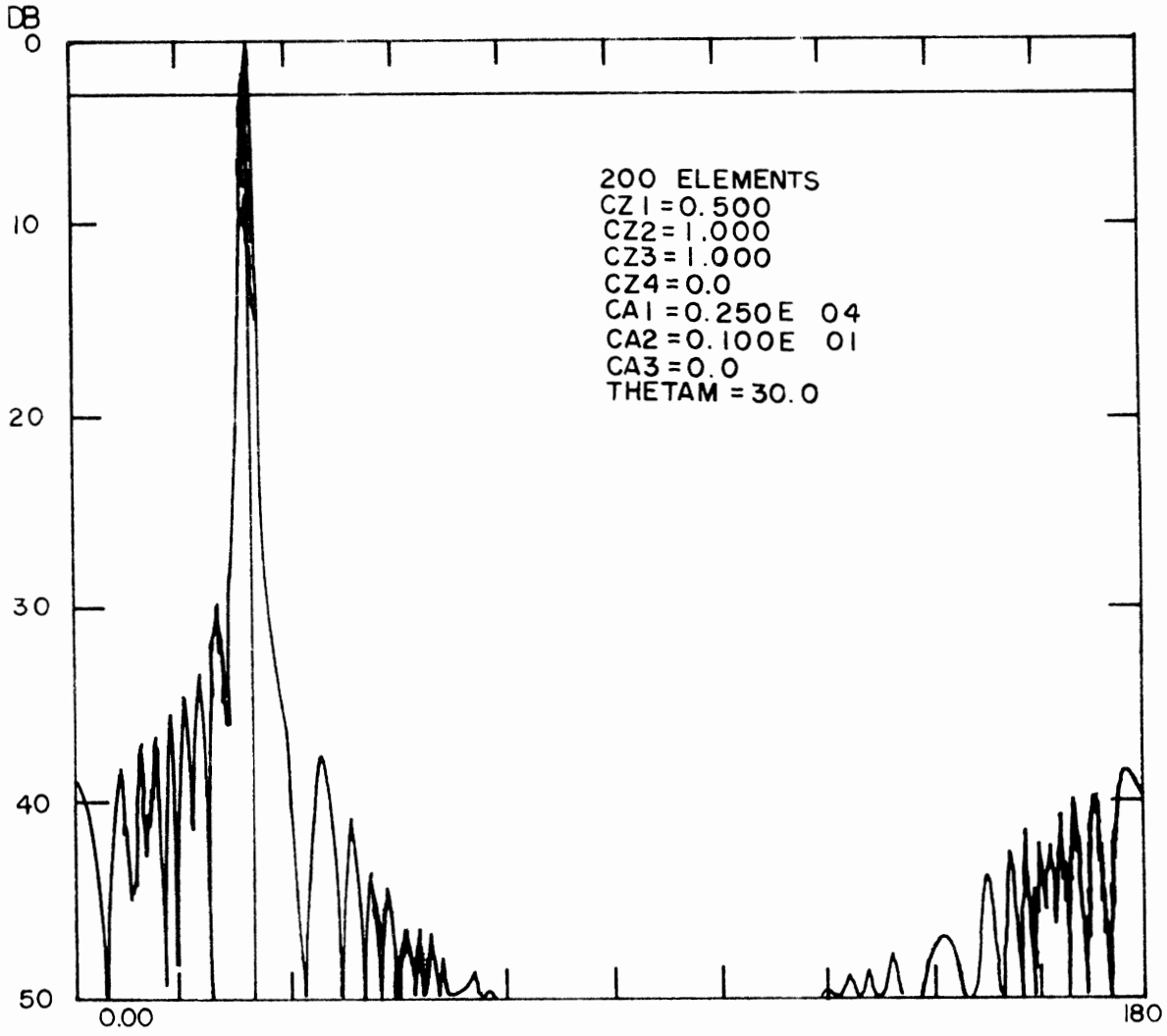

Fig. 43: Study E-1. 9 dB Power Constraint. 200 Elements with Uniform Spacing of 0.500λ. Taper Factor CA 1 = 0.250 x 10^4. Each Abscissa Scale Unit is 18^o.

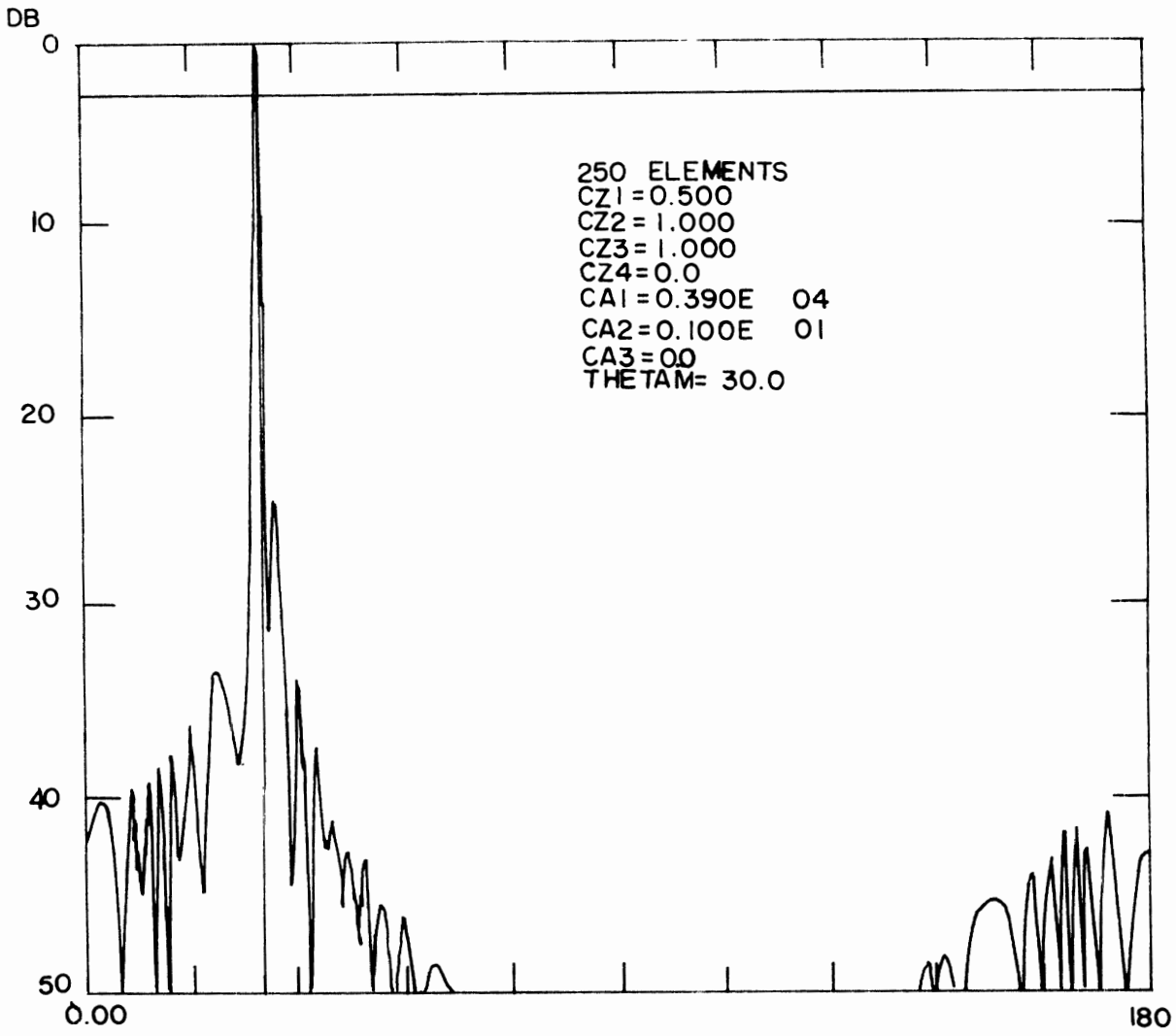

Fig. 44: Study E-2. 9 dB Power Constraint. 250 Elements with Uniform Spacing of 0.500λ. Taper Factor CA 1 = 0.390 x 10^4. Each Abscissa Scale Unit is 18^o.

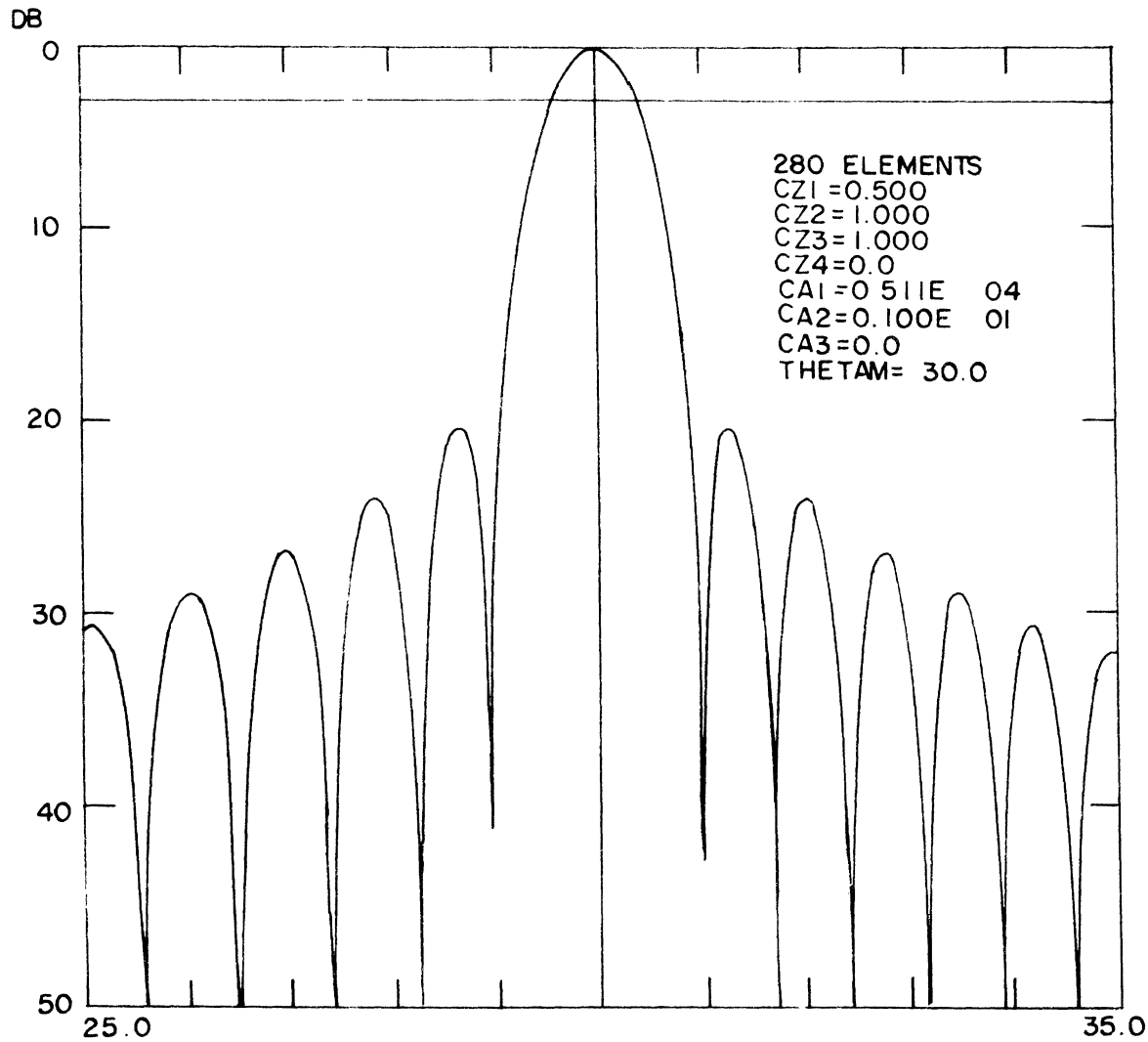

Fig. 45: Study E-3. 9 dB Power Constraint. 280 Elements with Uniform Spacing of 0.500λ. Taper Factor CA 1 = 0.511 x 10^4. Each Abscissa Scale Unit is 1^o.

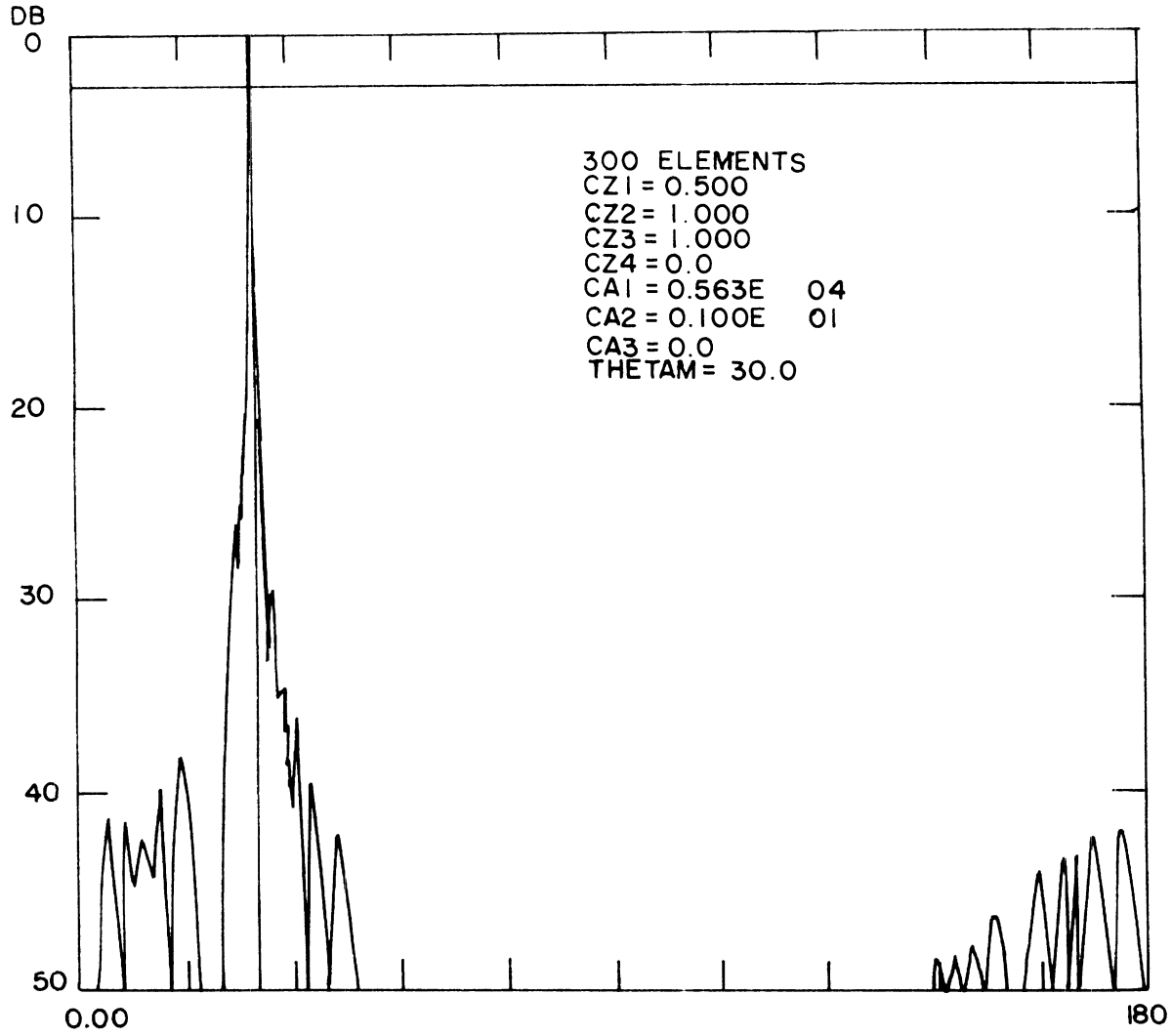

Fig. 46: Study E-4. 9 dB Power Constraint. 300 Elements with Uniform Spacing of 0.500λ. Taper Factor CA 1 = 0.563×10^4. Each Abscissa Scale Unit is 18^o.

design level of 0.8^{o} is reached somewhere between 250 and 300 elements. (For 250 elements, BW = 0.9^{o}, for 300 elements, BW = 0.7^{o}.)

Next, a -12 dB power constraint was applied to a set of uniformly spaced arrays. The patterns for this case are denoted by the letter F and are shown in Figs. 47 to 54, inclusively. As in the previous case, the patterns indicate that the sidelobe level remains relatively constant, independent of the number of elements in the array. The sidelobe level was -30 dB for this set of arrays, a noticeable improvement over the case where a -9 dB constraint was applied. As before, the beamwidth tended to decrease as the number of elements increased. The design level of 0.8^{o} was reached somewhere between 250 and 300 elements.

The final case studies in this section utilized a -9 dB power constraint on a spaced tapered array. The patterns for this case are denoted by the letter G and are shown in Figs. 55 to 61, inclusively. The tapering parameters used were CZ 1 = 0.5, CZ 2 = 1.05, and CZ 3 = 1.00. (Please refer to subsection 2.1 for a detailed explanation of these terms.) This means that the distance of the nth element from the center of the array is $(0.5)(1.05)^{n}$ wavelengths. The sidelobe structure obtained for this case was very poor due to the grating lobe effect discussed earlier. This fact yields further evidence to the thought that one must have a more systematic way of obtaining space tapering if grating lobes are to be avoided. Such a method is developed subsection 2.10 dealing with the steepest descent method.

Finally, it should be noted that there was nothing magic about choosing -9 dB and -12dB for the level of power constraint. Depending upon mutual coupling effects and the actual size of the array, less restrictive constraints could be applied to yield lower sidelobe levels. In the absence of detailed coupling data for large arrays, the value of this section is in observing general trends rather than in designing specific arrays.

2.10 Optimization by Steepest Descent Technique

A computer program was written to implement the steepest descent technique. in the synthesis of antenna patterns. The resulting patterns are for linear arrays

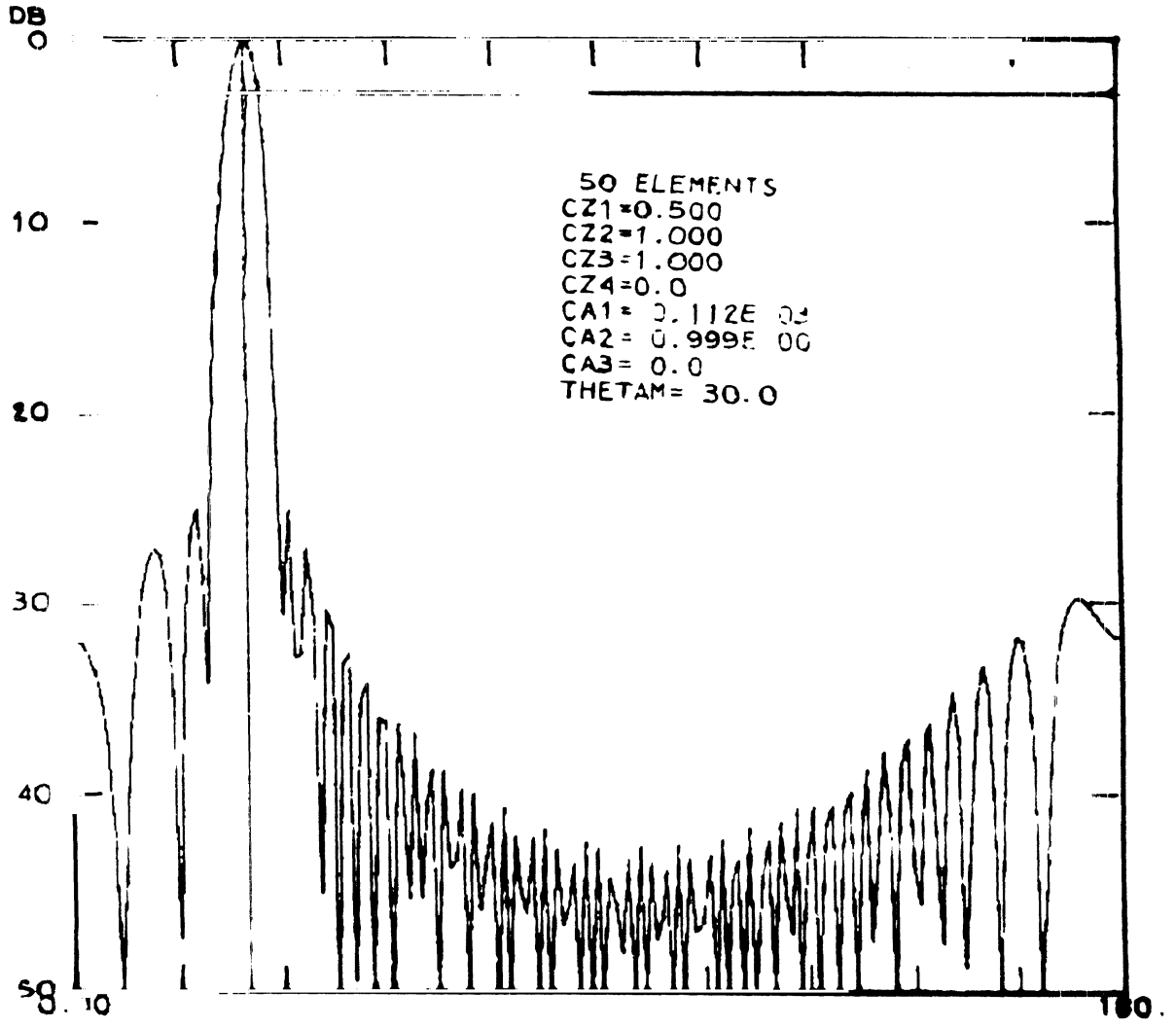

Fig. 47: Study F-1. 12 dB Constraint. 50 Elements with Uniform Spacing of 0.500λ. Taper Factor CA 1 = 0.112×10^3. Each Abscissa Scale Unit is 18^o.

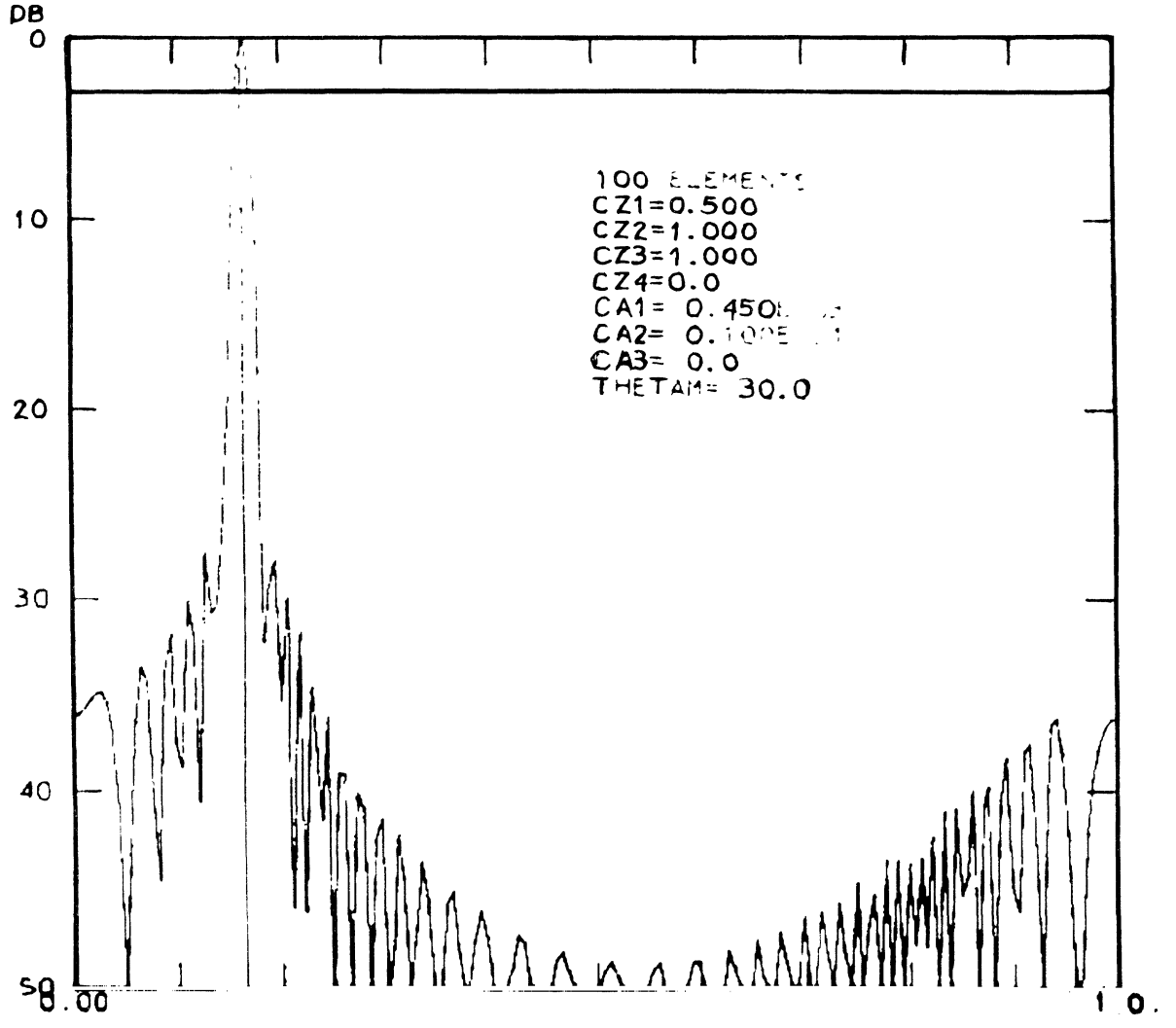

Fig. 48: Study I -2. 12 dB Constraint. 100 Elements with Uniform Spacing of 0.500λ. Taper Factor CA1 = 0.450×10^{-3}. Each Abscissa Scale Unit is 18^{0}.

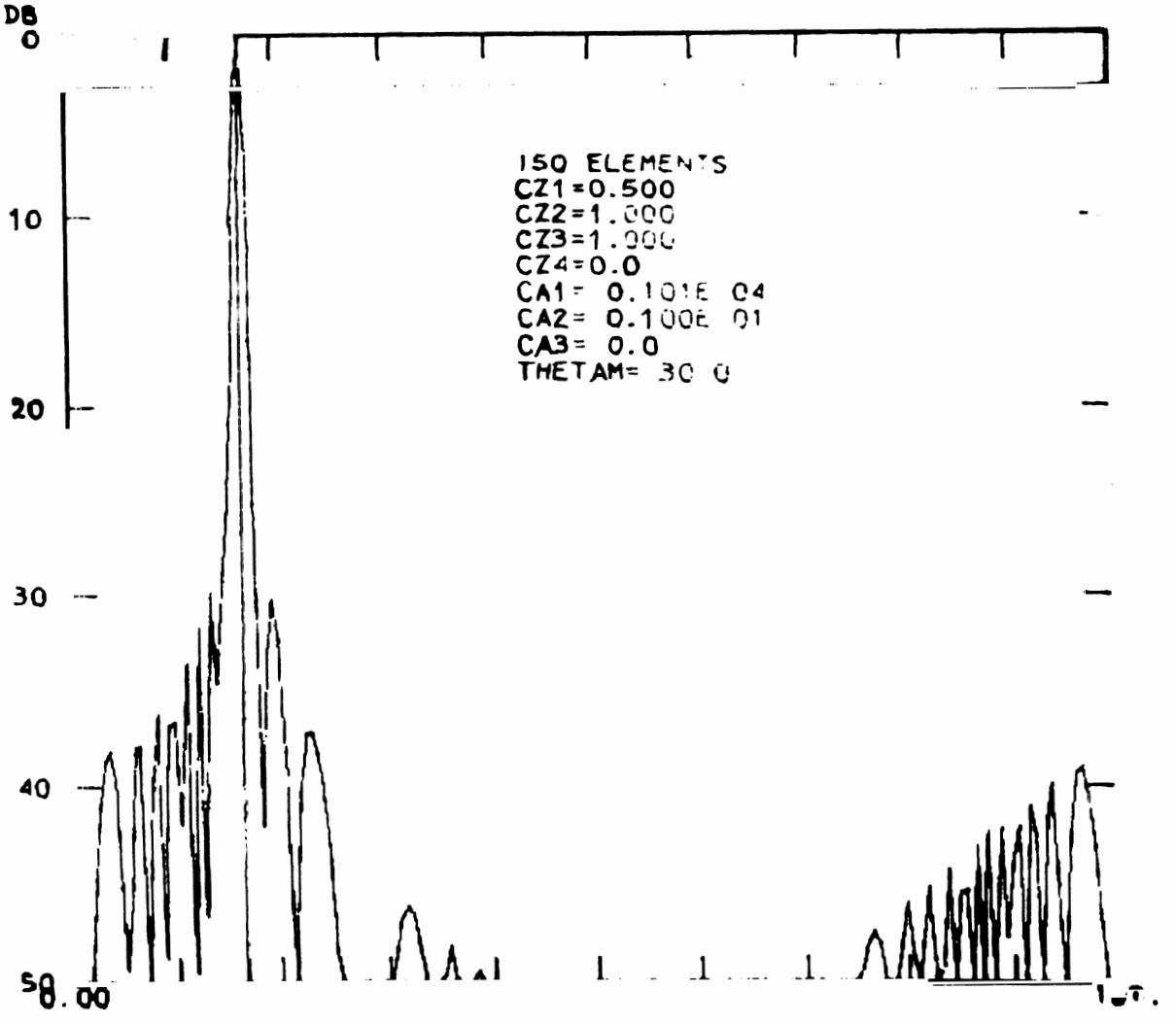

Fig. 49: Study F-3. 12 dB Constraint. 150 Elements with Uniform Spacing of 0.500λ. Taper Factor CA 1 = 0.101×10^4. Each Abscissa Scale Unit is 18^o.

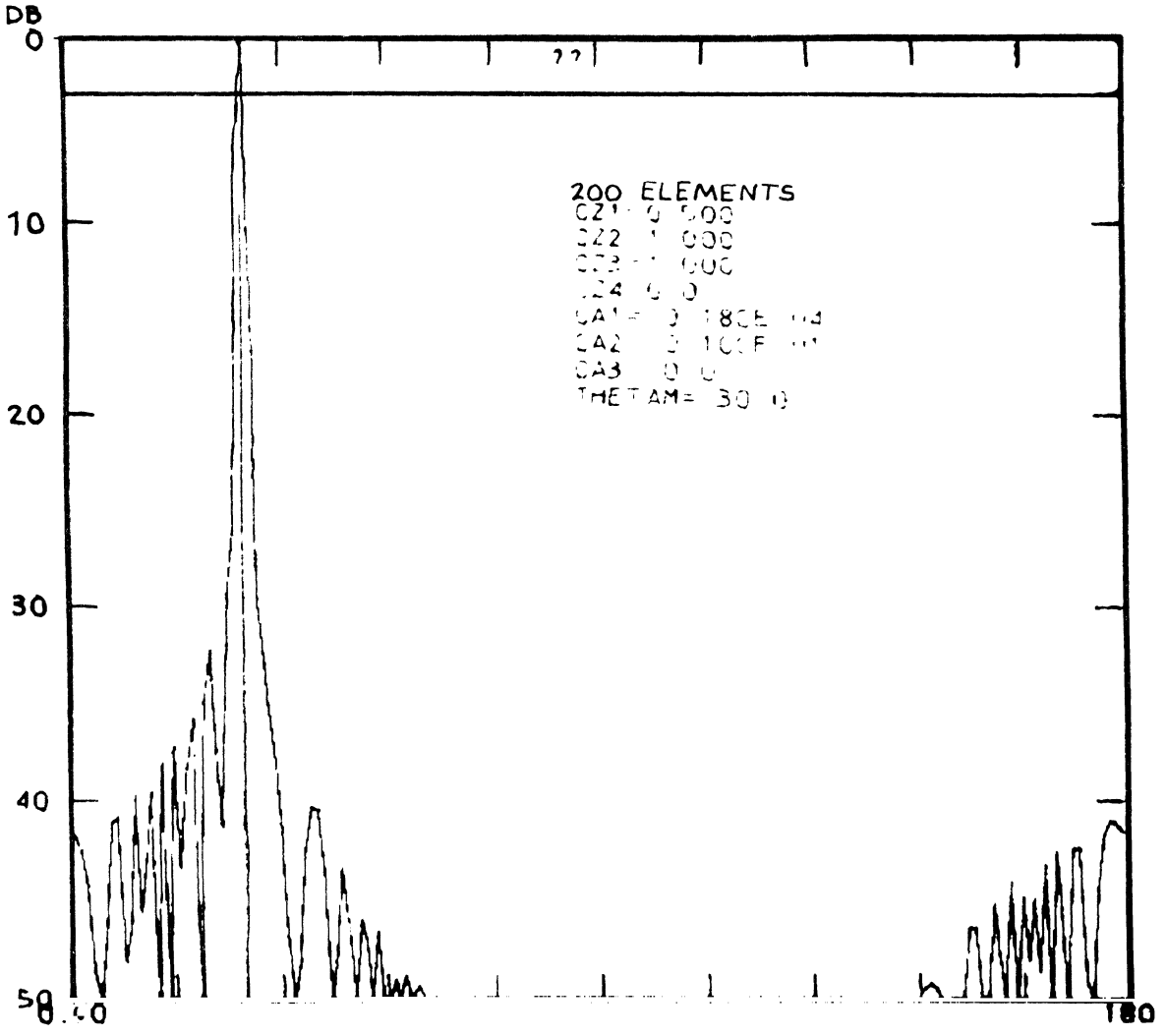

Fig. 50: Study F-4. 12 dB Constraint. 200 Elements with Uniform Spacing of 0.500λ. Taper Factor CA1 = 0.180 x 10^4. Each Abscissa Scale Unit is 18^o.

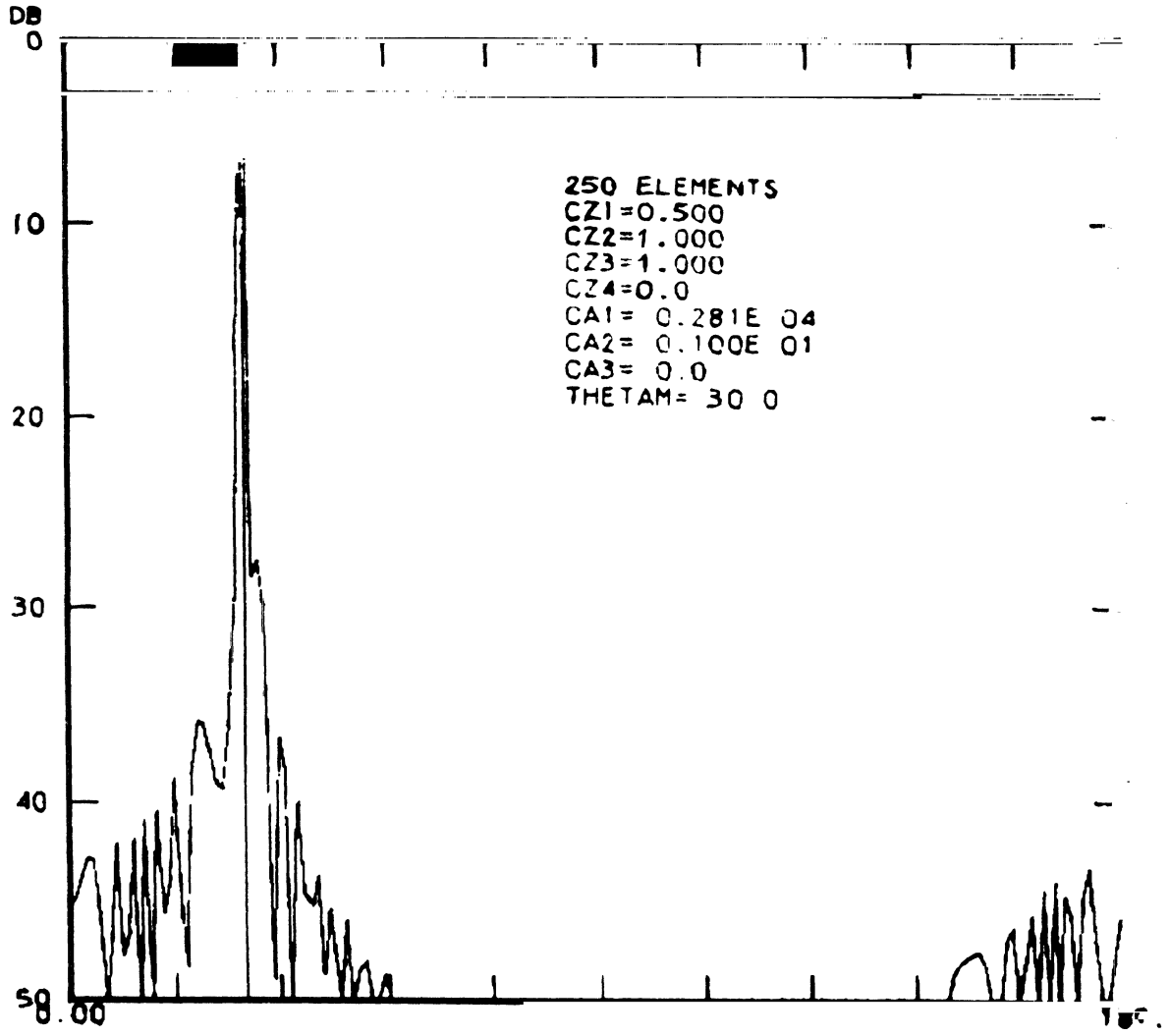

Fig. 51: Study F-5. 12 dB Constraint. 250 Elements with Uniform Spacing of 0.500λ. Taper Factor CA 1 = 0.281×10^4. Each Abscissa Scale Unit is 18^o.

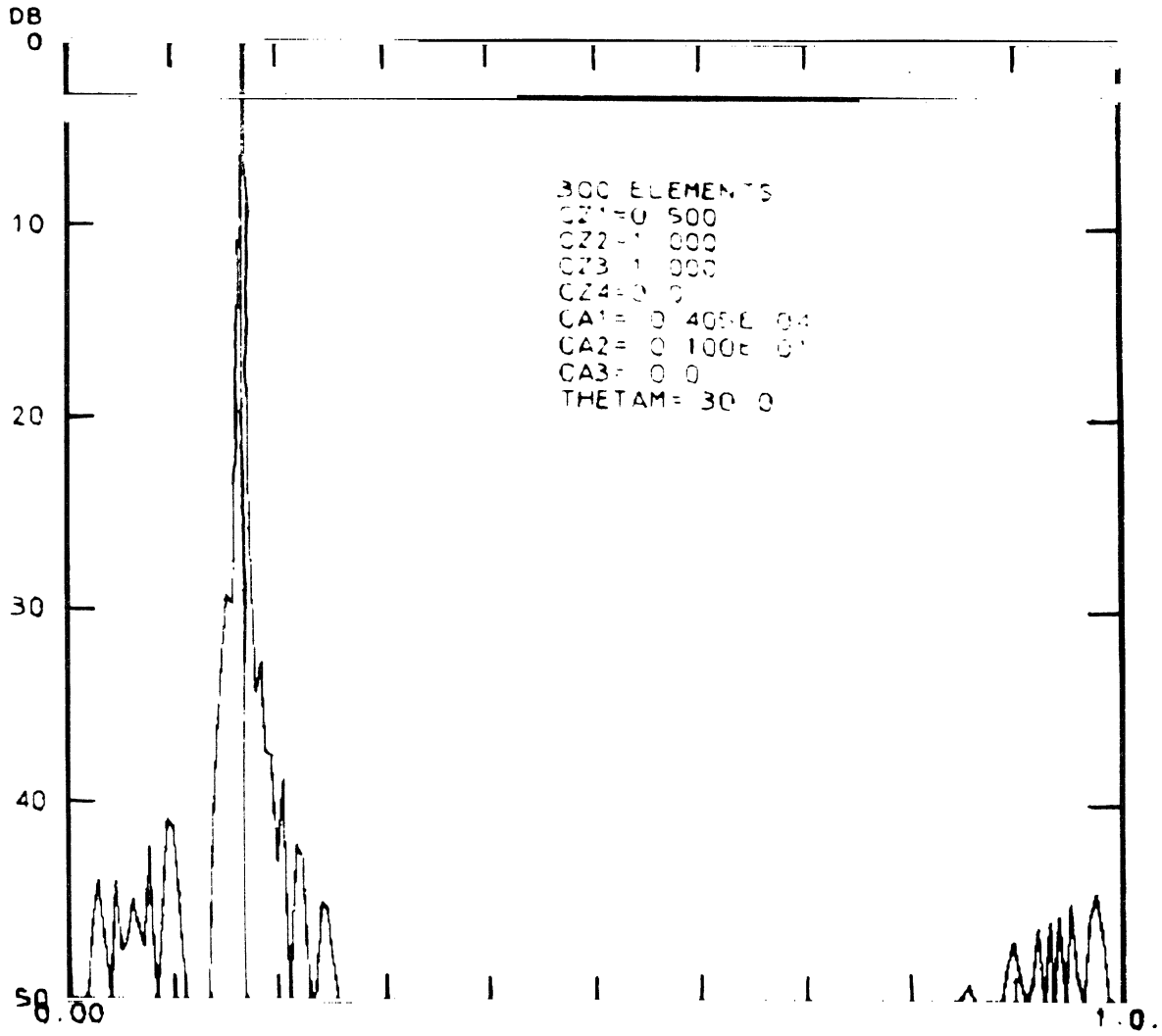

Fig. 52: Study F-6. 12 dB Constraint. 300 Elements with Uniform Spacing of 0.500λ Taper Factor CA 1 = 0.405×10^{4}. Each Abscissa Scale Unit is 18^{o}.

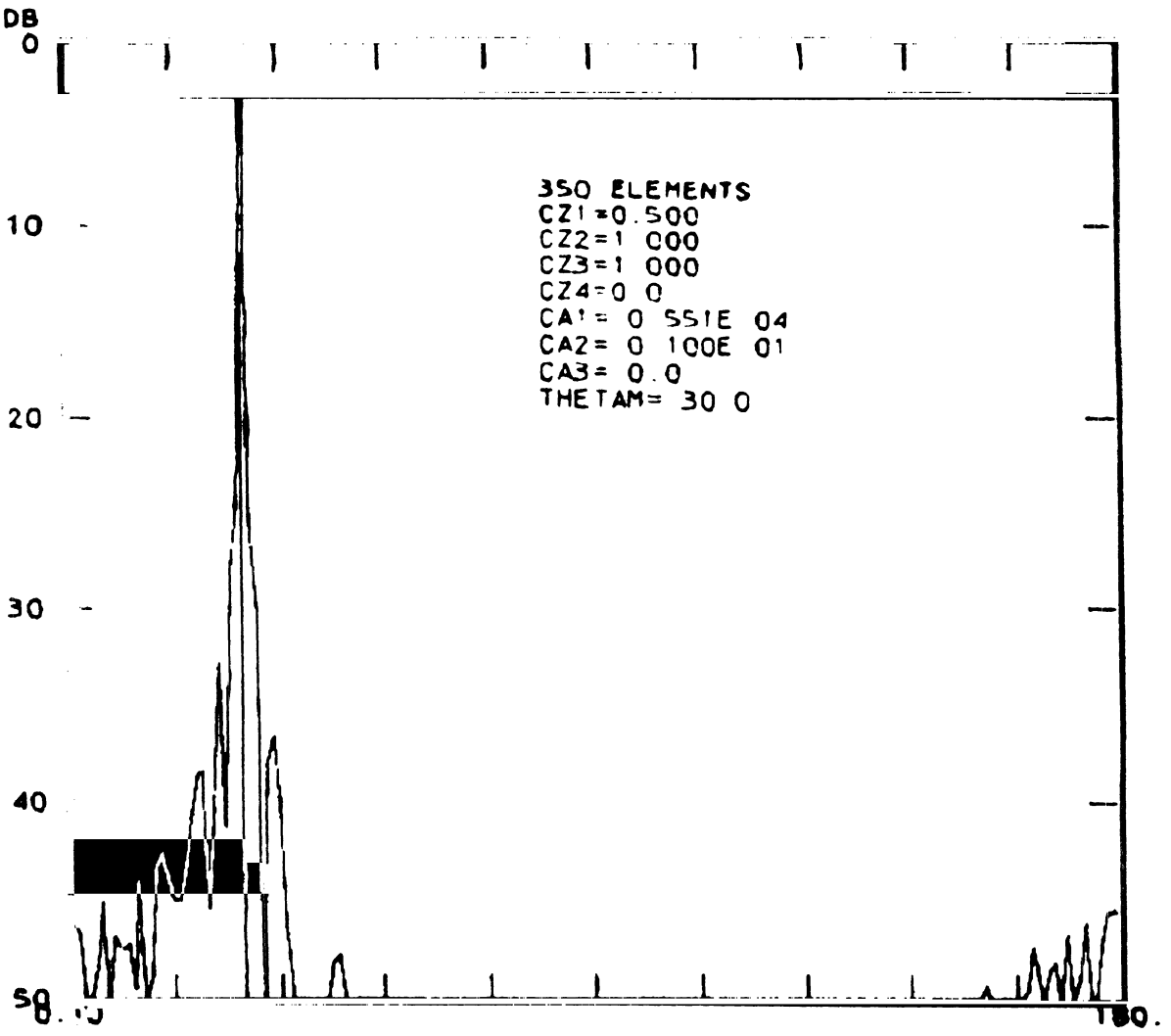

Fig. 53: Study F-7. 12 dB Constraint. 350 Elements with Uniform Spacing of 0.500λ. Taper Factor CA 1 = 0.551×10^4. Each Abscissa Scale Unit is 18^o.

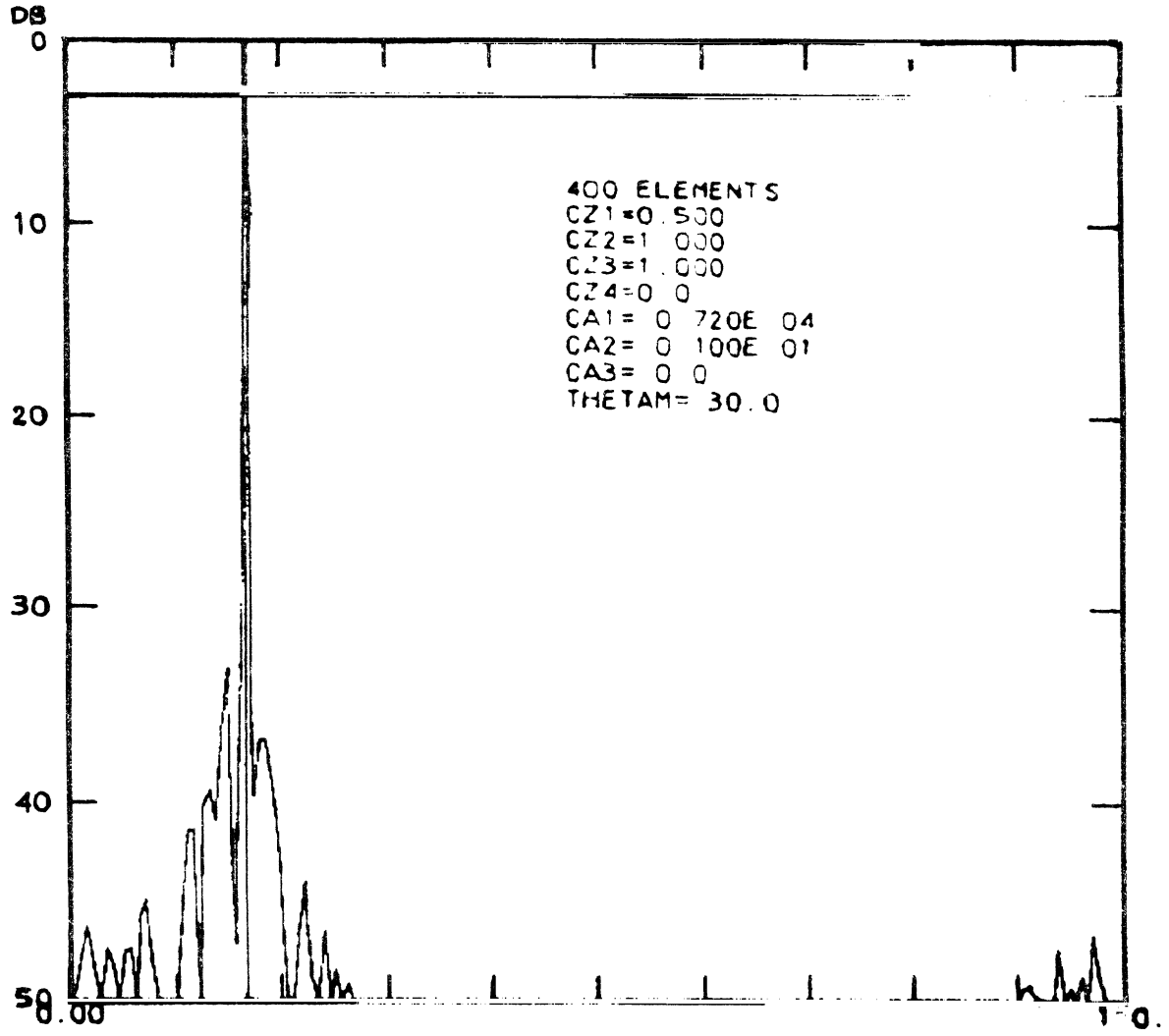

Fig. 54: Study F-8. 12 dB Constraint. 400 Elements with Uniform Spacing of 0.500λ. Taper Factor CA 1 = 0.720×10^4. Each Abscissa Scale Unit is 18^o.

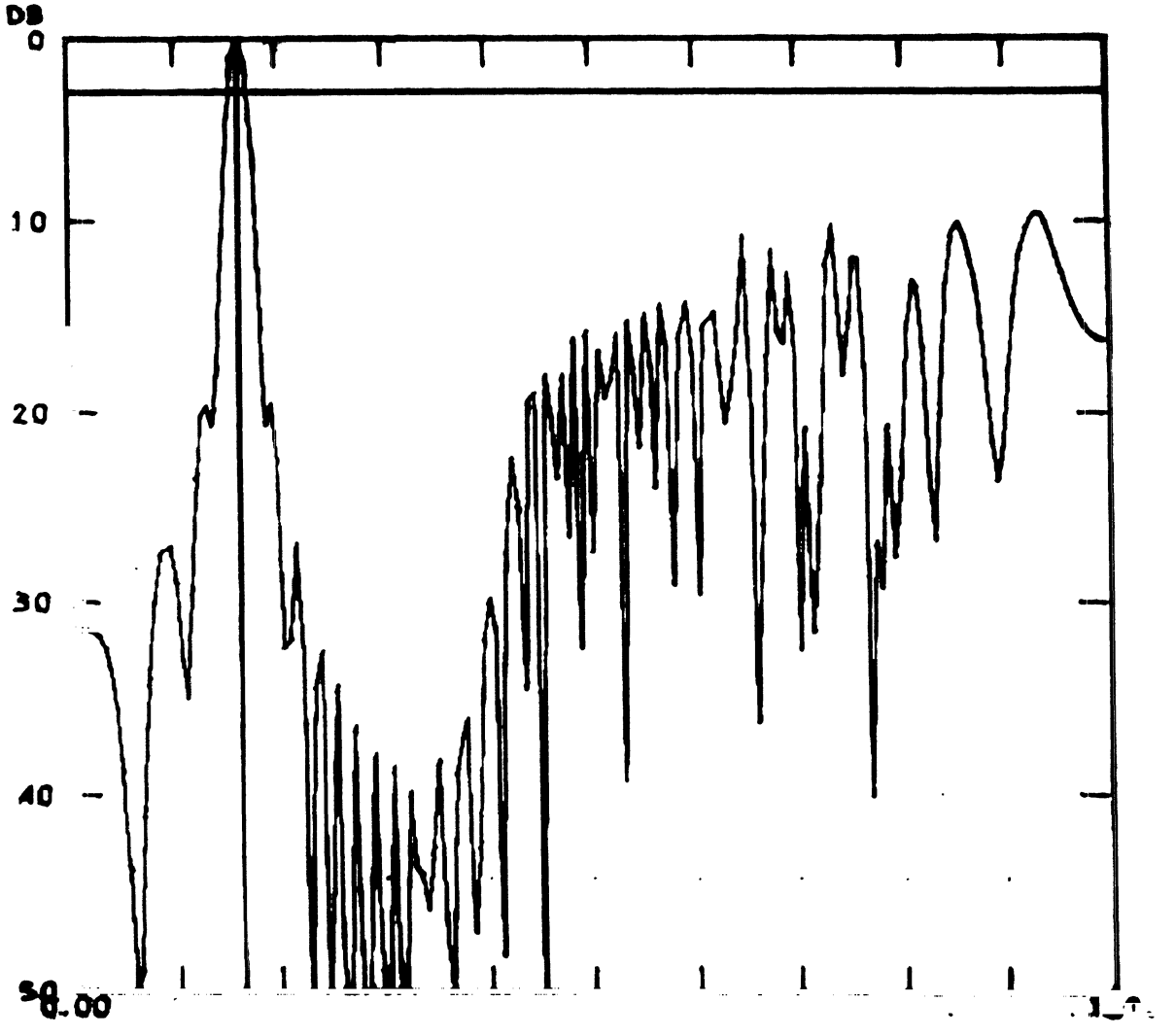

50 ELEMENTS
CZ1=0.500
CZ2=1.050
CZ3=1.000
CZ4=0.0
CA1= 0.571E 03
CA2= 0.100E 01
CA3= 0.0
THETAM= 30.0

Fig. 55: Study G-1. 9 dB Power Constraint with Varied Spacing. 50 Elements. Range of Spacing 0.500λ to 1.54λ. Taper Factor CA 1 = 0.571×10^3. Each Abscissa Scale Unit is 18^o.

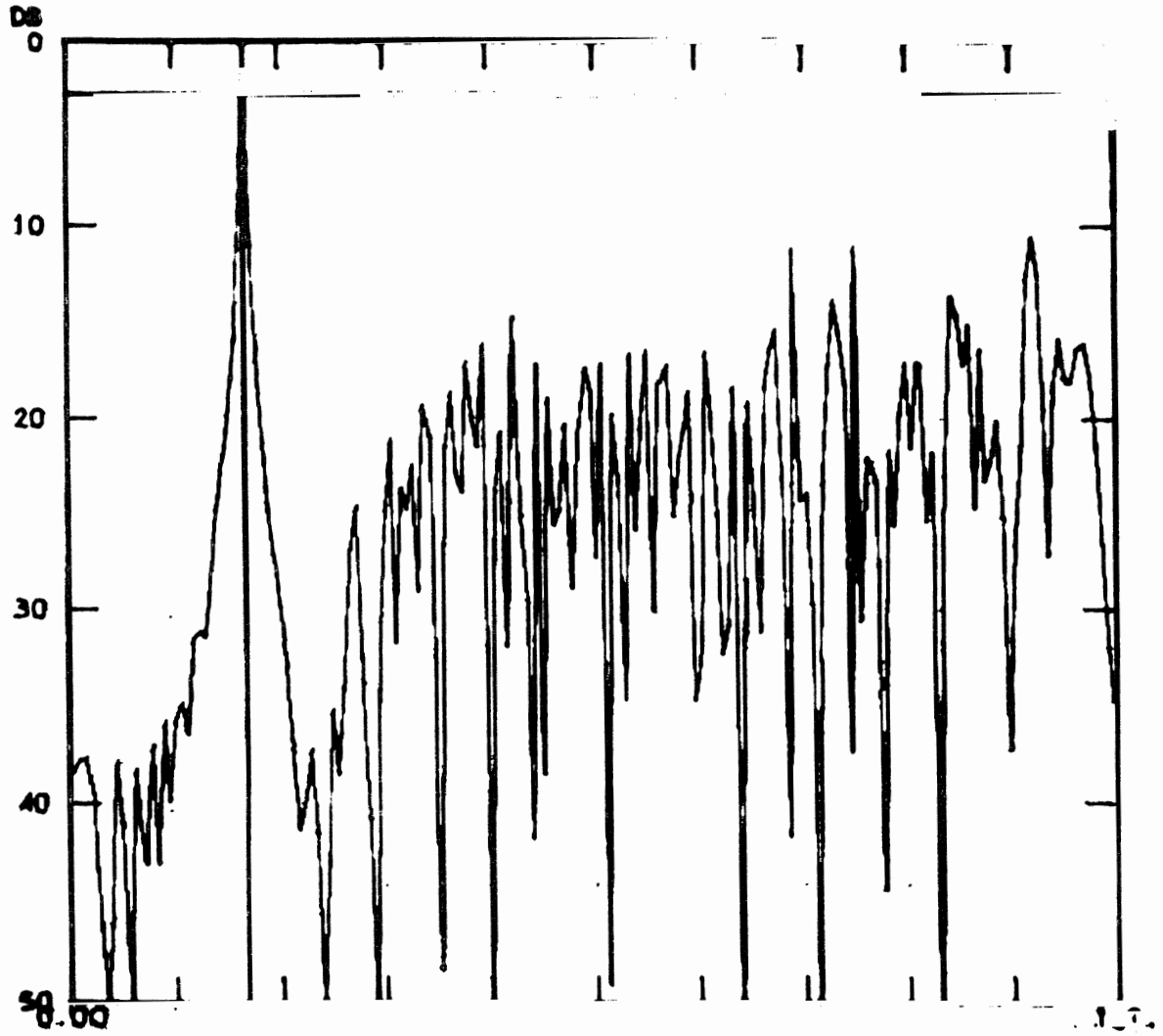

100 ELEMENTS
CZ1=0.500
CZ2=1.050
CZ3=1.000
CZ4=0.0
CA1= 0.115E 05
CA2= 0.100E 01
CA3= 0.0
THETAM= 30.0

Fig. 56: Study G-2. 9 dB Power Constraint with Varied Spacing. 100 Elements. Range of Spacing 0.500λ to 5.2λ. Taper Factor CA 1 = 0.115×10^5. Each Abscissa Scale Unit is 18^o.

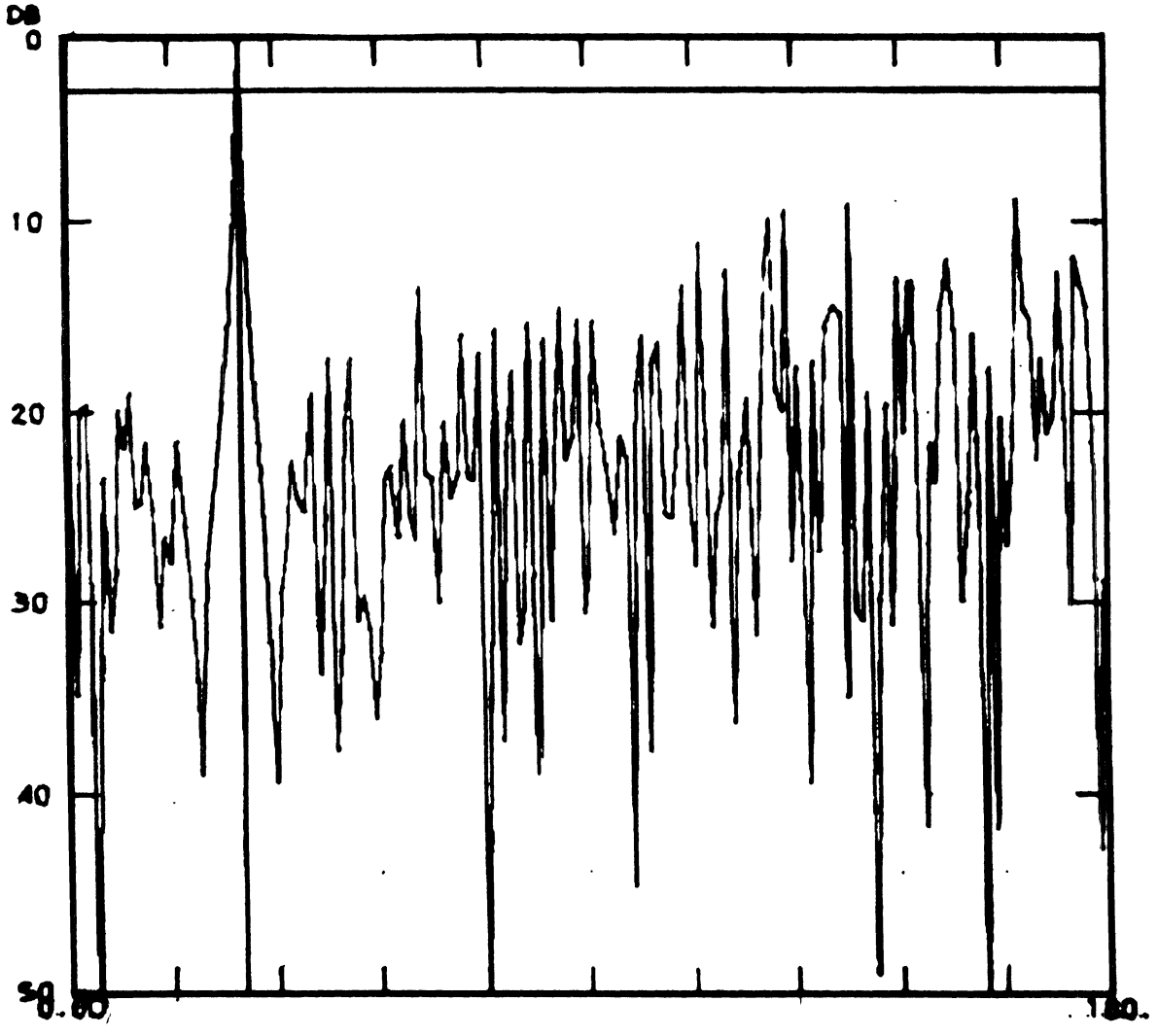

150. ELEMENTS
CZ1=0.500
CZ2=1.050
CZ3=1.000
CZ4=0.0
CA1= 0.144E 06
CA2= 0.100E 01
CA3= 0.0
THETAM= 30.0

Fig. 57: Study G-3. 9 dB Power Constraint with Varied Spacing. 150 Elements. Range of Spacing 0.500λ to 17.65λ. Taper Factor CA $1 \leq 0.144 \times 10^6$. Each Abscissa Scale Unit is 18^o.

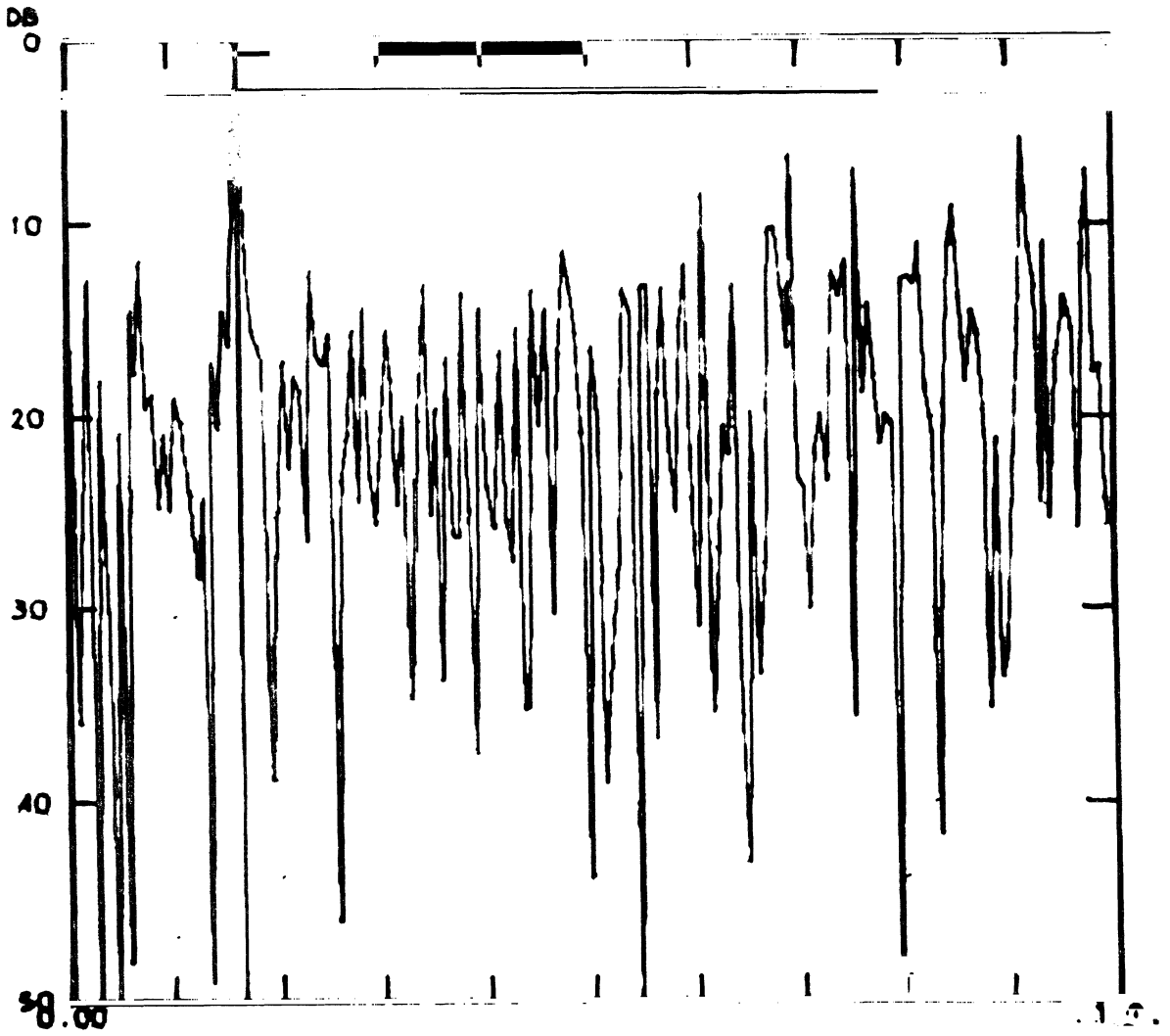

200 ELEMENTS
CZ1=0.500
CZ2=1.050
CZ3=1.000
CZ4=0.0
CA1= 0.169E 07
CA2= 0.100E 01
CA3= 0.0
THETAM= 30.0

Fig. 58: Study G-4. 9 dB Power Constraint with Varied Spacing. 200 Elements. Range of Spacing 0.500λ to 60.0λ. Taper Factor CA 1 = 0.169×10^7. Each Abscissa Scale Unit is 18^o.

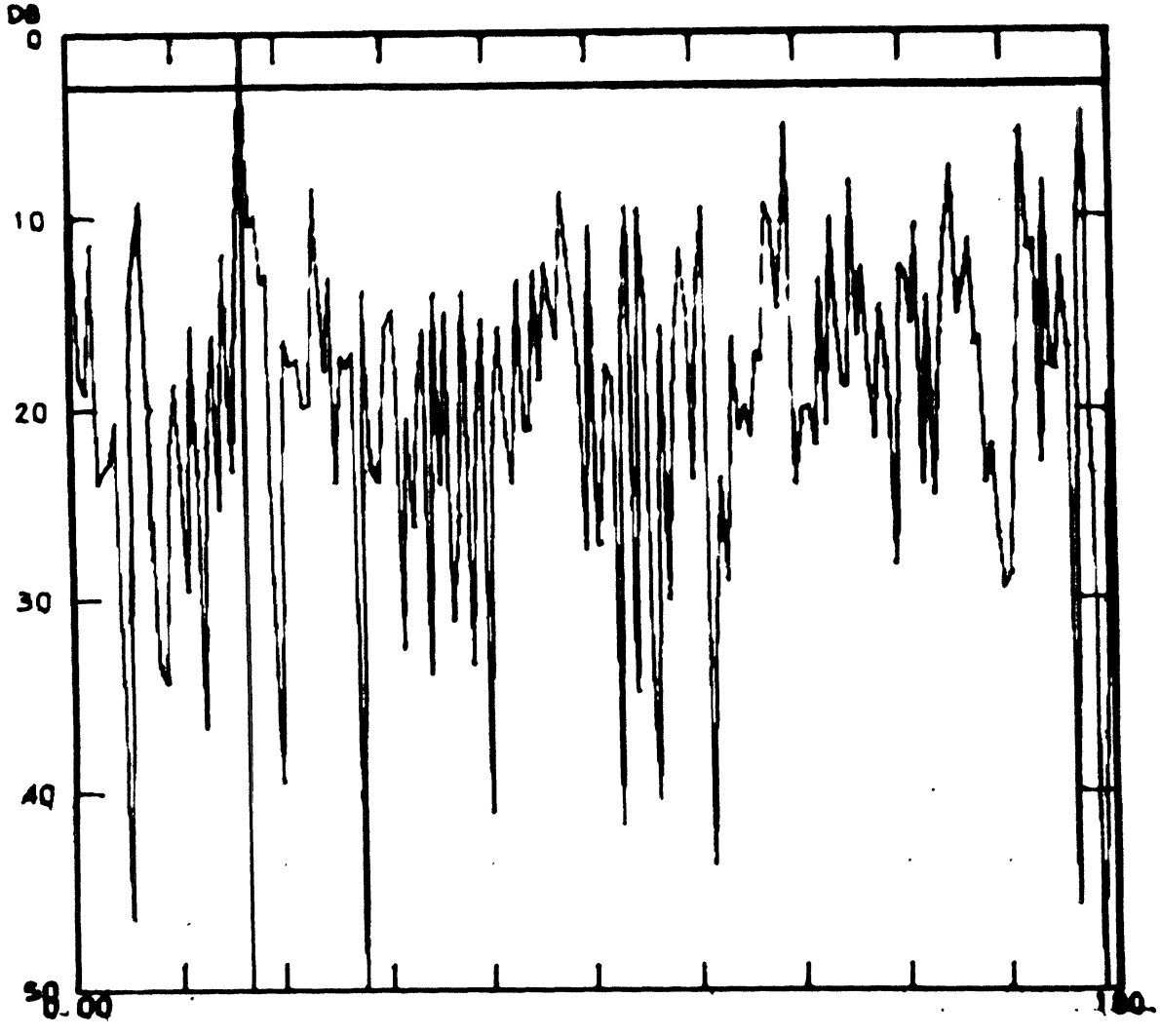

250 ELEMENTS
CZ1=0.500
CZ2=1.050
CZ3=1.000
CZ4=0.0
CA1= 0.200E 08
CA2= 0.100E 01
CA3= 0.0
THETAM= 30.0

Fig. 59: Study G-5. 9 dB Power Constraint with Varied Spacing. 250 Elements. Range of Spacing 0.500λ to 202.0λ. Taper Factor CA 1 = 0.200×10^8. Each Abscissa Scale Unit is 18^o.

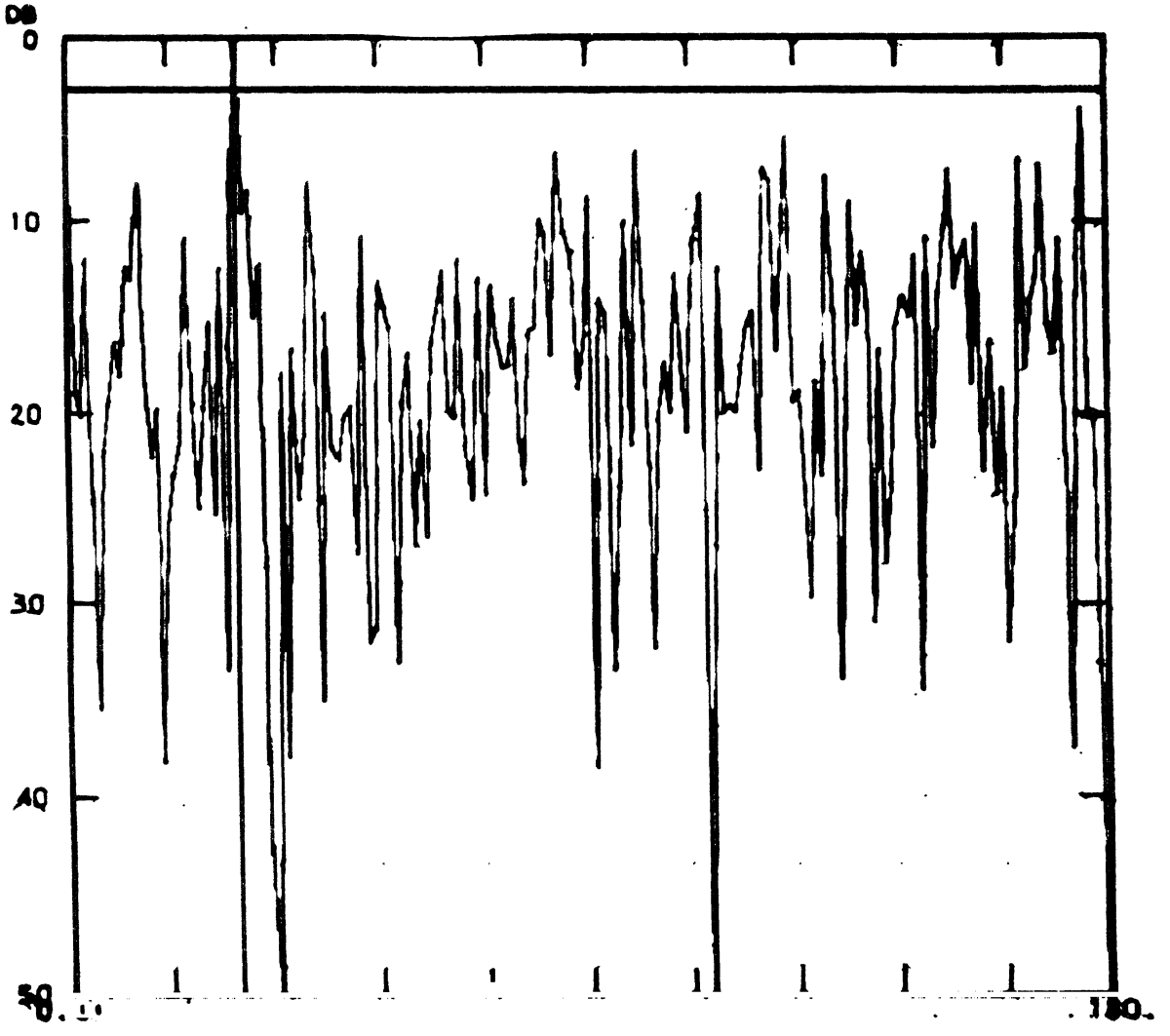

300 ELEMENTS
CZ1=0.500
CZ2=1.050
CZ3=1.000
CZ4=0.0
CA1= 0.225E 09
CA2= 0.100E 01
CA3= 0.0
THETAM= 30 0

Fig. 60: Study G-6. 9 dB Power Constraint with Varied Spacing. 300 Elements. Range of Spacing 0.500λ to 690.0λ. Taper Factor CA 1 = 0.225×10^{9}. Each Abscissa Scale Unit is 18^{o}.

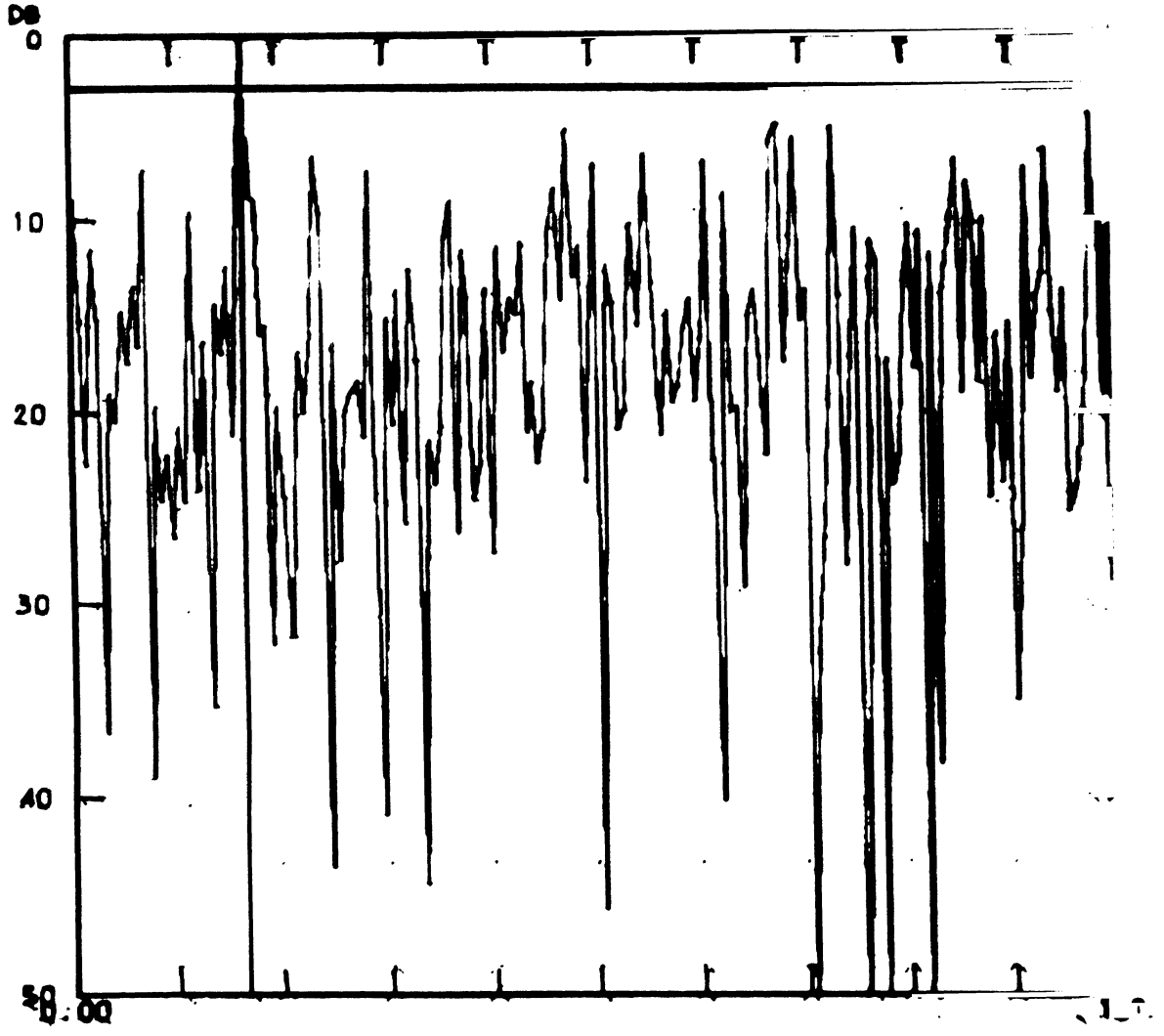

350 ELEMENTS
CZ1=0.500
CZ2=1.050
CZ3=1.000
CZ4=0.0
CA1= 0.260E 10
CA2= 0.100E 01
CA3= 0.0
THETAM= 30.0

Fig. 61: Study G-7. 9 dB Power Constraint with Varied Spacing. 350 Elements. Range of Spacing 0.500λ to 2300λ. Taper Factor CA 1 = 0.260×10^{10}. Each Abscissa Scale Unit is 18^{o}.

symmetrical about a center point. In this first use of the steepest descent technique, the amplitudes of the elements are specified, and the element positions are varied to obtain the desired pattern.

The steepest descent technique is a general method and is not restricted to the examples described. It should be applicable to planar as well as linear arrays. Other parameters could be adjusted instead of the element positions to obtain the desired pattern, or they could be adjusted in addition to the element positions.

The synthesis of the non-uniformly spaced linear array is now considered. The array pattern P is defined:

$$P = \sum_{n=1}^{N} b_n e^{ik\bar{R}_N \cdot \hat{R}} \tag{2.13}$$

where b_n is the relative level of excitation of the nth element including phase, and R_N is the distance of the nth element from the origin. Let

$$b_n = a_n e^{-jz_n \cos\theta_m} . \tag{2.14}$$

Then for an even number of elements the calculated pattern is:

$$P_c = \sum_{n=1}^{N/2} a_n \cos\left[kz_n (\cos\theta_m - \cos\theta) \right] \tag{2.15}$$

where the elements are numbered from the center. Note that P_c has a maximum value when $\theta = \theta_m$. It is assumed that the a_n are real and have magnitudes adjusted so that the maximum value of P_c is unity.

Let $P_s(\theta)$ be some specified array pattern given as a function of θ. An example is shown in Fig. 62. The synthesis problem is to find a combination of the element positions z_n producing a pattern P_c, which matches as closely as possible the specified pattern P_s. Define an error function $E_1(\theta) = \left[P_s(\theta) - P_c(\theta) \right]^2$. An error function over the entire synthesis range of θ is defined:

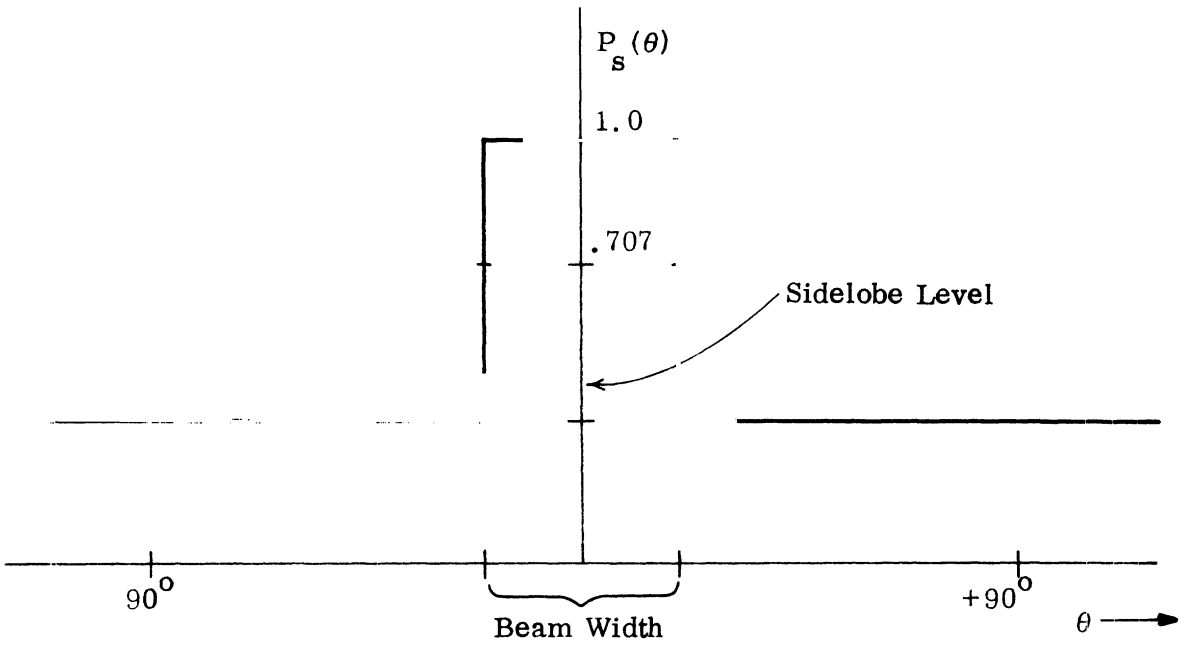

Fig. 62: Specified Array Pattern

$$E_1 = \sum_{i=1}^{M} \left[P_s(\theta_i) - P_c(\theta_i) \right]^2 \qquad (2.16)$$

where $\theta_1, \ldots, \theta_M$ are n specified directions. It is assumed that the θ_i are spaced closely enough to give an accurate value of the error for all values of θ in the synthesis range. If more emphasis is placed on certain values of θ than on others in the design procedure, a weighting function $W_{(\theta_i)}$ can be introduced so that equation (2.16) becomes

$$E_1 = \sum_{i=1}^{M} W_{(\theta_i)} \left[P_s(\theta_i) - P_c(\theta_i) \right]^2 \quad . \qquad (2.17)$$

For simplicity in specifying the pattern P_s, it will be defined positive and the

error function will be defined

$$E = \sum_{i=1}^{M} W_{(\theta_i)} \left[P_s(\theta_i) - \left| P_c(\theta_i) \right| \right]^2 \tag{2.18}$$

From equations (2.15) and (2.18) it is seen that E is a function of the z_n. Let $\bar{z}$ be the vector

$$\bar{z} = (kz_1, kz_2, \ldots, kz_N). \tag{2.19}$$

Then

$$E = E(\bar{z}) \quad . \tag{2.20}$$

The problem then is to find the minimum value of $\bar{E}(\bar{z})$.

The method of solution (Perini and Idselis, 1971) is known as the conjugate gradient method or the method of steepest descent. A gradient can be defined

$$\nabla E(\bar{z}) = \left(\frac{\partial E}{\partial kz_1}, \frac{\partial E}{\partial kz_2}, \ldots, \frac{\partial E}{\partial kz_N} \right) \tag{2.21}$$

where from equation (2.18)

$$\frac{\partial E}{\partial kz_j} = 2 \sum_{i=1}^{M} W(\theta_i) \left[P_s(\theta_i) - \left| P_c(\theta_i) \right| \right] (-1) \frac{\partial}{\partial kz_j} \left| P_c(\theta_i) \right| \tag{2.22}$$

and from equation (2.15)

$$\frac{\partial \left| P_c(\theta_i) \right|}{\partial kz_j} = -\operatorname{sign}\left[P_c(\theta_i) \right] a_N (\cos\theta_m - \cos\theta_i) \sin\left[kz_j (\cos\theta_m - \cos\theta_i) \right] . \tag{2.23}$$

Suppose that initially one has a vector $\bar{z}^o$ and an error E^o. For example, $\bar{z}^o$ might correspond to a uniformly spaced array. From equation (2.21) the greatest decrease in E is accomplished for a given change in magnitude of $\bar{z}$ when the change in $\bar{z}$ is opposed to the gradient of E. That is,

$$\bar{z}' = \bar{z}^o - K \nabla E^o \quad . \tag{2.24}$$

This represents the n equations

$$\begin{aligned} kz_1' &= kz_1^o - K \frac{\partial E}{\partial kz_1} \\ &\vdots \\ kz_N' &= kz_N^o - K \frac{\partial E}{\partial kz_N} \end{aligned} \quad . \tag{2.25}$$

The corresponding near value for E is approximately

$$E_p(\bar{z}') \cong E^o + \left.\frac{\partial E}{\partial kz_1}\right|_{\bar{z}^o} \Delta kz_1 + \ldots + \left.\frac{\partial E}{\partial kz_N}\right|_{\bar{z}^o} \Delta kz_N \tag{2.26}$$

where Δkz_i represents the change in the i th position and $E^o = E(z^o)$. Equation (2.26) can be written

$$E_p(\bar{z}') \cong E^o + \nabla E^o (\bar{z}' - \bar{z}^o) \tag{2.27}$$

or from equation (2.24)

$$\bar{E}_p(\bar{z}') \cong E^o - K (\nabla E^o)^2 \quad . \tag{2.28}$$

The constant K is chosen so that the value for $E(\bar{z}')$ given by equation (2.27) is comparable with the true value given by equation (2.18) (Eveleigh, 1967). The purpose of this restriction is to assure that the gradient $\nabla E^o = \nabla E\Big|_{\bar{z}=\bar{z}^o}$ is not greatly different from the gradient $\nabla E' = \nabla E\Big|_{\bar{z}=\bar{z}'}$. A practical condition (Eveleigh, 1967) is that

$$\left| \frac{\Delta E_p - \Delta E_c}{\Delta E_c} \right| < .6 \tag{2.29}$$

$$\left| \frac{\Delta E_p - \Delta E_c}{\Delta E_c} \right| > .2 \tag{2.30}$$

where ΔE_p, the predicted change in error, is given by equation (2.29)

$$\Delta E_p = -K (\nabla E^o)^2 \tag{2.31}$$

and ΔE_c, the calculated change in error, is given using equation (2.18)

$$\Delta E_c = E\left[\bar{z}^o\right] - E\left[\bar{z}'\right] \quad . \tag{2.32}$$

If K is so small that E_p is very close to the value E_c, then it will take more iterations than necessary to find the minimum error. However, if K is so large that E_p is very different from E_c, it is not assured that the iterative procedure will converge.

The first step in using criteria of equations (2.29) and (2.30) is to get an initial value of K. The criterion for choosing an initial K in the example is to specify that the spacing between any two elements should change no more than five percent at the first iteration. Then it is desired that:

$$\left|(z'_i - z'_{i-1}) - (z^o_i - z^o_{i-1})\right| \leq 0.05\,(z^o_i - z^o_{i-1}) \quad . \tag{2.33}$$

From equation (2.24) then

$$\left| -K \frac{\partial E}{\partial (kz_i)} + K \frac{\partial E}{\partial (kz_{i-1})} \right| \leq 0.05\,(z^o_i - z^o_{i-1}) \quad . \tag{2.34}$$

Thus:

$$K \leq 0.05 \left| \frac{z^o_i - z^o_{i-1}}{\frac{\partial E}{\partial kz_i} - \frac{\partial E}{\partial (kz_{i-1})}} \right| \quad . \tag{2.35}$$

Noting equation (2.19) there results:

$$K = 0.05 \max \left\{ \left| \frac{(kz_\ell) - (kz_{\ell-1})}{\frac{\partial E}{\partial (kz_\ell)} - \frac{\partial E}{\partial (kz_{\ell-1})}} \right| \quad \ell = 2, \ldots, \frac{N}{2} \right\} . \tag{2.36}$$

Once the iterative procedure is begun the value of K is controlled by the tests indicated in equations (2.29) and (2.30). If equation (2.29) is true K is increased by 50 percent. If equation (2.30) is true K is decreased by 20 percent. Otherwise, K remains the same. After the above tests are made, the test is made to see if the new value for the error E' is less than the error at the previous step E^o. If it is a new step in the iteration is taken. However, if $E' > E^o$, the previous step is repeated with the new value for K. That is, the just calculated element positions are dumped, the element positions are restored to the values they had at the beginning of the step, and a new set of element positions is calculated using the new value of K.

A numerical example will be used for illustration. It is desired to lower the sidelobe level of a 200-element uniformly spaced symmetrically excited array by varying the element spacings. The spacings must be varied so that the elements are spaced symmetrically about the center. The design is to be terminated if the element spacing is required to be less than 0.42. The element excitation is shown in Fig. 63. The specified pattern P_s is of the same form as Fig.

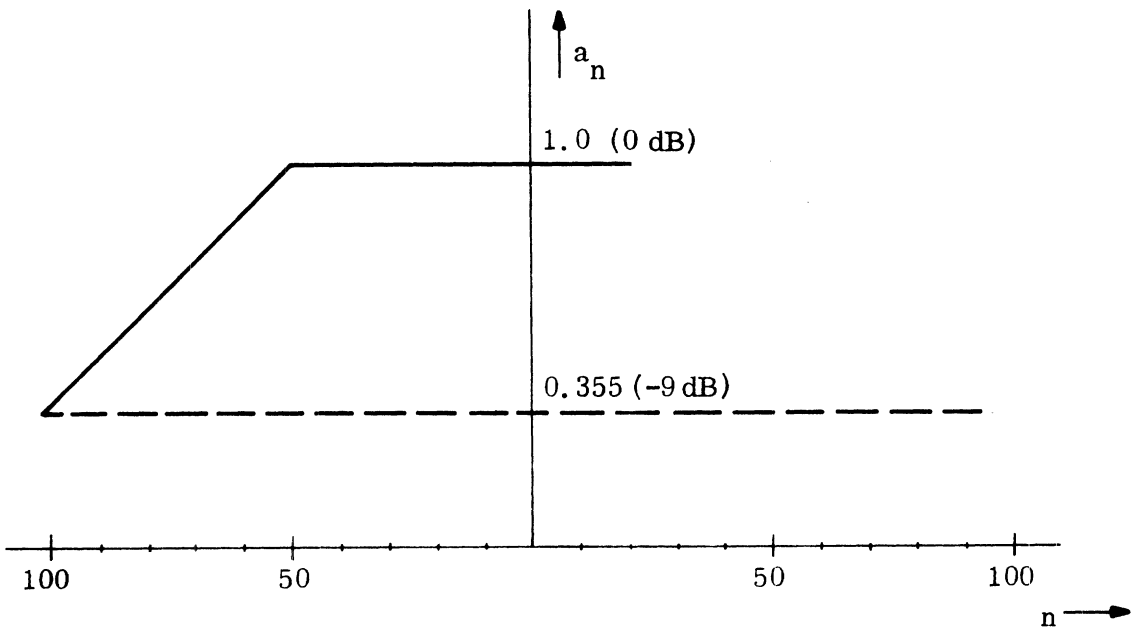

Fig. 63: Element Excitation

with a beamwidth of 1^{o} and a uniform sidelobe level of 0.01. The pattern is assumed to be normalized with the maximum value at $\theta_m = 90^{o}$. The weighting function $W(\theta_i)$ is chosen so that $W(89.5^{o}) = 225$ and all the remaining values are unity or zero, depending on whether $P_s < P_c$ or $P_s > P_c$, respectively. The z vector is initially chosen so that the spacing between any two elements is $\lambda/2$. There are 450 values of θ_i chosen to assure a good pattern match. These angles are chosen so that the point density close to the main beam is greater than it is away from the main beam.

After two iterations the height of the maximum sidelobe was reduced from -17.8 dB to -25 dB. The flow chart for the numerical work is given in Fig. 67. The initial pattern $P_c(z_o)$ is given in Fig. 64, and the pattern after two iterations is shown in Fig. 65. After the second iteration, the minimum spacing was 0.408λ and the maximum spacing was 0.56λ. The total array width was 98.6λ as compared to 99.5λ for the original uniformly spaced array.

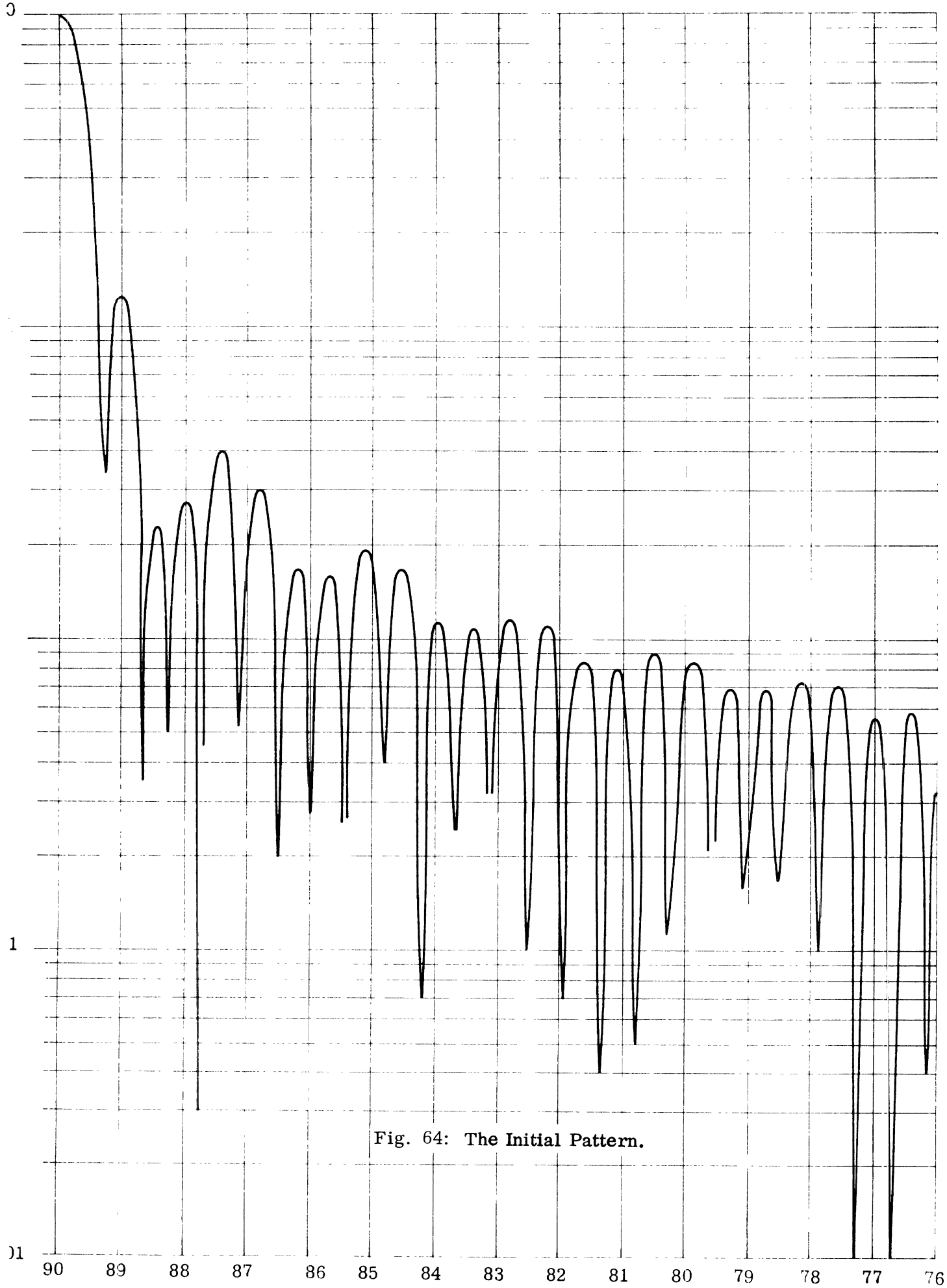

Fig. 64: **The Initial Pattern.**

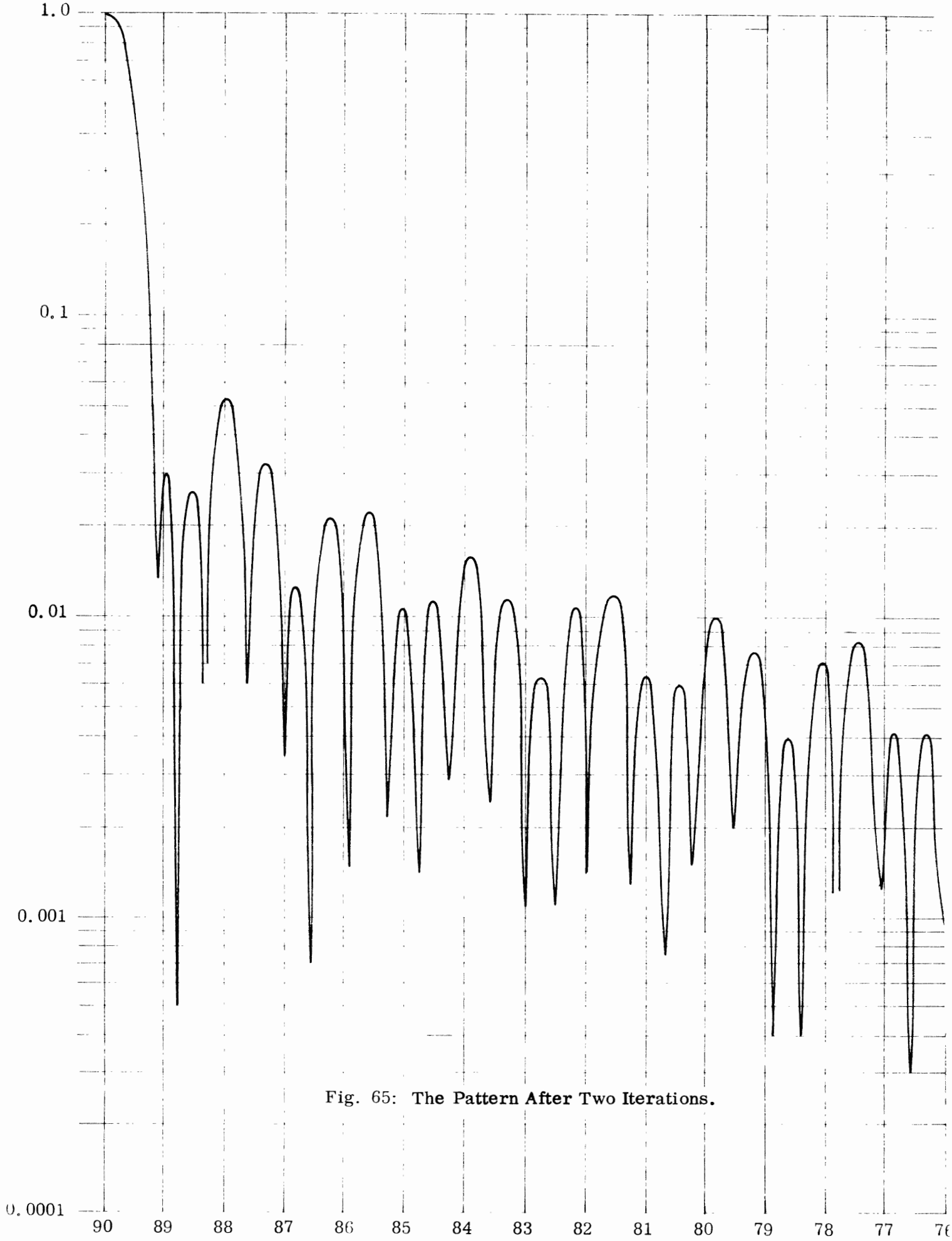

Fig. 65: **The Pattern After Two Iterations.**

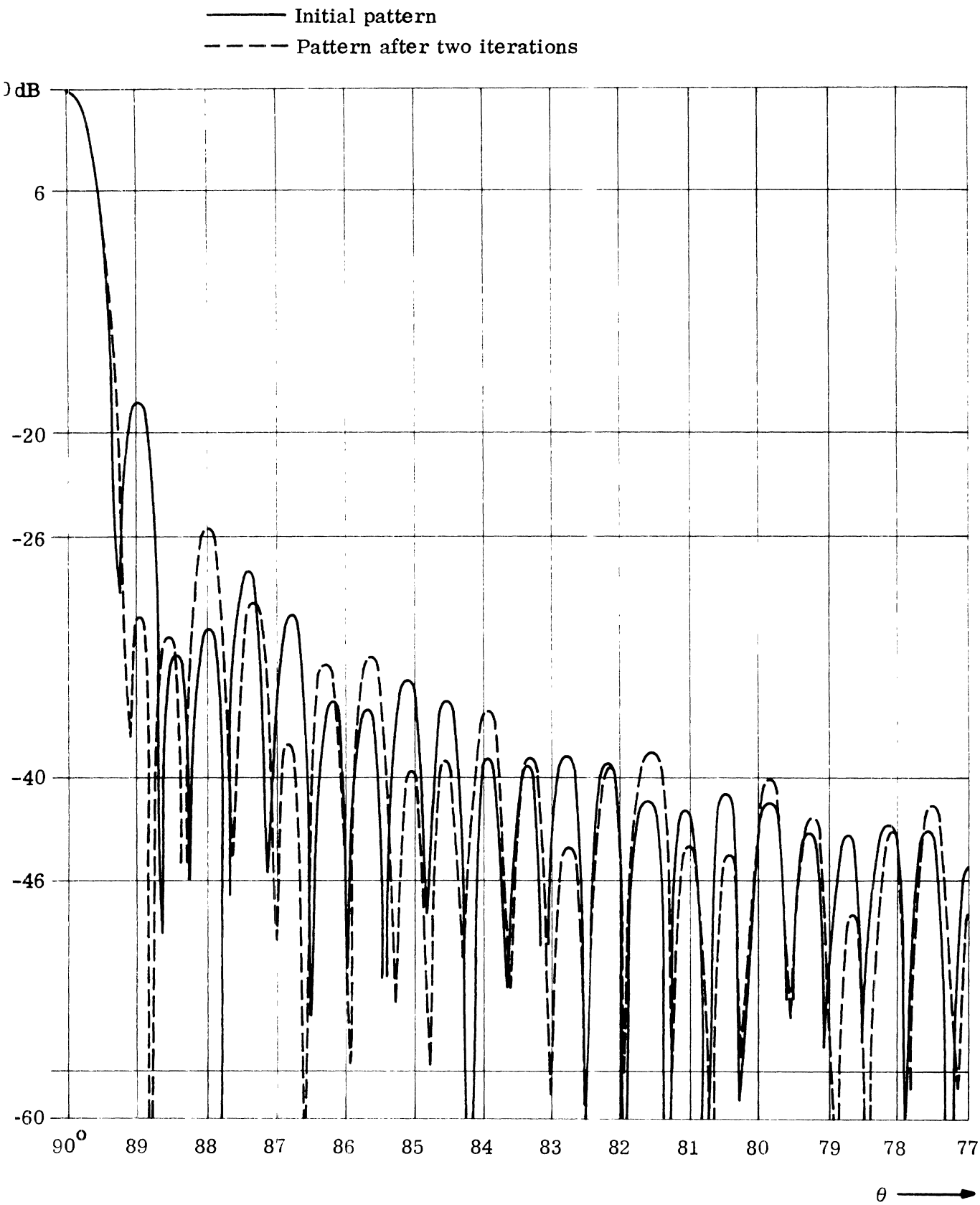

Fig. 66: Overlay of original pattern and pattern after two iterations.

Fig. 67: Flow chart for synthesis of an unequally spaced array.

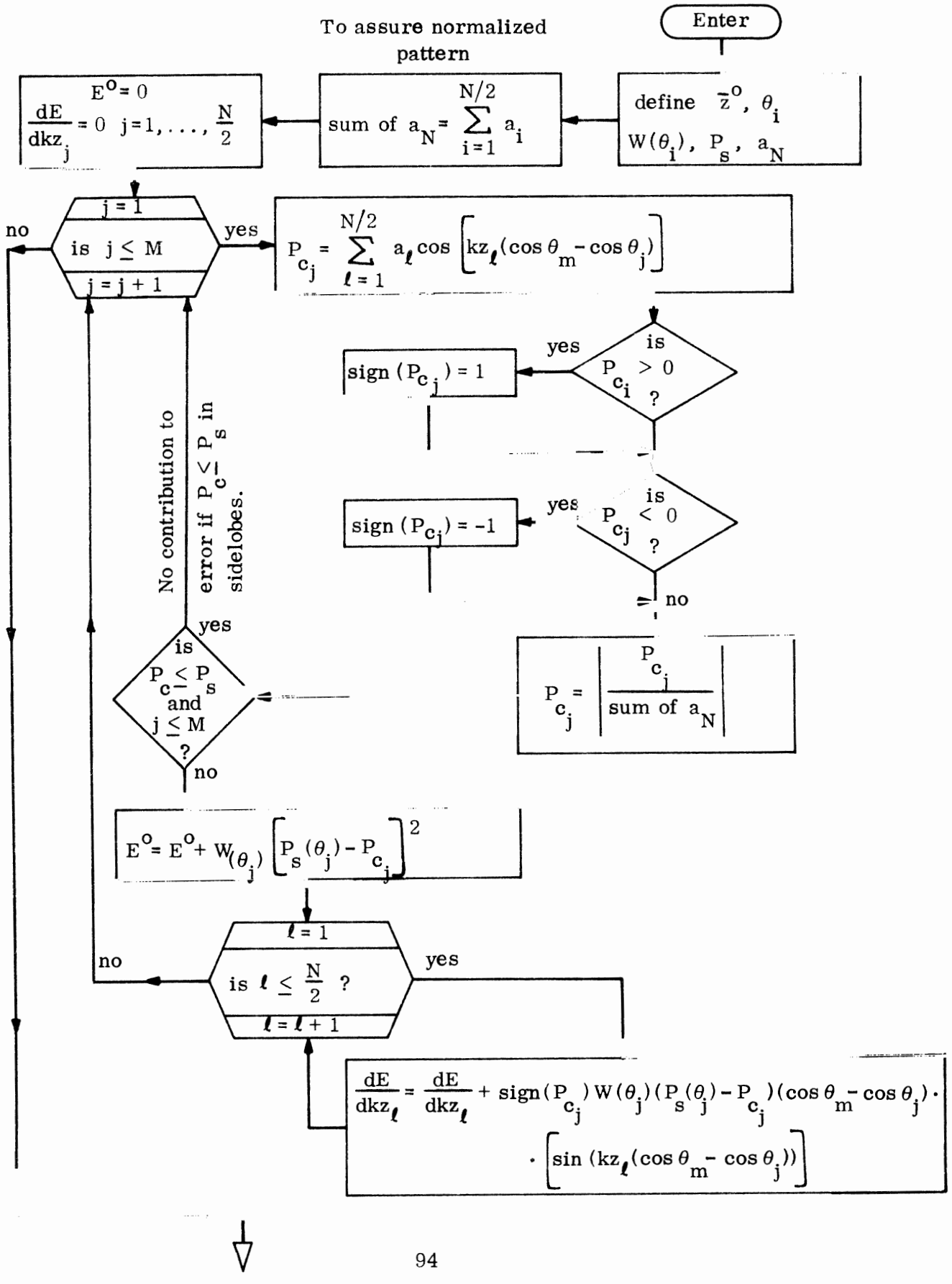

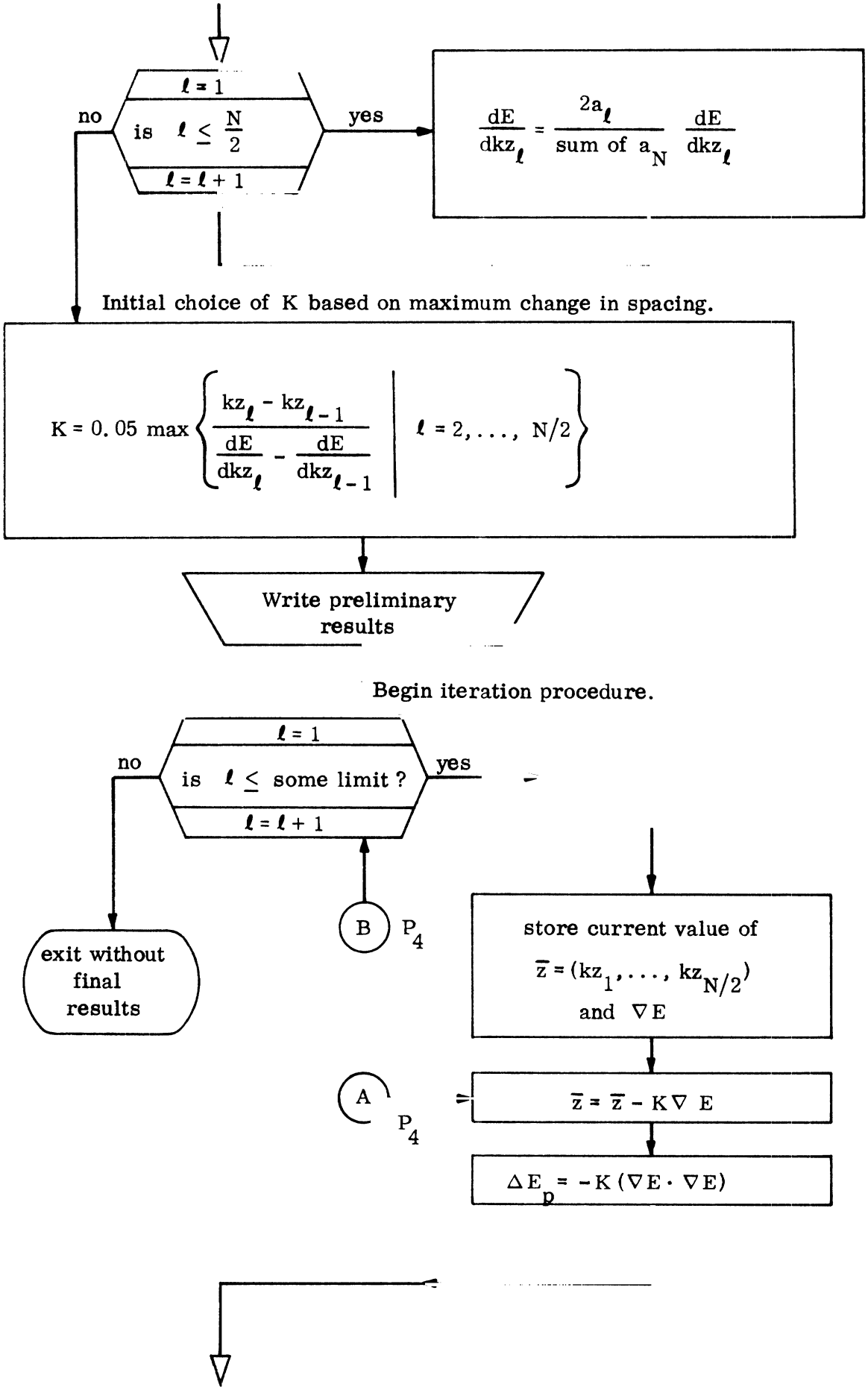
$\ell = 1$
no
is $\ell \leq \frac{N}{2}$
yes
$\ell = \ell + 1$
$\frac{dE}{dkz_\ell} = \frac{2a_\ell}{\text{sum of } a_N} \frac{dE}{dkz_\ell}$
Initial choice of K based on maximum change in spacing.
$K = 0.05 \max \left\{ \frac{kz_\ell - kz_{\ell-1}}{\frac{dE}{dkz_\ell} - \frac{dE}{dkz_{\ell-1}}} \;\middle|\; \ell = 2, \ldots, N/2 \right\}$
Write preliminary results
Begin iteration procedure.
$\ell = 1$
no
is $\ell \leq$ some limit ?
yes
$\ell = \ell + 1$
exit without final results
B
P_4
store current value of $\bar{z} = (kz_1, \ldots, kz_{N/2})$ and ∇E
A
P_4
$\bar{z} = \bar{z} - K \nabla E$
$\Delta E_p = -K (\nabla E \cdot \nabla E)$

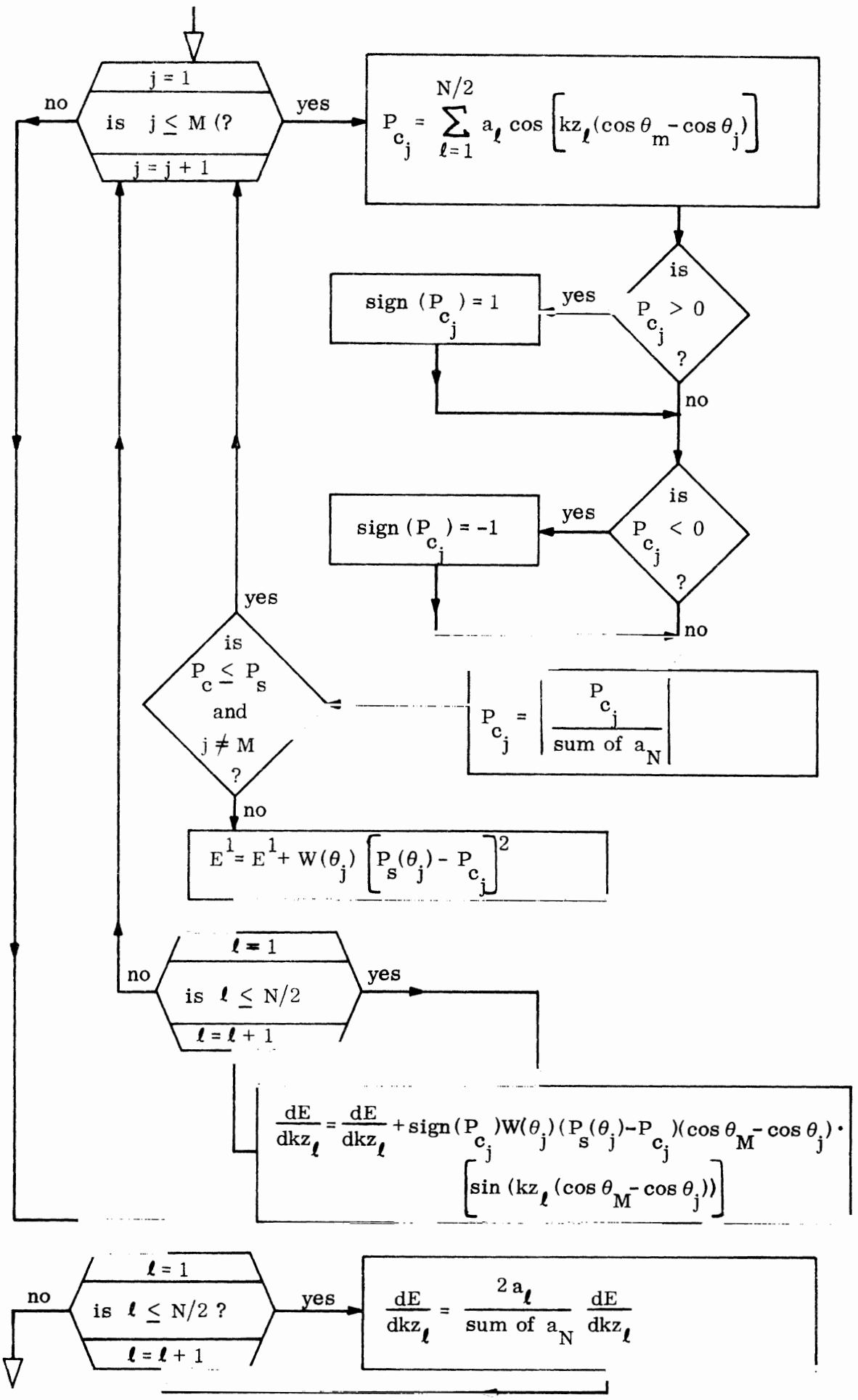
j = 1
is j ≤ M (?
j = j + 1
no
yes
$P_{c_j} = \sum_{\ell=1}^{N/2} a_\ell \cos\left[kz_\ell(\cos\theta_m - \cos\theta_j)\right]$
is $P_{c_j} > 0$?
yes
sign (P_{c_j}) = 1
no
is $P_{c_j} < 0$?
yes
sign (P_{c_j}) = -1
no
is $P_c \leq P_s$ and $j \neq M$?
yes
$P_{c_j} = \left|\frac{P_{c_j}}{\text{sum of } a_N}\right|$
no
$E^1 = E^1 + W(\theta_j)\left[P_s(\theta_j) - P_{c_j}\right]^2$
$\ell = 1$
is $\ell \leq N/2$
$\ell = \ell + 1$
no
yes
$\frac{dE}{dkz_\ell} = \frac{dE}{dkz_\ell} + \text{sign}(P_{c_j})W(\theta_j)(P_s(\theta_j) - P_{c_j})(\cos\theta_M - \cos\theta_j) \cdot \left[\sin(kz_\ell(\cos\theta_M - \cos\theta_j))\right]$
$\ell = 1$
is $\ell \leq N/2$?
$\ell = \ell + 1$
no
yes
$\frac{dE}{dkz_\ell} = \frac{2a_\ell}{\text{sum of } a_N} \frac{dE}{dkz_\ell}$

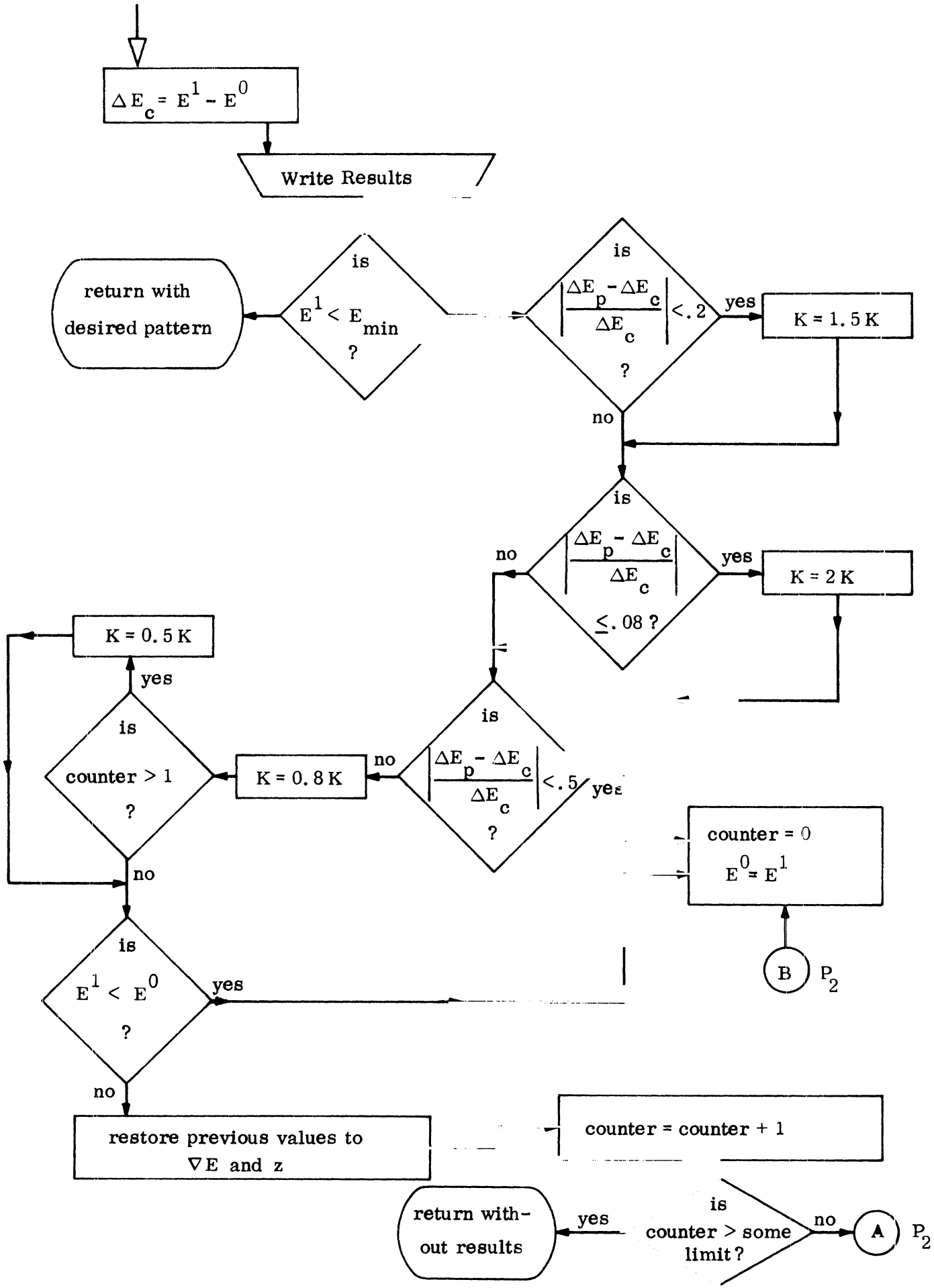
$\Delta E_c = E^1 - E^0$
Write Results
is $E^1 < E_{min}$?
return with desired pattern
is $\left|\frac{\Delta E_p - \Delta E_c}{\Delta E_c}\right| < .2$?
yes
K = 1.5 K
no
is $\left|\frac{\Delta E_p - \Delta E_c}{\Delta E_c}\right| \leq .08$?
no
yes
K = 2 K
is $\left|\frac{\Delta E_p - \Delta E_c}{\Delta E_c}\right| < .5$?
no
K = 0.8 K
yes
is counter > 1 ?
yes
K = 0.5 K
no
is $E^1 < E^0$?
yes
no
restore previous values to ∇E and z
counter = 0
$E^0 = E^1$
B
P_2
counter = counter + 1
is counter > some limit?
no
A
P_2
yes
return without results

III. DISCUSSION AND CONCLUSIONS

The use of the CALCOMP Unit in connection with the IBM 360/67 computer was helpful in portraying the influence on linear array characteristics in response to changes of various parameters. The series of computer studies did not result in new principles being evolved. Rather, the accomplishment was to observe the influence of changing many parameters. The series of studies showed approximately what would be necessary in the number of elements, spacings and gradation of illumination in order to satisfy the requirements of a high performance linear array. The CALCOMP method utilized could possible be extended to planar array work. However, this would require a considerable complication in the programming. Furthermore, for this CALCOMP display it would be necessary to obtain various cuts for the pattern of a planar array.

As would be expected the various computed patterns verify the following established dependencies: (1) increasing the length of the array results in a narrower beam, (2) for a uniformly spaced array tapering the illumination of the elements from the center to the extreme ends results in lower sidelobe levels, (3) increasing the spacing of a uniformly spaced array ultimately results in the presence of grating lobes in the visible region, (4) the beamwidth of an array increases as the position of the beam departs from the broadside position, (5) with unequal spacings of elements it is possible to have some spacings exceed the critical value of 0.55λ without the occurrence of grating lobes, (6) for a linear array of uniformly spaced elements it is possible to have an illumination taper such that the resulting array pattern is the same shape as a Tschebyscheff polynomial.

The mathematical method of "steepest descent" has been made applicable to a simple linear array. The results of computations on a 200-element linear array using the "steepest descent" method shows an improvement is obtained. This means that it is possible to take a linear array which roughly approximates

the desired performance of the array and then by the method of steepest descent calculate the changes necessary to make the final array come up to the required performance, i.e., to make the required array have the radiation pattern that has been prescribed.

REFERENCES

[1] Perini, Jose and Manfred Idselis, "Note on antenna pattern synthesis using numerical iterative methods," IEEE Trans. on Antennas and Propagation, Vol. AP-19, No. 2, March 1971, p. 284-286.

[2] Eveleigh, V., Adaptive Control and Optimization Techniques. New York: McGraw-Hill, 1967, ch. 5.

[3] Skolnik, Merrill I., Radar Handbook. New York: McGraw-Hill, 1970, ch. 11, p. 11.

UNCLASSIFIED

Security Classification

DOCUMENT CONTROL DATA - R & D

(Security classification of title, body of abstract and indexing annotation must be entered when the overall report is classified)

1 ORIGINATING ACTIVITY (Corporate author)

The University of Michigan Radiation Laboratory
2216 Space Research Bldg. North Campus
Ann Arbor Michigan 48105

2a. REPORT SECURITY CLASSIFICATION

UNCLASSIFIED

2b GROUP

N/A

3 REPORT TITLE

VHF-UHF PHASED ARRAY TECHNIQUES
PART I: CALCOMP STUDIES OF LINEAR ARRAYS WITH NON-UNIFORMLY SPACED ISOTROPIC ELEMENTS

4 DESCRIPTIVE NOTES (Type of report and inclusive dates)

Technical Report, Scientific, Interim

5 AUTHOR(S) (First name, middle initial, last name)

John A.M. Lyon, Philip H. Fiske, Mohamed A. Hidayet and Jess B. Scott

6 REPORT DATE	7a. TOTAL NO OF PAGES	7b NO OF REFS
November 1973	100	3

8a CONTRACT OR GRANT NO	9a ORIGINATOR'S REPORT NUMBER(S)
F33615-71-C-1495 b. PROJECT NO 6099 c Task 05 d.	004970-1-T 9b. OTHER REPORT NO(S) (Any other numbers that may be assigned this report) AFAL-TR-73-399, PART I

10 DISTRIBUTION STATEMENT

Distribution limited to U.S. Government Agencies only; Test and Evaluation Data; November 1973. Other requests for this document must be referred to AFAL/TEN.

11 SUPPLEMENTARY NOTES	12 SPONSORING MILITARY ACTIVITY
	Air Force Avionics Laboratory Air Force Systems Command Wright-Patterson Air Force Base, Ohio

13 ABSTRACT

This report contains information obtained by numerous computer studies of linear arrays of isotropic elements. A large range of numbers of elements were used. Various formulations were used to provide control on the degree of non-uniformity of spacing. Provision was made so as to provide a gradation in the illumination of the various elements used. It was found that a simple exponential relation provided illumination corresponding simultaneously to a Tchebyscheff type radiation pattern.

It was decided that for practical purposes some restraint should be provided on the grading of the slot illumination from the center slot to either extreme end slot. Therefore, in some of the studies utilizing an exponential variation of illumination, an arbitrary limit was imposed which required the illumination on the end slot to be either 9 or 12 dB below that of the center slot.

Considerable work was done on an optimization process, which has been classified as the method of steepest descent. In the steepest descent method a change in spacing is made in the direction that causes the most rapid rate of change (reduction) in the difference between a prescribed radiation pattern and the obtained radiation pattern. In other words, the change to be made was always in the direction so as to decrease the error or difference between the two patterns most rapidly. In applying this optimization procedure it was decided that it was appropriate to start with an array already reasonably designed. For instance, if a broadside Tschebyscheff array was selected, the optimization process would be applied and changes would be made in the spacings of the elements so that the sidelobe levels would be reduced.

DD FORM 1 NOV 68 1473

UNCLASSIFIED

Security Classification

14 KEY WORDS	LINK A		LINK B		LINK C	
	ROLE	WT	ROLE	WT	ROLE	WT
Antenna Array Analysis						
Unequal Spacing of Array Elements						
Grating Lobes in Arrays						
Simulated Tschebyscheff Arrays						
Computer Graphic Techniques						